Arch. Rational Mech. Anal. (2024) 248:103
Digital Object Identifier (DOI) https://doi.org/10.1007/s00205-024-02043-2

From Incommensurate Bilayer Heterostructures to Allen–Cahn: An Exact Thermodynamic Limit

Michael Hott, Alexander B. Watson & Mitchell Luskin

Communicated by A. Braides

Abstract

We give a complete and rigorous derivation of the mechanical energy for twisted 2D bilayer heterostructures without any approximation beyond the existence of an empirical many-body site energy. Our results apply to both the continuous and discontinuous continuum limit. Approximating the intralayer Cauchy–Born energy by linear elasticity theory and assuming an interlayer coupling via pair potentials, our model reduces to a modified Allen–Cahn functional. We rigorously control the error, and, in the case of sufficiently smooth lattice displacements, provide a rate of convergence for twist angles satisfying a Diophantine condition.

Contents

List of Symbols

A_j Matrix of primitive translation vectors in layer j (2.1)
$\mathcal{R}_j$ Lattice of layer j (2.2)
$D_{j\to 3-j}$ Disregistry matrix of layer j with respect to layer $3-j$ (1.1)
$\Gamma_{\mathcal{M}}$ Moiré unit cell (2.12)
Γ_j Unit cell of layer j (2.3)
$\mathcal{R}_j(N)$ Square truncated lattice in layer j, of side-length $2N+1$ (2.4)
B_j Matrix of reciprocal primitive translation vectors in layer j (2.5)
$\mathcal{R}_j^*$ Reciprocal lattice of layer j (2.6)
$\mathcal{A}_j$ Sublattice degrees associated with layer j (2.7)
$\tau_j^{(\alpha_j)}$ Shift vector in layer j corresponding to the subllatice degree $\alpha_j \in \mathcal{A}_j$ (2.7)
$B_{\mathcal{M}}$ Matrix of moiré reciprocal primitive translation vectors (2.8)
$\mathcal{R}_{\mathcal{M}}^*$ Reciprocal moiré lattice (2.9)
$A_{\mathcal{M}}$ Matrix of moiré primitive translation vectors (2.10)
$\mathcal{R}_{\mathcal{M}}$ Moiré lattice (2.11)
$\rho_{\mathcal{M}}$ Moiré length scale ratio, see (2.14)
$\{x\}_{\mathcal{M}}$ Moiré disregistry (2.15)
$\lfloor x \rfloor_{\mathcal{M}}$ Projection onto moiré lattice (2.16)
$\lfloor x \rfloor_j$ Projection onto $\mathcal{R}_j$ (2.17)
$\{x\}_j$ Disregistry with respect to layer j (2.17)
$Y_j(x, \alpha_j)$ Total (generalized) lattice position in layer j, associated with position x and sublattice degree $\alpha_j \in \mathcal{A}_j$ (2.20), (2.21)
$\mathbf{u}$ Vector $\mathbf{u} = (u_1, u_2)$ consisting of the (moiré-periodic) displacement functions u_j of layer j, $j = 1, 2$ (2.22)
$\boldsymbol{\gamma}$ Vector $\boldsymbol{\gamma} = (\gamma_1, \gamma_2)$ consisting of the origins γ_j of layer j, $j = 1, 2$ (2.22)
$\boldsymbol{\alpha}$ Vector $\boldsymbol{\alpha} = (\alpha_1, \alpha_2)$ consisting of the sublattice degrees $\alpha_j \in \mathcal{A}_j$ of layer j, $j = 1, 2$ (2.22)
$V_{j,\alpha_j}^{(\text{mono})}$ Monolayer manybody potential in layer j, acting on an atom of sublattice degree $\alpha_j \in \mathcal{A}_j$, Sect. 2.1.2
$\Phi_j^{(\text{mono})}$ Sublattice-averaged monolayer site-potential in layer j (2.24)
$V_{j,\alpha_j}^{(\text{inter})}$ Interlayer manybody potential in layer j, acting on an atom of sublattice degree $\alpha_j \in \mathcal{A}_j$, Sect. 2.1.2
$v_{\boldsymbol{\alpha}}$ Interlayer pair potential between atoms of types $\alpha_1 \in \mathcal{A}_1$ in layer 1 and $\alpha_2 \in \mathcal{A}_2$ in layer 2, $\boldsymbol{\alpha} = (\alpha_1, \alpha_2)$ (2.26)
$\Psi_j^{(\text{inter})}$ Sublattice-averaged interlayer site-potential in layer j dependent on opposite layer and moiré disregistry (2.28)

$\Phi_{j,\boldsymbol{\gamma}}^{(\text{inter})}$ Diagonal of $\Psi_j^{(\text{inter})}$ (2.30)
$\mathcal{F}_{\Gamma_{\mathcal{M}}}$ Fourier transform over the domain $\Gamma_{\mathcal{M}}$, see (2.35); similarly defines $\mathcal{F}_{\Gamma_{\mathcal{M}}\times\Gamma_j}$ as Fourier transform over the domain $\Gamma_{\mathcal{M}} \times \Gamma_j$, see (3.1)
$\mathbb{1}_{\mathcal{R}_j^*}^{(N)}$ Rescaled Dirichlet kernel associated with the truncated lattice $\mathcal{R}_j(N)$ (3.2)

1. Introduction

Setting a two-dimensional lattice on another with a small rotation creates quasi-periodic moiré patterns on a superlattice scale given by the period of oscillation of the interlayer disregistry, see Fig. 1. This moiré effect can be understood as being analoguous to the *beating phenomenon* in acoustics. At small twist angles, the moiré scale acts as a slow variable, whereas the individual layer constants act as fast variables. Consequently, moiré heterostructures are a suitable playground for multiscale analysis.

In recent years, moiré materials consisting of a few relatively twisted layers of 2D-crystal structures have attracted great attention since the moiré length scale offers the possibility of discovering previously inaccessible electronic phases and other phenomena [38].

The seminal paper in 2011 by Bistritzer and MacDonald [15] predicted that twisted bilayer graphene (TBG), at an angle of $\theta \approx 1.1°$—referred to as the magic angle—exhibits almost flat electronic bands near the charge neutrality point. As a consequence of the flat bands, there is a high density of states, which has been known to provide a platform for emergent electronic phases involving strong electron interactions. This has been experimentally verified, e.g., in [22,23], where both a superconducting and a correlated insulating phase have been established. A class of other 2D materials is given by *transition metal dichalcogenides* (TMDs). Popular choices for transition metals include Mo and W and for chalcogens include Se, S, and Te. In particular, moiré materials have become quantum simulators, i.e., highly tunable experimental realizations for effective theories predicted by theorists. For overviews on moiré materials, we refer to, e.g., [26,55,71].

Structural relaxation, the process by which atoms deviate from their monolayer equilibrium positions in order to minimize the total mechanical energy of the twisted bilayer, can significantly modify the electronic properties of moiré materials. For example, relaxation enhances the band gap between the flat electronic bands and other bands in twisted bilayer graphene [87]. In a simplified model of twisted bilayer graphene with strong relaxation, the chiral model, the almost flat bands become exactly flat [5,6,83,86]. It is thus critical to develop systematic methods for modeling structural relaxation and its effects on electronic properties of moiré materials.

Modeling structural relaxation is complicated by the fact that the atomic structure of twisted bilayer 2D materials is generally aperiodic (incommensurate) except at special commensurate angles [85]. Phenomenological continuum models for structural relaxation at commensurate twist angles have been proposed in [72,77,88,90].

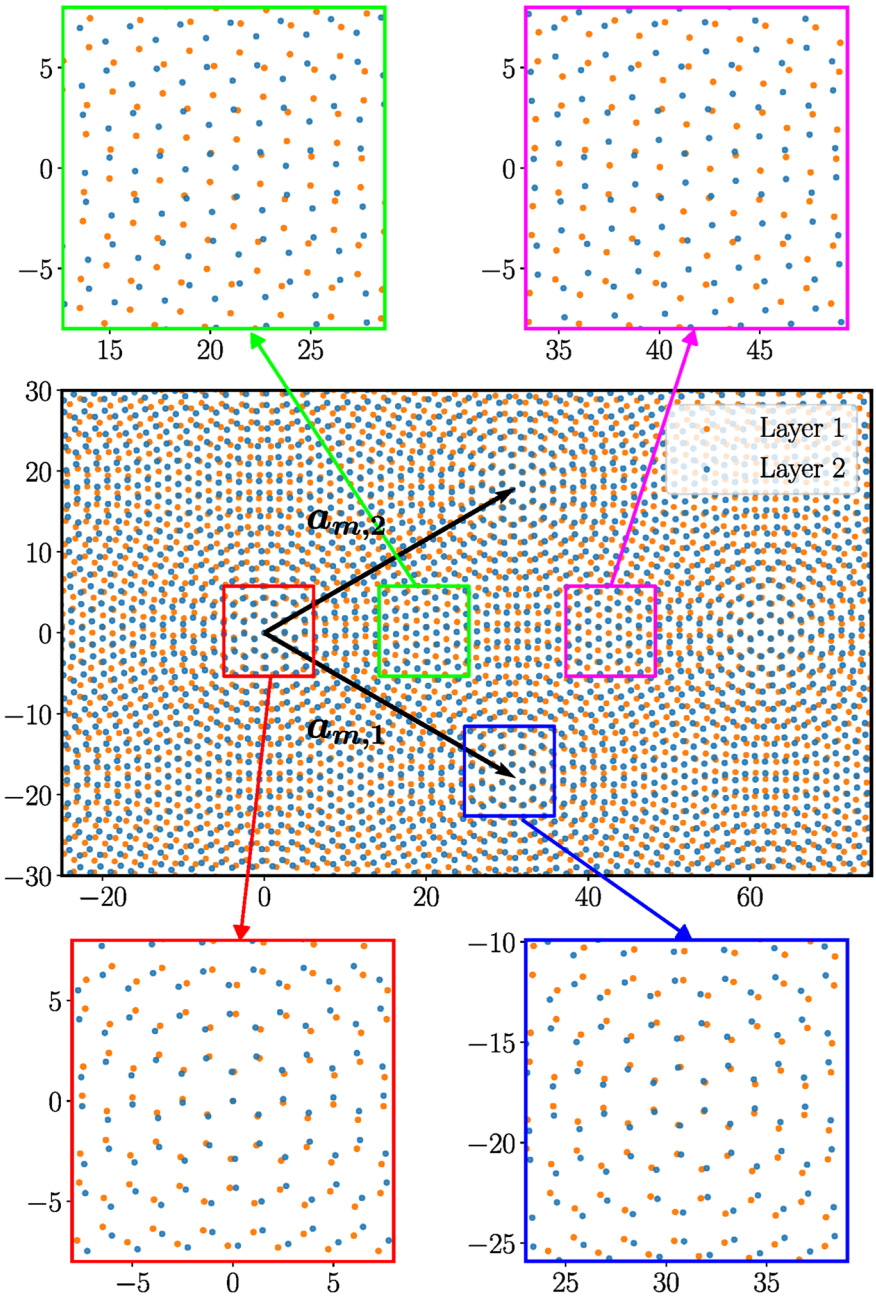

Fig. 1. Twisted bilayer, with moiré vectors; pictures on top show local environment in symmetry-related AB and BA (Bernal) stacked regions, pictures below zoom in on two AA stacked regions separated by a moiré superlattice vector. See Sect. 2.3.3 for a description and discussion of the energetics of AA, AB, and BA stacking

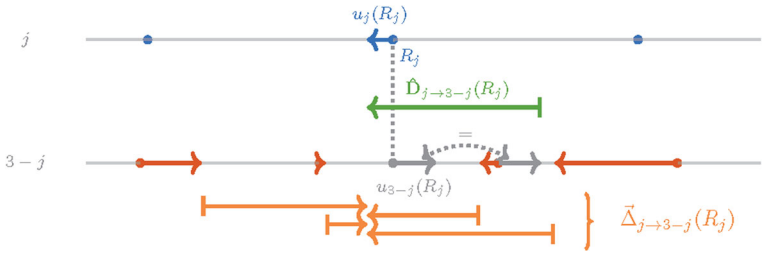

Fig. 2. Modulated disregistry $\hat{\mathbf{D}}_{j\to 3-j}(R_j)$ chosen in [28]. In comparison, the sequence $\vec{\Delta}_{j\to 3-j}(R_j)$ of all modulated disregistries chosen in the present work

A systematic approach not restricted to commensurate twist angles or bilayer structures was proposed in [28]. In this approach, the displacements u_j of atoms in layer j of an incommensurate twisted 2D bilayer structure are assumed to be continuous functions of the local configuration, or disregistry, which can be identified with a two-dimensional torus. This is based on the more general concept of a *hull*, a compact parametrization of all possible local environments, which has been introduced in the context of electronic properties of general aperiodic structures, see, e.g., [7–9] and references therein.

For more general multilayer structures with $p > 2$ layers [89,91], the hull can be identified with a $2p-2$ dimensional torus and hence there does not exist a two-dimensional periodic continuum model in real space. The configuration-space model proposed in [28] has become increasingly used to model trilayer and more general structures [92].

Such a parametrization is known to be valid for the Frenkel-Kontorova model in one dimension, using Aubry-Mather theory [2–4]. In addition, as a function of the disregistry, a minimizer, if it exists, is smooth as long as the intralayer potential dominates the interlayer coupling; see [2–4] and also [29] for a simplified model. When this condition does not hold, the minimizer can be discontinuous at a dense set of points [2–4,29]. This motivated us to extend the previous framework to include non-smooth displacements. In two dimensions, we are not aware of any proof that minimizers of the twisted bilayer energy necessarily admit such a continuous parameterization, although the assumption is well-motivated given that intralayer lattice bonds are known to be much stronger than interlayer couplings in TBG and other van der Waals 2D heterostructures.

The total mechanical energy of the bilayer is, then, assumed to be decomposable into a monolayer and an interlayer coupling contribution. For the monolayer part, [28] starts with many-body site potentials and then passes directly to the Cauchy–Born approximation, inspired by, e.g., [16,74]. For the interlayer coupling, they utilize a stacking penalization, the *generalized stacking fault energy* (GSFE), see also [36], dependent on a *modulated disregistry*, i.e., on the relaxed local environment. Their modulated disregistry is obtained by projecting an interpolated relaxed position onto the relaxed structure of the other layer, see Fig. 2.

To define the modulated disregistry more precisely, let A_j denote the matrix whose columns are the primitive translation vectors of lattice $\mathcal{R}_j = A_j\mathbb{Z}^2$ describ-

ing layer j (see the beginning of Sect. 2), and let

$$D_{j\to 3-j} := I - A_{3-j}A_j^{-1} \tag{1.1}$$

denote the *disregistry matrix of layer j with respect to layer* $3-j$, see Sect. 2 below for more context. We choose Lagrangian coordinates for the lattice displacements u_j. Then the modulated disregistry chosen in [28] is given by

$$\hat{\mathbf{D}}_{j\to 3-j}(R_j) = D_{j\to 3-j}R_j + u_j(R_j) - u_{3-j}(R_j)\,, \quad R_j \in \mathcal{R}_j\,,$$

see Fig. 2. In particular, since u_{3-j} is not evaluated at a lattice vector of layer $3-j$, the chosen modulated disregistry in [28] only approximates the difference vectors of nearby atoms from different layers; see Sect. 2.3.4 for a more thorough discussion.

In order to pass to a thermodynamic limit, [28] employs an ergodic property for continuous functions of the interlayer disregistry in incommensurate lattices, derived in [21,68] in the context of 2D incommensurate systems—systems with a relative irrational angle, see Assumption 1 below. After they approximate the Cauchy–Born energy by linear elasticity, their resulting model is given by

$$\begin{aligned}\frac{1}{2}\sum_{j=1}^{2}\fint_{\Gamma_{\mathcal{M}}}\mathrm{d}x\,\Big(&Du_j(x):\mathcal{E}_j:Du_j(x)\\&+\Phi_j^{(\mathrm{GSFE})}\big(D_{j\to 3-j}x+u_j(x)-u_{3-j}(x)\big)\Big)\,,\end{aligned} \tag{1.2}$$

where $\Gamma_{\mathcal{M}}$ denotes a moiré unit cell, see (2.12) below, and the GSFE $\Phi_j^{(\mathrm{GSFE})}:\mathbb{R}^2\to\mathbb{R}$ is periodic with respect to to lattice $\mathcal{R}_{3-j}$ of the other layer. Furthermore, we abbreviate by

$$\mathcal{E}_{j,abcd} := \lambda_j\delta_{ab}\delta_{cd} + \mu_j(\delta_{ad}\delta_{bc}+\delta_{ac}\delta_{bd})\,, \tag{1.3}$$

the elasticity tensor where $\lambda_j, \mu_j > 0$ are referred to as *Lamé parameters*. We adjusted the sign-convention in (1.2) to that chosen in the present work.

In applications, the GSFE is obtained via a density functional theory (DFT) approach by minimizing the energy of two untwisted parallel layers at a given xy-shift corresponding to the disregistry, while the system is allowed to relax in the z-direction, see [24,36]. Periodic boundary conditions can then be chosen to account for the lattice periodicity.

The relaxation model obtained in [28] has been very successfully applied to determine the relaxed structure of twisted bilayer systems at small twist angles, see, e.g., [24]. The goal of the present work is to develop a new approach to modeling relaxation of twisted bilayer 2D materials which builds on and refines several aspects of the approach of [28]. In particular, we expect our model to retain accuracy even at relatively large twist angles, and lend itself better to the systematic study of lattice vibrations (phonons), which are known to play a significant role in the electronic properties of many materials.

The first key point of our approach is that we start from an exact, i.e., not interpolated, discrete model for the interlayer energy. More precisely, the interlayer site potentials depend on the *finite difference stencils*

$$\vec{\Delta}_{j\to 3-j}(R_j) = \big(R_j + u_j(R_j) - R_{3-j} - u_{3-j}(R_{3-j})\big)_{R_{3-j}\in\mathcal{R}_{3-j}}$$

of displaced lattice positions, see Fig. 2. This approach allows us to pass to the thermodynamic limit, without first requiring other approximations. Crucially, our approach still relies on the assumption that the lattice displacements depend on the local disregistry. Under this assumption, our model encodes all of the structure of the underlying discrete model, and allows for further approximations at later steps. Passing to the thermodynamic limit with such a penalization requires a more general form of the Birkhoff theorem used in [28]. Since we do not invoke any interpolation or small-angle approximation here, we expect this interlayer energy to retain accuracy for arbitrary twist angles. We additionally generalize [28] in allowing for finitely-many independent sublattice degrees of freedom, and relaxation in the vertical direction, perpendicular to the layers.

Although we emphasize the generality of our approach, it is illuminating to present our configuration-space model under simplifying assumptions. In particular, this allows for comparison between our model and (1.2). Let us assume the interlayer many-body potential is given by an even pair potential v. We ignore sublattice degrees of freedom and lattice shifts, and restrict u_j to take values in $\mathbb{R}^2$, i.e., we ignore out-of-plane relaxation, and assume smooth u_j so that the Cauchy–Born approximation applies. After further approximation by linear elasticity, our model is given by

$$\begin{aligned}\frac{1}{2}\sum_{j=1}^{2}\fint_{\Gamma_{\mathcal{M}}}\mathrm{d}x\; Du_j(x) : \mathcal{E}_j : Du_j(x)\\ + \frac{1}{|\Gamma_{\mathcal{M}}|}\int_{\mathbb{R}^2}\mathrm{d}\xi\; v\big(A_1\xi + u_1(A_1\xi) - A_2\xi - u_2(A_2\xi)\big)\,.\end{aligned} \tag{1.4}$$

For the most general case of monolayer and interlayer coupling energy, we refer to Eqs. (2.25), and (2.29), respectively. We show the difference between the models for a specific choice of GSFE depending on v in Sect. 2.3.4. A crucial benefit of our approach is that it is formulated for the more general case of many-body potentials; another advantage is that our result holds for arbitrary angles, while the result in [28] was derived only in the small-angle limit. We believe that our analysis is extendable to multiple layers as in [28]. In Sect. 2.3.2, we provide some more details on the Cauchy–Born and linear elasticity approximation. We would like to point out that the interlayer term in (1.4) takes into account that all distances between points of different layers are attained.

The next main result is, under additional regularity assumptions on the displacements u_j, an estimate on the convergence rate for passage to the thermodynamic limit. For this, we introduce the notion of *Diophantine 2D rotations*, a two-dimensional analogue of Diophantine numbers, to quantify the incommensurability of twisted 2D bilayer lattices. We show that an ergodic average can be

rewritten in Fourier representation as a weighted sum involving an appropriately rescaled Dirichlet kernel. The leading order term in orders of the truncation corresponds to the limit of the ergodic average. The lower order terms can be bounded by the tail-behavior of the Dirichlet kernel, if we assume an appropriate Diophantine angle condition, defining Diophantine 2D rotations. Our concept of Diophantine 2D rotations extends the ideas developed in [30] in the context of coupled one-dimensional chains. Metric Diophantine approximation theory is a vibrant research area in analytic number theory. We refer to [10,12,59] and references therein for historic reviews, and, e.g., to [13,14,32,50,73] and references therein for more recent results.

The final contribution of the present work is that we prove the existence of a thermodynamic limit for the energy density under least restrictive assumptions. These assumptions ensure integrability in the limit energy density functional. The starting point of our approach is a weaker, namely L^1, parametrization of the atomic displacement functions u_j as functions of their relative position with respect to the moiré unit cell $\Gamma_{\mathcal{M}}$, modulo a moiré lattice shift. To be more precise, we pass to the thermodynamic limit for any (u_1, u_2) such that the limiting site energy is in $L^1(\Gamma_{\mathcal{M}})$, where $\Gamma_{\mathcal{M}}$ is the moiré cell; see Proposition 2.14, and Theorem 2.17. We show that $u_j \in L^\infty(\Gamma_{\mathcal{M}}) \subset L^1(\Gamma_{\mathcal{M}})$ is sufficient for this in Lemma 4.5.

This parametrization is given meaning by embedding the twisted bilayer model within the family of models defined by all possible layer shifts (modulo shifts which leave the bilayer invariant) and applying Birkhoff-type ergodic theorems which hold up to a measure zero set of shifts, see Sect. 2.4 for more details. In particular, this perspective allows us to pass to an almost sure thermodynamic limit without assuming a continuous parametrization of the atomic displacements as in [28].

One of the promising properties of the models presented here and in [28] are that they lend themselves to methods from calculus of variations for continuous systems, even though the underlying system is discrete. As we will discuss below in Sect. 2.3.3, the resulting model is connected to the Allen–Cahn or Ginzburg–Landau energy functional [44,45]. For references on the study of the Allen–Cahn equation, we refer to, e.g., [20,35,46,65,82] and references therein, for the Ginzburg–Landau equations, e.g., to [49,52,78,80] and references therein, and for results on more general semilinear elliptic equations, e.g., to [1,31,39,41,42,53], and references therein.

An interesting question is whether an existence and regularity theory can be developed for the thermodynamic limit energy involving many-body monolayer potentials, before passing to the Cauchy–Born approximation. We do not address this question in the present work, instead developing the existence and regularity theory only for displacements for which the intralayer energy can be simplified using the Cauchy–Born approximation, such as C^2-displacements. After this simplification, the existence and regularity theory are standard, since the Euler–Lagrange equation is, then, elliptic; see, e.g., [28].

We comment on the practical application of our results, especially to the study of lattice vibrations (phonons) in twisted bilayer materials. First, we note that passing to the thermodynamic limit without restricting to smooth or even continuous

displacements u_j should allow us to model more subtle relaxation patterns and vibrations than those which can be described using the Cauchy–Born or linear elasticity approximation. The use of the GSFE in [58] is limited to nearest neighbor interactions and does not include out-of-plane displacement. The phonon dispersion method given in [64] includes longer-ranged interactions in the GSFE and out-of-plane displacements. Our interlayer energy is exact, but it needs approximation since it includes infinite range interactions. A systematic approximation of our interlayer energy can give a method to compute the phonon dispersion with controlled accuracy. Finally, we note that our new interlayer misfit energy has the potential to be highly accurate if implemented with the new generation of machine learned empirical potentials [70,81]. These issues will be the subjects of forthcoming works.

2. Model Description

In order to state our model, we start by introducing standard notation to describe general Bravais lattices, see, e.g., [69]. A 2D Bravais lattice consists of 2 *primitive translation vectors*, as well as a *basis* with associated translation vectors, see Fig. 3. We associate the basis with *sublattice degrees of freedom*.

In the case of hexagonal lattices, the sublattice degrees of freedom refer to an additional atom position given a fixed unit cell. In the case of TMDs, it allows to distinguish between various species of atoms, the metals and chalcogens. Atomic orbitals present another choice of sublattice degrees of freedom. To understand the main ideas, the reader may want to ignore the sublattice degrees of freedom on first reading.

2.1. Notation

2.1.1. Lattices Let $\theta \in \mathbb{R}$, $q > 0$, and $A \in \mathrm{GL}_2(\mathbb{R})$. Define

$$A_1 := q^{-1/2} R_{-\theta/2} A\,, \quad A_2 := q^{1/2} R_{\theta/2} A\,, \quad R_\phi := \begin{pmatrix} \cos\phi & -\sin\phi \\ \sin\phi & \cos\phi \end{pmatrix}. \tag{2.1}$$

Let

$$\mathcal{R}_j := A_j \mathbb{Z}^2\,,\ j \in \{1,2\}, \tag{2.2}$$

denote two crystal layers at a relative twist angle θ and with a relative lattice mismatch q, and abbreviate the respective unit cells

$$\Gamma_j := A_j [0,1)^2\,,\ j \in \{1,2\}\,. \tag{2.3}$$

In addition, denoting $[\![n_1, n_2]\!] := [n_1, n_2] \cap \mathbb{Z}$ whenever $n_1, n_2 \in \mathbb{Z}$, $n_1 \le n_2$, we introduce the truncated lattices

$$\mathcal{R}_j(N) := A_j [\![-N, N]\!]^2\,,\ j \in \{1,2\}\,,\ N \in \mathbb{N}\,. \tag{2.4}$$

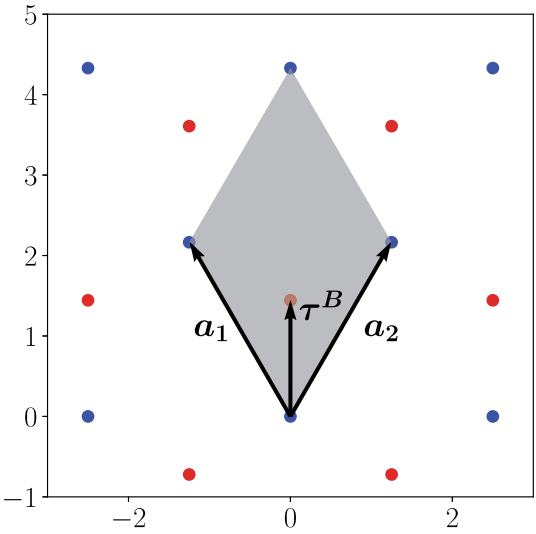

Fig. 3. Hexagonal graphene lattice. a_j refers to the primitive translation vectors, while τ^B is the translation vector for an additional position within a given unit cell. Blue dots refer to the A lattice, while red dots refer to the B lattice

Furthermore, let

$$B_j := 2\pi A_j^{-T}, \ j \in \{1, 2\} \tag{2.5}$$

denote the matrix of reciprocal vectors, and define the reciprocal lattices

$$\mathcal{R}_j^* := B_j \mathbb{Z}^2, \ j \in \{1, 2\}. \tag{2.6}$$

Throughout this work, we let $j \in \{1, 2\}$.

In addition to the lattices $\mathcal{R}_j$, we also introduce the *sublattice degrees of freedom* $\mathcal{A}_j$, $j \in \{1, 2\}$. $\mathcal{A}_j$ is assumed to be a finite set, and to each $\alpha_j \in \mathcal{A}_j$, we assign a unique shift vector $\tau_j^{(\alpha_j)} \in \mathbb{R}^2$, see Fig. 3. Moreover, as an additional degree of freedom, we allow layer j to be shifted by $\gamma_j \in \Gamma_j$. Consequently, the unrelaxed positions of layer j are given by

$$\gamma_j + R_j + \tau_j^{(\alpha_j)}, \ \alpha_j \in \mathcal{A}_j. \tag{2.7}$$

As explained above, the moiré lattice is another important lattice in incommensurate bilayer heterostructures. We will first define this lattice and then explain its importance. The primitive translation vectors for the *moiré frequency lattice* then are given by

$$B_{\mathcal{M}} := B_1 - B_2, \tag{2.8}$$

generating the *moiré frequency lattice*

$$\mathcal{R}_{\mathcal{M}}^* := B_{\mathcal{M}} \mathbb{Z}^2. \tag{2.9}$$

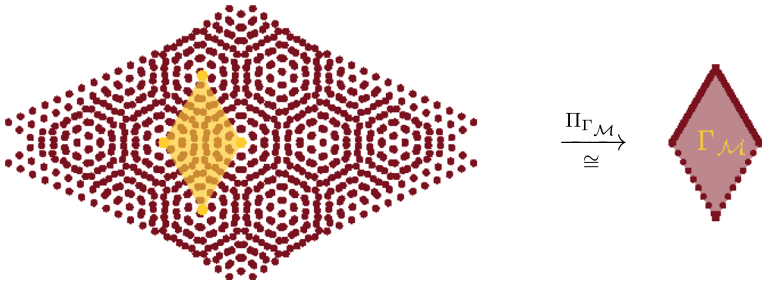

Fig. 4. Twisted bilayer with its moiré lattice highlighted in yellow

The corresponding moiré direct lattice vectors are given by

$$A_{\mathcal{M}} := 2\pi B_{\mathcal{M}}^{-T} = (A_1^{-1} - A_2^{-1})^{-1}. \tag{2.10}$$

Then we define the *moiré lattice*

$$\mathcal{R}_{\mathcal{M}} := A_{\mathcal{M}}\mathbb{Z}^2, \tag{2.11}$$

together with its unit cell

$$\Gamma_{\mathcal{M}} := A_{\mathcal{M}}[0,1)^2. \tag{2.12}$$

We now explain the importance of the moiré lattice. As can be seen in Fig. 4, the moiré lattice is the lattice with respect to which the union of the lattices $\mathcal{R}_1 \cup \mathcal{R}_2$ appears almost periodic. This phenomenon can be explained from two different perspectives.

First, the moiré lattice is the lattice of periodicity for the beating pattern created by superposing plane waves with the periodicity of each layer.

Observe that we have that

$$e^{i(B_1 e_j)\cdot x} = e^{i(B_2 e_j)\cdot x} \text{ for } j = 1,2 \quad \Longleftrightarrow \quad x \in 2\pi(B_1 - B_2)^{-T}\mathbb{Z}^2,$$

and hence constructive interference at the points of the moiré lattice.

Second, we would like to formalize the idea that the local environment is moiré (quasi-)periodic, as can be seen in Fig. 1.

For that, observe that, for a lattice vector $R_1 \in \mathcal{R}_1$ in layer 1, its position relative to the lattice of layer 2 is

$$R_1 \mod \mathcal{R}_2.$$

Equivalently, we can consider the position of R_1 relative to its projection into layer 2

$$(I - A_2 A_1^{-1})R_1 \mod \mathcal{R}_2.$$

This motivates the definition of the disregistry matrices $D_{j\to 3-j}$ introduced in (1.1), given by

$$D_{1\to 2} = I - A_2 A_1^{-1} = -A_2 A_{\mathcal{M}}^{-1}, \quad D_{2\to 1} = I - A_1 A_2^{-1} = A_1 A_{\mathcal{M}}^{-1} \tag{2.13}$$

With these, we define the *local configuration functions*

$$x \mapsto (I - A_2 A_1^{-1})x \mod \mathcal{R}_2\,, \quad x \mapsto (I - A_1 A_2^{-1})x \mod \mathcal{R}_1\,.$$

Due to (2.13), both of these local configuration functions are periodic with respect to the moiré lattice $\mathcal{R}_\mathcal{M}$. This establishes the moiré periodicity for a notion of the local environment.

Notice that there are other descriptions of the local environment which are not moiré-periodic, such as the *disregistries* defined below in (2.15) and (2.17), although these notions are related to moiré-periodic quantities through (2.18).

Lemma 2.1. (Moiré length scale) *For any $x \in \mathbb{R}^2$, we have that*

$$|A_\mathcal{M} x| \,=\, [(q^{1/2} - q^{-1/2})^2 + 4\sin^2(\theta/2)]^{-\frac{1}{2}} |Ax|\,.$$

Similarly, we have for any $k \in \mathbb{R}^2$ that

$$|B_\mathcal{M} k| \,=\, [(q^{1/2} - q^{-1/2})^2 + 4\sin^2(\theta/2)]^{\frac{1}{2}} |2\pi A^{-T} k|\,.$$

For a proof, we refer to Appendix A. Motivated by this lemma, we define the characteristic *moiré length scale ratio* given by

$$\rho_\mathcal{M} \,:=\, [(q - q^{-1})^2 + 4\sin^2(\theta/2)]^{-\frac{1}{2}}\,. \tag{2.14}$$

In order to specify almost periodicity, we impose the following restrictions:

Assumption 1. $(\mathcal{R}_1, \mathcal{R}_2)$ is *incommensurate*, i.e.,

$$G_1 \,+\, G_2 \,=\, 0 \text{ for } G_j \in \mathcal{R}_j^* \quad \text{iff} \quad G_1 = G_2 = 0\,.$$

Assumption 1 has been introduced in [21,68]. In addition, we impose the following condition:

Assumption 2. $(\mathcal{R}_1^*, \mathcal{R}_2^*)$ is incommensurate.

Remark 2.2. Under Assumption 1, it can be readily verified that also $\mathcal{R}_j$ and $\mathcal{R}_\mathcal{M}$ are incommensurate. In fact, let $G_\mathcal{M} = B_\mathcal{M} m \in \mathcal{R}_\mathcal{M}^*$, $m \in \mathbb{Z}^2$, and $G_1 = B_1 n \in \mathcal{R}_1^*$, $n \in \mathbb{Z}^2$. Then we have that

$$G_\mathcal{M} \,+\, G_1 \,=\, B_1(m+n) \,-\, B_2 n \,=\, 0$$

iff $m = n = 0$, see (2.8). Analogously, $(\mathcal{R}_1^*, \mathcal{R}_2^*)$ being incommensurate implies that $(\mathcal{R}_j^*, \mathcal{R}_\mathcal{M}^*)$, $j = 1, 2$ is incommensurate.

A straight-forward calculation yields the following result:

Lemma 2.3. *We have that $(\mathcal{R}_1, \mathcal{R}_2)$ is incommensurate iff $(q, \theta) \in \mathbb{R}^+ \times [0, 2\pi)$ satisfy*

$$q A^T R_\theta A^{-T} \mathbb{Z}^2 \cap \mathbb{Z}^2 \,=\, \{0\}\,.$$

As a consequence of Assumption 2, the relative positions of $\mathcal{R}_j$ with respect to the moiré lattice never repeat. We want to use this assumption to define a continuous extension of the displacement functions, defined on the (discrete) lattice $\gamma_j + \mathcal{R}_j$, and corresponding energies. In particular, we use Assumption 2 to relabel lattice positions by their relative position within a translate of a moiré unit cell.

To this end, we define for $x \in \mathbb{R}^2$

$$\{x\}_{\mathcal{M}} := \sum_{R_{\mathcal{M}} \in \mathcal{R}_{\mathcal{M}}} (x - R_{\mathcal{M}}) \mathbb{1}_{\Gamma_{\mathcal{M}}}(x - R_{\mathcal{M}}) \, (= x \mod \mathcal{R}_{\mathcal{M}}) \,, \tag{2.15}$$

and

$$\lfloor x \rfloor_{\mathcal{M}} := x - \{x\}_{\mathcal{M}} \,. \tag{2.16}$$

Observe that

$$\mathbb{1}_{\Gamma_{\mathcal{M}}}(x - R_{\mathcal{M}}) = 0 \quad \Leftrightarrow \quad x \in \Gamma_{\mathcal{M}} + R_{\mathcal{M}} \,.$$

Analogously, we define the decomposition with respect to the lattices $\mathcal{R}_j$

$$x = \lfloor x \rfloor_j + \{x\}_j \tag{2.17}$$

with $\lfloor x \rfloor_j \in \mathcal{R}_j$, $\{x\}_j \in \Gamma_j$. An analogous notation has already been used in [21]. We call $\{\cdot\}_{\mathcal{M}}$ the *(local) disregistry* with respect to $\mathcal{R}_{\mathcal{M}}$ and $\{\cdot\}_j$ the *(local) disregistry* with respect to $\mathcal{R}_j$.

The quasi-moiré-periodicity of the local disregistry can also be understood by virtue of Lemma 4.2, for we have that

$$\{R_1\}_2 = D_{1\to 2}\{R_1\}_{\mathcal{M}} + A_2 \begin{pmatrix} 1 \\ 1 \end{pmatrix}, \quad \{R_2\}_1 = D_{2\to 1}\{R_2\}_{\mathcal{M}} \,. \tag{2.18}$$

Exact periodicity would mean that similar formulas relating the moiré disregistry and the individual layer disregistry would hold for general $x \in \mathbb{R}^2$ instead of lattice points R_j. However, in Remark 4.3, we prove that there exists no such affine transformation. In the incommensurate case, there is only quasi-periodicity. However, in case of *commensurate* layers, the local disregistry is periodic with respect to a lattice which is a subset of the moiré lattice $\mathcal{R}_{\mathcal{M}}$. Note that in the commensurate case, methods for periodic systems, such as Bloch-Floquet theory, become available. For this reason, and since the commensurate case is in any case not generic, see Proposition 2.5, we ignore this case in the present work.

As a consequence of incommensurability of $(\mathcal{R}_1^*, \mathcal{R}_2^*)$ and $(\mathcal{R}_j^*, \mathcal{R}_{\mathcal{M}}^*)$, respectively, both

$$\Pi_{\Gamma_{3-j}} : \mathcal{R}_j + \gamma_j \to \Gamma_{3-j} \,, \quad R_j + \gamma_j \mapsto \left\{R_j + \gamma_j\right\}_{3-j} \,,$$
$$\Pi_{\Gamma_{\mathcal{M}}} : \mathcal{R}_j + \gamma_j \to \Gamma_{\mathcal{M}} \,, \quad R_j + \gamma_j \mapsto \left\{R_j + \gamma_j\right\}_{\mathcal{M}} \,,$$

are one-to-one, $j = 1, 2$. For a discussion of this bijection, we refer, e.g., to [67]. We call both, $\Pi_{\Gamma_{3-j}}$ and $\Pi_{\Gamma_{\mathcal{M}}}$, *configuration space projections*, see also Fig. 4.

Before continuing, we briefly want to comment why we can simultaneously choose $(\mathcal{R}_1, \mathcal{R}_2)$ *and* $(\mathcal{R}_1^*, \mathcal{R}_2^*)$ to be incommensurate. For that, we introduce the notion of *Diophantine* $2D$*-rotations*, that corresponds to a quantified version of incommensurability.

Definition 2.4. Given $q > 0$, we call $\theta \in \mathbb{R}$ a (q, K, σ)-*Diophantine 2D rotation* iff $K > 0, \sigma > 0$, and, for all $n \in \mathbb{Z}^2 \setminus \{0\}$,

$$\operatorname{dist}\left(q^{\pm 1} A^T R_{\pm\theta} A^{-T} n, \mathbb{Z}^2\right) \geq \frac{K}{|n|^{2\sigma}} . \tag{2.19}$$

This notion of Diophantine 2D rotations is exactly the condition that allows us to quantify the error in the ergodic approximation, see Proposition 3.5 below. As in the case of Diophantine numbers, we have that Diophantine 2D rotations are generic.

Proposition 2.5. *For all $q > 0$, $\sigma > \frac{1433}{1248} \approx 1.1482$ and for Lebesgue-almost all $\theta \in \mathbb{R}$ there exists $K > 0$ s.t. θ is a (q, K, σ)-Diophantine 2D rotation.*

Since almost every angle θ is a Diophantine 2D rotation, the corresponding lattice $(\mathcal{R}_1, \mathcal{R}_2)$ is incommensurate. By applying the same argument to the reciprocal lattices, we also have that for almost every θ, $(\mathcal{R}_1^*, \mathcal{R}_2^*)$ is incommensurate. In particular, for (Lebesgue-)almost every θ, both, $(\mathcal{R}_1, \mathcal{R}_2)$ and $(\mathcal{R}_1^*, \mathcal{R}_2^*)$, are incommensurate.

As the classical results for the one-dimensional case, our proof of Proposition 2.5, see Appendix B, relies on the Borel-Cantelli Lemma.

As usual, the absolute value function $|\cdot|$ will have a context-dependent meaning. For finite sets M, $|M|$ denotes the cardinality of M, for bounded measurable sets $\Omega \subseteq \mathbb{R}^n$, $|\Omega|$ denotes the respective Lebesgue measure, and for $x \in \mathbb{R}^n$, $|x|$ denotes the Euclidean norm.

Remark 2.6. Bourgain-Watt [18] proposed the bound

$$|B_r \cap \mathbb{Z}^2| = \pi r^2 + O_{r\to\infty}\left(r^{\frac{517}{824}+\varepsilon}\right)$$

for any $\varepsilon > 0$, where $\frac{517}{824} \approx 0.6274$, compared to $\frac{131}{208} \approx 0.6298$ in B in the proof of Proposition 2.5. In particular, this would allow us to lower the lower bound of σ to $\frac{5671}{4944} \approx 1.1471$ compared to $\frac{1433}{1248} \approx 1.1482$ above.

The general lattice problem is a very active research area. For related works, we refer to [17,19,43,48] and references therein.

2.1.2. Energies As described in the introduction, we assume that the lattice displacements u_j are periodic functions of their respective disregistry. Since we assume that $(\mathcal{R}_1, \mathcal{R}_2)$ is incommensurate, this is equivalent to parametrizing u_j as moiré-periodic functions instead. For simplicity, we assume that $u_j \in C_{\text{per}}(\Gamma_{\mathcal{M}}; (\mathbb{R}^3)^{\mathcal{A}_j})$, s.t. the total lattice positions are given by

$$Y_j(\gamma_j + R_j, \alpha_j) := \gamma_j + R_j + \tau_j^{(\alpha_j)} + u_j\left(\left\{\gamma_j + R_j\right\}_{\mathcal{M}}, \alpha_j\right) . \tag{2.20}$$

Here, we identified the $\mathbb{R}^2$-valued points R_j, γ_j, $\tau_j^{(\alpha_j)}$ with their respective $\mathbb{R}^3$-embeddings $(R_j, 0)$ resp. $(\gamma_j, 0)$ resp. $(\tau_j^{(\alpha_j)}, 0)$. We allow the lattice displacement u_j to take values in $\mathbb{R}^3$, in order to account for relaxation in z-direction.

By identifying u_j with its periodic extension to $\mathbb{R}^2$, we also define the generalized total lattice positions

$$Y_j(x, \alpha_j) := x + \tau_j^{(\alpha_j)} + u_j(x, \alpha_j), \quad (x, \alpha_j) \in \mathbb{R}^2 \times \mathcal{A}_j. \tag{2.21}$$

Throughout this work, we abbreviate

$$\mathbf{u} = (u_1, u_2), \quad \boldsymbol{\gamma} = (\gamma_1, \gamma_2) \in \Gamma_1 \times \Gamma_2, \quad \boldsymbol{\alpha} = (\alpha_1, \alpha_2) \in \mathcal{A}_1 \times \mathcal{A}_2. \tag{2.22}$$

As stated above, we assume that the total energy of the coupled bilayer system can be decomposed into a monolayer and interlayer contribution. For each, we assume that they can be expressed via sums over site-energies over the individual layers. We assume that these site-energies depend on the finite difference stencils originating at the respective site, as well as the sublattice degree type.

We will now present the monolayer and interlayer energy densities, and explain how their thermodynamic limits can be obtained via ergodic theorems. Here, we state our results in a general context that only requires the existence of the limiting energy functional, in order to state results that hold both, in the cases of smooth and non-smooth displacements. In the case of smooth displacements and for lattice shifts $\gamma_j = 0$, we even establish a rate of convergence, see Sect. 2.2. We postpone a discussion of the non-smooth case to Sect. 2.4.

We present our results in terms of many-body potentials dependent on finite difference stencils, which yield a more accurate description of materials than just interatomic pair potentials, such as Kolmogorov-Crespi [57]. However, to better illustrate our ideas, we decided to also include the case of interlayer pair potentials.

Monolayer potential Let

$$V_{j,\alpha_j}^{(\mathrm{mono})} : (\mathbb{R}^3)^{\mathcal{R}_j \times \mathcal{A}_j} \to \mathbb{R}$$

with $\alpha_j \in \mathcal{A}_j$ be given. We assume that $V_{j,\alpha_j}^{(\mathrm{mono})}$ only depends on the finite (relative) difference stencils

$$\big(u_j(R_j + \gamma_j + R_j', \alpha_j') - u_j(R_j + \gamma_j, \alpha_j)\big)_{R_j' \in \mathcal{R}_j, \alpha_j' \in \mathcal{A}_j}.$$

The reason, for which we may consider dependence only on relative difference stencils for the monolayer potential, is that the index R_j' encodes a distance between the evaluation points in the finite differences; this distance is independent of the reference point $R_j + \gamma_j$.

Example 2.7. (Monolayer pair potentials) In order to illustrate the needed decay assumptions, we may consider pair potentials w_j. For simplicity, let us reduce to a single sublattice degree of freedom and ignore lattice shifts. Then the model many-body site potential takes the form

$$R_j \mapsto \sum_{R_j' \in \mathcal{R}_j \setminus \{0\}} \big(w_j\big(R_j' + u_j(R_j + R_j') - u_j(R_j)\big) - w_j(R_j')\big).$$

For this reason, one needs to assume a decay assumption in R'_j in the case of monolayer potentials. Below, we will state assumptions on the site potentials

$$R_j \mapsto V^{(\mathrm{mono})}_{j,\alpha_j}\Big(\big(u_j(R_j+\gamma_j+R'_j,\alpha'_j)-u_j(R_j+\gamma_j,\alpha_j)\big)_{R'_j\in\mathcal{R}_j,\alpha'_j\in\mathcal{A}_j}\Big)$$

that allow us to pass to a thermodynamic limit. For clarity, we omit sufficient assumptions on $V^{(\mathrm{mono})}_{j,\alpha_j}$ and u_j individually which would imply our assumptions on the site potentials; these could be obtained by adapting the ideas of, e.g., [16,74].

For $\gamma_j \in \Gamma_j$, we introduce the monolayer energy density

$$\begin{aligned} e^{(\mathrm{mono})}_{j,N,\gamma_j}(u_j) &:= \frac{1}{|\Gamma_j|(2N+1)^2}\sum_{\alpha_j\in\mathcal{A}_j}\sum_{R_j\in\mathcal{R}_j(N)} \\ &V^{(\mathrm{mono})}_{j,\alpha_j}\Big(\big(u_j(R_j+\gamma_j+R'_j,\alpha'_j)\,-\,u_j(R_j+\gamma_j,\alpha_j)\big)_{(R'_j,\alpha'_j)\in\mathcal{R}_j\times\mathcal{A}_j}\Big), \end{aligned} \tag{2.23}$$

where

$$|A_j[-N-1/2,N+1/2]^2| \,=\, |\Gamma_j|(2N+1)^2$$

is the area of the corresponding truncated region covered by the nuclei in layer j.

Observe that, since we defined u_j as $\mathcal{R}_{\mathcal{M}}$-periodic extensions,

$$\begin{aligned} &\Phi^{(\mathrm{mono})}_j[u_j](x) \\ &:= \frac{1}{|\Gamma_j|}\sum_{\alpha_j\in\mathcal{A}_j} V^{(\mathrm{mono})}_{j,\alpha_j}\left(\Big(u_j(x+R'_j,\alpha'_j)\,-\,u_j(x,\alpha_j)\Big)_{\substack{R'_j\in\mathcal{R}_j,\\ \alpha'_j\in\mathcal{A}_j}}\right) \end{aligned} \tag{2.24}$$

is $\mathcal{R}_{\mathcal{M}}$-periodic. If $R_j\in\mathcal{R}_j, \gamma_j\in\Gamma_j$, $\Phi^{(\mathrm{mono})}_j[u_j](R_j+\gamma_j)$ denotes the sublattice-averaged site-potential experienced at $R_j+\gamma_j$. In particular, (2.23) becomes

$$e^{(\mathrm{mono})}_{j,N,\gamma_j}(u_j) \,=\, \frac{1}{(2N+1)^2}\sum_{R_j\in\mathcal{R}_j(N)}\Phi^{(\mathrm{mono})}_j[u_j]\big(\{R_j+\gamma_j\}_{\mathcal{M}}\big)\,.$$

Then, the ergodic theorem Proposition 2.14 implies, after substituting $x\mapsto A_j x$, that the thermodynamic limit of the monolayer energy is given by

$$\begin{aligned} &e^{(\mathrm{mono})}_j(u_j) \\ &:= \frac{1}{|\Gamma_j|}\sum_{\alpha_j\in\mathcal{A}_j}\fint_{A_j^{-1}\Gamma_{\mathcal{M}}}\mathrm{d}\xi\; V^{(\mathrm{mono})}_{j,\alpha_j}\left(\Big(u_j(A_j\xi+R'_j,\alpha'_j)\,-\,u_j(A_j\xi,\alpha_j)\Big)_{\substack{R'_j\in\mathcal{R}_j,\\ \alpha'_j\in\mathcal{A}_j}}\right) \\ &= \fint_{\Gamma_{\mathcal{M}}}\mathrm{d}x\;\Phi^{(\mathrm{mono})}_j[u_j](x)\,, \end{aligned} \tag{2.25}$$

where $\fint_\Omega = \frac{1}{|\Omega|}\int_\Omega$ denotes the averaging integral over Ω. This result is given in Theorem 2.10.

Interlayer coupling

Definition 2.8. A function

$$V \,:\, (\mathbb{R}^3)^{\mathcal{R}_j \times \mathcal{A}_j} \to \mathbb{R}$$

is *translation-invariant* iff for any $(a_{R_j,\alpha_j})_{(R_j,\alpha_j)\in\mathcal{R}_j\times\mathcal{A}_j} \in (\mathbb{R}^3)^{\mathcal{R}_j\times\mathcal{A}_j}$ and any $R_j' \in \mathcal{R}_j$, we have that

$$V\big((a_{R_j+R_j',\alpha_j})_{(R_j,\alpha_j)\in\mathcal{R}_j\times\mathcal{A}_j}\big) \,=\, V\big((a_{R_j,\alpha_j})_{(R_j,\alpha_j)\in\mathcal{R}_j\times\mathcal{A}_j}\big)\,.$$

In addition, V is *even* iff $V(x) = V(-x)$.

Let

$$V^{(\mathrm{inter})}_{j,\alpha_j} \,:\, (\mathbb{R}^3)^{\mathcal{R}_{3-j}\times\mathcal{A}_{3-j}} \to \mathbb{R}\,,$$

with $\alpha_j \in \mathcal{A}_j$ be even and translation-invariant. As a special instance, let $v_{\boldsymbol{\alpha}} : \mathbb{R}^3 \to \mathbb{R}$, with $\alpha_k \in \mathcal{A}_k$, $k = 1, 2$, $\boldsymbol{\alpha} = (\alpha_1, \alpha_2)$, denote an even pair potential, and consider

$$V^{(\mathrm{inter})}_{j,\alpha_j}\left((a_{R_{3-j},\alpha_{3-j}})_{\substack{R_{3-j}\in\mathcal{R}_{3-j},\\ \alpha_{3-j}\in\mathcal{A}_{3-j}}}\right) \,=\, \frac{1}{2}\sum_{\substack{R_{3-j}\in\mathcal{R}_{3-j}\\ \alpha_{3-j}\in\mathcal{A}_{3-j}}} v_{\boldsymbol{\alpha}}(a_{R_{3-j},\alpha_{3-j}})\,. \tag{2.26}$$

Such interatomic pair potentials $v_{\boldsymbol{\alpha}}$ have been constructed using DFT, e.g., in [62, 66, 79].

The fact that we are using the ordered index $\boldsymbol{\alpha} = (\alpha_1, \alpha_2)$ to label pair potentials, as opposed to, e.g., (α_j, α_{3-j}), is to indicate that pair interactions only depend on the pair of involved atoms, as opposed to the order of the pair. Whenever there is a α_j or α_{3-j} on the LHS of an equation, and α_1 or α_2 on the RHS, the corresponding equation is to be read individually for $j = 1$ or $j = 2$, to avoid confusion.

We assume that $V^{(\mathrm{inter})}_{j,\alpha_j}$ depends on the finite (total) difference stencils

$$\big(Y_j(R_j + \gamma_j, \alpha_j) - Y_{3-j}(R_{3-j} + \gamma_{3-j}, \alpha_{3-j})\big)_{R_{3-j}\in\mathcal{R}_{3-j},\alpha_{3-j}\in\mathcal{A}_{3-j}}\,.$$

In the case of the interlayer potential, the distance between the evaluation points does depend on the reference point $R_j + \gamma_j$, or its disregistry, respectively.

Example 2.9. (Interlayer pair potentials) For simplicity we can again consider the special case of pair potentials. Let us again restrict to a single sublattice degree of freedom, and assume $\gamma_j = 0$. Then the interlayer site-potential is given by

$$\begin{aligned} R_j \mapsto & \sum_{R_{3-j}\in\mathcal{R}_{3-j}} v\big(R_{3-j} + u_{3-j}(R_{3-j}) - R_j - u_j(R_j)\big) \\ = & \sum_{R_{3-j}\in\mathcal{R}_{3-j}} v\big(R_{3-j} - \big\{R_j\big\}_{3-j} + u_{3-j}(R_j + R_{3-j} - \big\{R_j\big\}_{3-j}) - u_j(R_j)\big)\,, \end{aligned}$$

where we recall (2.17). In contrast to monolayer potentials, we now have to correct the positions by their local disregistry. For a generalization of this idea to many-body potentials, we refer to Lemma 4.4. Here one could also, analogously to Example 2.7, subtract the constant contribution $\sum_{R_{3-j}\in\mathcal{R}_{3-j}} v(R_{3-j} - R_j)$. Since it does not affect our results, we chose not to include it.

Consequently, we need to impose a decay assumption which is based on the magnitude of the total distance $Y_j(x) - Y_{3-j}(y)$ in the argument. We prove the existence of a thermodynamic limit based on regularity of the site potentials

$$R_j \mapsto V^{(\mathrm{inter})}_{j,\alpha_j}\Big(\big(Y_j(R_j+\gamma_j,\alpha_j) - Y_{3-j}(R_{3-j}+\gamma_{3-j},\alpha_{3-j})\big)_{R_{3-j}\in\mathcal{R}_{3-j},\alpha_{3-j}\in\mathcal{A}_{3-j}}\Big).$$

Again, we expect that this regularity would follow from appropriate assumptions on $V^{(\mathrm{inter})}_{j,\alpha_j}$ and u_j along the lines of [16,74].

Recalling (2.21), define the interlayer coupling energy density of the j-th layer

$$\begin{aligned} e^{(\mathrm{inter})}_{j,N,\boldsymbol{\gamma}}(\mathbf{u}) := \frac{1}{|\Gamma_j|(2N+1)^2} \sum_{R_j\in\mathcal{R}_j(N)} \sum_{\alpha_j\in\mathcal{A}_j} V^{(\mathrm{inter})}_{j,\alpha_j}\Big(\big(Y_j(R_j+\gamma_j,\alpha_j) \\ - Y_{3-j}(R_{3-j}+\gamma_{3-j},\alpha_{3-j})\big)_{\substack{R_{3-j}\in\mathcal{R}_{3-j},\\ \alpha_{3-j}\in\mathcal{A}_{3-j}}}\Big). \end{aligned} \tag{2.27}$$

We would like to study the thermodynamic limit of the energy density (2.27) by employing an appropriate ergodic theorem. Such an ergodic theorem lets us map a functional defined on the discrete systems $\mathcal{R}_j$ to a functional defined on the continuous system $\Gamma_{\mathcal{M}}$, via the configuration space isomorphism $\Pi_{\Gamma_{\mathcal{M}}}$. As a useful tool to map in between unit cells of the involved lattices, we recall from (1.1), see also (2.13), the disregistry matrices:

$$D_{1\to 2} = I - A_2A_1^{-1} = -A_2A_{\mathcal{M}}^{-1}, \quad D_{2\to 1} = I - A_1A_2^{-1} = A_1A_{\mathcal{M}}^{-1}.$$

In particular, we have that

$$D_{j\to 3-j}\Gamma_{\mathcal{M}} = (-1)^j\Gamma_{3-j}.$$

The disregistry matrices $D_{j\to 3-j}$ have the crucial property that they map between the different notions of configurations if restricted to the individual non-shifted lattices, see Lemma 4.2.

As above, we define the sublattice-averaged generalized interlayer site potentials

$$\begin{aligned} &\Psi^{(\mathrm{inter})}_j[\mathbf{u}](x,y) \\ &:= \frac{1}{|\Gamma_j|}\sum_{\alpha_j\in\mathcal{A}_j} V^{(\mathrm{inter})}_{j,\alpha_j}\Big(\big(y - R_{3-j} + \tau_j^{(\alpha_j)} - \tau_{3-j}^{(\alpha_{3-j})} + u_j(x,\alpha_j) \\ &\quad - u_{3-j}(x-y+R_{3-j},\alpha_{3-j})\big)_{\substack{R_{3-j}\in\mathcal{R}_{3-j},\\ \alpha_{3-j}\in\mathcal{A}_{3-j}}}\Big) \end{aligned} \tag{2.28}$$

for all $x, y \in \mathbb{R}^2$. Employing Lemma 4.4, we obtain that

$$e^{(\mathrm{inter})}_{j,N,\boldsymbol{\gamma}}(\mathbf{u}) = \frac{1}{(2N+1)^2} \sum_{R_j \in \mathcal{R}_j(N)} \Psi^{(\mathrm{inter})}_j[\mathbf{u}]\left(\left\{R_j + \gamma_j\right\}_{\mathcal{M}}, \left\{R_j + \gamma_j - \gamma_{3-j}\right\}_{3-j}\right).$$

Observe that, due to the $\mathcal{R}_{\mathcal{M}}$-periodic extension of u_j and due to the dependence on the collection of all lattice shifts with respect to $\mathcal{R}_{3-j}$, $\Psi^{(\mathrm{inter})}_j[u]$ is $\mathcal{R}_{\mathcal{M}} \times \mathcal{R}_{3-j}$-periodic.

Here, we prove a mean ergodic theorem, Proposition 3.3: Let $h \in L^1_{loc}(\mathbb{R}^4)$ be $\mathcal{R}_{\mathcal{M}} \times \mathcal{R}_{3-j}$-periodic.

Recalling (2.18), we then show that

$$\begin{aligned}
&\frac{1}{(2N+1)^2} \sum_{R_j \in \mathcal{R}_{j(N)}} h\left(\left\{R_j + \omega_{\mathcal{M}}\right\}_{\mathcal{M}}, \left\{R_j + \omega_{3-j}\right\}_{3-j}\right) \\
&\xrightarrow{N\to\infty} \fint_{\Gamma_{\mathcal{M}}} \mathrm{d}x\, h\left(x, D_{j\to 3-j}x + A_{3-j}A_j^{-1}\omega_{\mathcal{M}} - \omega_{3-j}\right) \\
&= \fint_{A_j^{-1}\Gamma_{\mathcal{M}}} \mathrm{d}\xi\, h\big(A_j\xi + \omega_{\mathcal{M}}, (A_j - A_{3-j})\xi + \omega_{3-j}\big)
\end{aligned}$$

converges for almost all $(\omega_{\mathcal{M}}, \omega_{3-j}) \in \Gamma_{\mathcal{M}} \times \Gamma_{3-j}$ and also in $L^1(\Gamma_{\mathcal{M}} \times \Gamma_{3-j})$. Both, this result and also the previously mentioned ergodic theorem Prop. 2.14, are special instances of a more general ergodic theorem for group actions, as can be found, e.g., in [37,54,56], see also Proposition 3.1. These ideas have been previously applied to incommensurate multilayer structures, see [69, Theorem 2.1], [21, Proposition 3.5].

We then obtain in Theorem 2.17 that, in the thermodynamic limit $N \to \infty$, the interlayer coupling potential converges to

$$\begin{aligned}
e^{(\mathrm{inter})}_{j,\boldsymbol{\gamma}}(\mathbf{u}) &:= \frac{1}{|\Gamma_j|} \sum_{\alpha_j \in \mathcal{A}_j} \fint_{A_j^{-1}\Gamma_{\mathcal{M}}} \mathrm{d}\xi\, V^{(\mathrm{inter})}_{j,\alpha_j}\Big(\big(Y_j(A_j\xi + \gamma_j, \alpha_j) \\
&\qquad - Y_{3-j}(A_{3-j}\xi + \gamma_{3-j} + R_{3-j}, \alpha_{3-j})\big)_{\substack{R_{3-j}\in\mathcal{R}_{3-j},\\ \alpha_{3-j}\in\mathcal{A}_{3-j}}}\Big) \qquad (2.29)\\
&= \fint_{\Gamma_{\mathcal{M}}} \mathrm{d}x\, \Phi^{(\mathrm{inter})}_{j,\boldsymbol{\gamma}}[\mathbf{u}](x),
\end{aligned}$$

where

$$\Phi^{(\mathrm{inter})}_{j,\boldsymbol{\gamma}}[\mathbf{u}](x) := \Psi^{(\mathrm{inter})}_j[\mathbf{u}](x, D_{j\to 3-j}x + A_{3-j}A_j^{-1}\gamma_j - \gamma_{3-j}). \qquad (2.30)$$

Lemma 4.6 yields in the special case of even pair potentials $v_{\boldsymbol{\alpha}}$ that

$$\begin{aligned}
e^{(\mathrm{inter})}_{j,\boldsymbol{\gamma}}(\mathbf{u}) &= \frac{1}{2|\Gamma_{\mathcal{M}}|} \sum_{\substack{\alpha_k\in\mathcal{A}_k\\ k=1,2}} \int_{\mathbb{R}^2} \mathrm{d}\xi\, v_{\boldsymbol{\alpha}}\big(A_1\xi + \gamma_1 + \tau_1^{(\alpha_1)} + u_1(A_1\xi + \gamma_1, \alpha_1) \\
&\qquad - A_2\xi - \gamma_2 - \tau_2^{(\alpha_2)} - u_2(A_2\xi + \gamma_2, \alpha_2)\big).
\end{aligned}$$

2.2. Results for Smooth Displacements

We now present our main result for the case of smooth displacements under some simplifying assumptions. Under these assumptions, our notion of Diophantine 2D rotations, recall Definition 2.4, allows us to establish a rate of convergence to the thermodynamic limit of the atomistic energy density. We emphasize that, even in this setting, our limiting energy functional appears to be novel.

We start by assuming that $\gamma_1 = \gamma_2 = 0$, and we abbreviate

$$\begin{aligned} \Phi_j^{(\mathrm{inter})} &:= \Phi_{j,\mathbf{0}}^{(\mathrm{inter})}, \quad e_{j,N}^{(\mathrm{inter})} := e_{j,N,\mathbf{0}}^{(\mathrm{inter})}, \\ e_j^{(\mathrm{inter})} &:= e_{j,\mathbf{0}}^{(\mathrm{inter})}, \quad e_{j,N}^{(\mathrm{mono})} := e_{j,N,0}^{(\mathrm{mono})}. \end{aligned}$$

We denote that

$$d_{\mathcal{A}_1,\mathcal{A}_2} := \max_{\substack{\alpha_\ell \in \mathcal{A}_\ell \\ \ell=1,2}} |\tau_1^{(\alpha_1)} - \tau_2^{(\alpha_2)}|, \tag{2.31}$$

and for $\mathbf{u} = (u_1, u_2) \in L^\infty(\mathbb{R}^2; \mathbb{R}^6)$, with components $u_{j,k}$, $j = 1, 2$, $k \in \{x, y, z\}$,

$$L_{\mathbf{u}}^z := d_{\mathcal{A}_1,\mathcal{A}_2} + \|u_{1,z}\|_\infty + \|u_{2,z}\|_\infty. \tag{2.32}$$

Moreover, let

$$\langle x \rangle := (1 + |x|^2)^{\frac{1}{2}}$$

for any $x \in \mathbb{R}^n$, $n \in \mathbb{N}$. For $k, n \in \mathbb{N}$ and $s > 0$ and a Lipschitz domain $\Omega \subseteq \mathbb{R}^n$, let

$$\|f\|_{W_s^{k,\infty}(\Omega)} := \sum_{j=0}^{k} \|\langle\cdot\rangle^s D^j f\|_{L^\infty(\Omega)} \tag{2.33}$$

denote the weighted Sobolev norm, and let

$$W_s^{k,\infty}(\Omega) := \{f \in W^{k,\infty}(\Omega) \mid \|f\|_{W_s^{k,\infty}(\Omega)} < \infty\} \tag{2.34}$$

denote the associated weighted Sobolev space. In addition, let

$$L_s^\infty(\Omega) := \{f \in L^\infty(\Omega) \mid \|\langle\cdot\rangle^s f\|_{L^\infty(\Omega)} < \infty\}$$

denote the weighted Lebesgue space.

For $f \in L^1(\Gamma_\mathcal{M})$ and $G_\mathcal{M} \in \mathcal{R}_\mathcal{M}^*$, we define the Fourier transform

$$\hat{f}(G_\mathcal{M}) := \mathcal{F}_{\Gamma_\mathcal{M}}(f)(G_\mathcal{M}) := \fint_{\Gamma_\mathcal{M}} \mathrm{d}x \, e^{-iG_\mathcal{M}\cdot x} f(x). \tag{2.35}$$

The next result is our main result in the case of smooth displacements.

Theorem 2.10. *Let $s > 1$, $\sigma > \frac{1433}{1248}$, and $\theta \in [0, 2\pi)$ be a (q, K, σ)-Diophantine 2D rotation for some $K > 0$. Let $\ell \in \{\text{mono}, \text{inter}\}$ and $j \in \{1, 2\}$. Assume that*

$$\Phi_j^{(\ell)}[u_j] \in L^1(\Gamma_{\mathcal{M}}) \,, \ \mathcal{F}_{\Gamma_{\mathcal{M}}}\big(|\nabla|^{2(\sigma+s)}\Phi_j^{(\ell)}[u_j]\big) \in \ell^\infty(\mathcal{R}_{\mathcal{M}}^*) \,.$$

In particular, if we assume pair interlayer potentials, assume that for $k = 1, 2$, $\alpha_k \in \mathcal{A}_k$, $u_k(\cdot, \alpha_k) \in W^{6,\infty}(\mathbb{R}^2)$, and that, see (2.34),

$$v_{\boldsymbol{\alpha}} \in W_{2r}^{6,\infty}(\mathbb{R}^2 \times [-L_{\mathbf{u}}^z, L_{\mathbf{u}}^z]) \,.$$

Then there exists a constant $C > 0$ such that

$$\big|e_{j,N}^{(\ell)} - e_j^{(\ell)}\big| \ \leq \ \frac{C}{2N+1} \,.$$

In the case of many-body potentials, this theorem is a consequence of the quantitative ergodic theorem, Proposition 3.5. The proof that the conditions in the case of interlayer pair potentials are sufficient, is contained in Sect. 4.3.

Remark 2.11. We provide bounds on the constants $C > 0$ that are explicit, except for the implicit dependence of the Diophantine constant $K > 0$ on the chosen angle θ and the decay σ. In the case of many-body potentials, we obtain

$$\begin{aligned} &\frac{2\sqrt{2}}{K}\Big(\frac{\rho_{\mathcal{M}}\|A\|_2}{2\pi}\Big)^{2(\sigma+s)}\big(\zeta(2s) + 2^{-s}\zeta(s)^2\big) \\ &\quad \sup_{G_{\mathcal{M}} \in \mathcal{R}_{\mathcal{M}}^*} |G_{\mathcal{M}}|^{2(\sigma+s)} |\mathcal{F}_{\Gamma_{\mathcal{M}}}(\Phi_j^{(\ell)}[u_j])(G_{\mathcal{M}})| \,, \end{aligned} \tag{2.36}$$

where $\zeta(\sigma)$ denotes the Riemann zeta function, and we recall $\rho_{\mathcal{M}}$ from (2.14). Now abbreviate

$$\kappa^{(\text{pair})}(\theta, \sigma) \ := \sup\Bigg(\bigcup_{N \in \mathbb{N}} \bigcap_{\substack{n \in \mathbb{Z}^2: \\ |n|^2 \geq N}} \bigg\{ K > 0 \mid \operatorname{dist}\big(A^T R_{\pm\theta} A^{-T} n, \mathbb{Z}^2\big) \geq \frac{K}{|n|^{2\sigma}} \bigg\} \Bigg) ,$$

and define

$$M^{(\text{pair})}(\theta) \ := \inf_{\sigma \in \left(\frac{1433}{1248}, 2\right)} \frac{1}{\kappa^{(\text{pair})}(\theta, \sigma)} \big(\zeta(6 - 2\sigma) + 2^{\sigma-3}\zeta(3 - \sigma)^2\big) \,. \tag{2.37}$$

Then an upper bound on the constant $C > 0$ in the case of interlayer pair potentials is given by

$$\begin{aligned} &\frac{203\sqrt{2}}{|\Gamma_1||\Gamma_2|}\Big(\frac{\rho_{\mathcal{M}}\|A\|_2}{2\pi}\Big)^6 M^{(\text{pair})}(\theta)(q^6 + q^{-6} + 1)\frac{5^{r-1}\pi}{r-1} \\ &\big(1 + d_{\mathcal{A}_1,\mathcal{A}_2} + \|u_1\|_{W^{6,\infty}} + \|u_2\|_{W^{6,\infty}}\big)^{6+2r} \sum_{\substack{\alpha_k \in \mathcal{A}_k \\ k=1,2}} \|v_{\boldsymbol{\alpha}}\|_{W_{2r}^{6,\infty}(\mathbb{R}^2 \times [-L_{\mathbf{u}}^z, L_{\mathbf{u}}^z])} \,. \end{aligned}$$

Remark 2.12. One could reduce the regularity assumption

$$\mathcal{F}_{\Gamma_{\mathcal{M}}}\big(|\nabla|^{2(\sigma+s)}\Phi_j^{(\text{mono})}[u_j]\big) \in \ell^\infty(\mathcal{R}_{\mathcal{M}}^*)$$

in Theorem 2.10 to assumptions on $V_{j,\alpha_j}^{(\ell)}$ and u_j individually, in analogy to the case of pair potentials. However, in order to maintain a clear presentation, we decided to omit such a result, and leave the details to the interested reader.

2.3. Discussion of Results

2.3.1. Regularity Assumptions We now want to comment on the imposed regularity on u_j and $v_{\boldsymbol{\alpha}}$. Our results require smoothness of u_j, i.e., $u_j \in W^{6,\infty}(\mathbb{R}^2)$, in order to show convergence with a rate. For an almost sure ergodic theorem to hold, see Proposition 3.3, we only require $u_j \in L^\infty(\mathbb{R}^2)$. We address this case in Sect. 2.4 below.

We do not expect general displacements u_j to be smooth. As explained above, if we consider a model consisting of a monolayer contribution and an interlayer coupling as constructed above, this has been analyzed for the Frenkel-Kontorova model [4] and a simplified coupled linear chain [29] in the one dimensional case. Their result is that the energy minimizer is a continuous function of the disregistry whenever the monolayer energy dominates the interlayer coupling. However, we do not address the question of smoothness of minimizers in our work. In the Cauchy–Born approximation, see Sect. 2.3.2 below, we believe that standard ideas in the theory of semi-linear elliptic equations, as applied in [28], can be utilized to show that, in case of C^∞-smooth and polynomially decaying pair potentials $v_{\boldsymbol{\alpha}}$, critical points $\mathbf{u} = (u_1, u_2)$ inherit C^∞-smoothness.

In order to obtain a rate of convergence, we require that the weighted Sobolev norm of $v_{\boldsymbol{\alpha}}$

$$\sum_{j=0}^{6} \| \langle \cdot \rangle^{2r} D^j v_{\boldsymbol{\alpha}} \|_{L^\infty(\mathbb{R}^2 \times [-L^z_{\mathbf{u}}, L^z_{\mathbf{u}}])} < \infty$$

for some $r > 1$ is finite, where $\langle \cdot \rangle = (1 + |x|^2)^{\frac{1}{2}}$ and

$$L^z_{\mathbf{u}} \sim 1 + \|u_{1,z}\|_\infty + \|u_{2,z}\|_\infty ,$$

where the involved constant depends on the lattice, see (2.32) below. In particular, $v_{\boldsymbol{\alpha}}$ obeys the tail-behavior

$$|v_{\boldsymbol{\alpha}}(\mathbf{x}, z)| \lesssim \frac{1}{|\mathbf{x}|^{2+}} \quad \text{as } |\mathbf{x}| \to \infty \tag{2.38}$$

for $\mathbf{x} \in \mathbb{R}^2$, $z \in [-L^z_{\mathbf{u}}, L^z_{\mathbf{u}}]$. As a special case, this includes the Yukawa potential $\frac{e^{-\kappa|\mathbf{x}|}}{|\mathbf{x}|}$, which accounts for screening effects. Observe that we need to regularize the potential near the origin.

Notice that in the perpendicular z-direction, we have no tail constraints, but again we need to regularize the potential near the origin. In particular, we are free to choose the potential to behave like a Lennard–Jones type potential in z-direction, away from the origin, which accounts for the van der Waals interaction between the layers.

In the case that no rate of convergence is obtained, we impose that

$$\| \langle \cdot \rangle^{2r} v_{\boldsymbol{\alpha}} \|_{L^\infty(\mathbb{R}^2 \times [-L^z_{\mathbf{u}}, L^z_{\mathbf{u}}])} < \infty$$

for some $r > 1$, amounting to the same decay rate (2.38).

2.3.2. Cauchy–Born Approximation We want to further approximate the monolayer contribution $e^{(\mathrm{mono})}$ by taking a continuum limit. This leads to the *Cauchy–Born approximation*, which is a popular approximation in elasticity theory. For that, we introduce a length-scale $a_0 \ll 1$ and rescale

$$A =: a_0 A_0 ,$$

where A_0 is independent of a_0. Consequently, $\mathcal{R}_j^{(0)} := \mathcal{R}_j / a_0$ is a_0-independent. For simplicity, we assume only a single sublattice degree of freedom, $|\mathcal{A}_j| = 1$.

In addition, we restrict u_j to take values in the xy-plane.

Recalling (2.24), and assuming that $\mathbf{u}$ is sufficiently regular, say $\mathbf{u} \in C^2(\Gamma_{\mathcal{M}}; \mathbb{R}^4)$, we then obtain for $a_0 \ll 1$ that

$$\begin{aligned} \Phi_j^{(\mathrm{mono})}[u_j](x) &\approx \frac{1}{|\Gamma_j|} V_j^{(\mathrm{mono})}\Big(a_0 Du_j(x) \cdot \mathcal{R}_j^{(0)}\Big) \\ &= W_j\big(Du_j(x)\big) , \end{aligned}$$

where W_j denotes the *Cauchy–Born energy density function*. In the linear elasticity approximation for $|Du_j|$ small enough, and assuming isotropy, one has

$$W_j(M) \approx \frac{1}{2} M : \mathcal{E}_j : M , \quad \text{for all } M \in \mathbb{R}^{2\times 2} ,$$

with the elasticity tensor $\mathcal{E}_j$ given in (1.3). In particular, the monolayer energy density (2.25) satisfies, for $a_0 \ll 1$,

$$e_j^{(\mathrm{mono})}(u_j) \approx \frac{1}{2} \fint_{\Gamma_{\mathcal{M}}} \mathrm{d}x \; Du_j(x) : \mathcal{E}_j : Du_j(x) . \tag{2.39}$$

Example 2.13. Let us, for instance, consider twisted bilayer graphene.

Let $\theta \in [0, 2\pi]$ be an incommensurate angle and let

$$a_0 := \sqrt{3} \cdot 1.42 \text{ nm} \approx 2.46 \text{ nm} .$$

Define

$$A := a_0 \begin{pmatrix} \frac{\sqrt{3}}{2} & \frac{\sqrt{3}}{2} \\ -\frac{1}{2} & \frac{1}{2} \end{pmatrix}$$

and recall from (2.1) that

$$A_1 = R_{-\theta/2} A , \quad A_2 = R_{\theta/2} A .$$

Graphene has two sublattice degrees of freedom, denoted by A and B, with associated shift vectors

$$\tau_j^{(A)} = -\frac{a_0}{2} R_{(-1)^j \theta/2} \hat{e}_1 , \quad \tau_j^{(B)} = \frac{a_0}{2} R_{(-1)^j \theta/2} \hat{e}_1 .$$

For simplicity, we can ignore the sublattice degree of freedom in order to compute the lattice displacements at the center of mass. Then we can set the relaxed lattice positions to

$$\tilde{Y}_j(R_j + \gamma_j, \alpha) := R_j + \gamma_j + \tau_j^{(\alpha)} + u_j(R_j + \gamma_j)$$

for $j = 1, 2$, $\alpha = A, B$.

The Lamé parameters for a single sheet of graphene are given by

$$\lambda = 37,950 \text{ meV/unit area}, \quad \mu = 47,352 \text{ meV/unit area},$$

see, e.g., [24]. In order to allow for out-of-plane relaxation, we need to extend the monolayer energy model, e.g., to

$$\fint_{\Gamma_{\mathcal{M}}} \mathrm{d}x \, \frac{1}{2} \left(\lambda \sum_{k=1}^{2} \varepsilon_{k,k;j}(x)^2 + 2\mu \sum_{k,\ell=1}^{2} \varepsilon_{k,\ell;j}(x)^2 + \kappa |D^2 u_{j,3}(x)|^2 \right),$$

where $\varepsilon_{k,\ell;j} := \frac{1}{2}(\partial_k u_{j,\ell} + \partial_\ell u_{j,k} + \partial_k u_{j,3} \partial_\ell u_{j,3})$ is the strain tensor, λ, μ are the Lamé parameters as before, and κ is the bending rigidity, see, e.g., [76]. As an interatomic pair potential, we may choose potentials that are radial in the horizontal direction. E.g., we may choose a Morse potential for the monolayer pair potentials, and a Lennard–Jones potential accounting for the van der Waals coupling between the layers, i.e.,

$$v_{\boldsymbol{\alpha}}(\mathbf{x}, z) \equiv v(\mathbf{x}, z) := v_{\mathrm{Morse}}(|\mathbf{x}|) v_{\mathrm{LJ}}(|z|)$$

with

$$\begin{aligned} v_{\mathrm{Morse}}(r) &:= E_0 \Big[\big(e^{-\kappa_0 (r - r_0)} - 1 \big)^2 - 1 \Big], \\ v_{\mathrm{LJ}}(r) &:= 4\varepsilon_0 \Big[\Big(\frac{\sigma}{r} \Big)^{12} - \Big(\frac{\sigma}{r} \Big)^{6} \Big]. \end{aligned}$$

Here E_0 denotes the dissociation energy, κ_0 relates to the stiffness, r_0 refers to the equilibrium position, see [79], $\varepsilon_0, \sigma > 0$ are van der Waals parameters. Strictly speaking, we need to regularize v_z to remove the singularity at the origin for our methods to apply.

More specialized interlayers potentials have been developed for graphene [57] and hBN [66], for example.

2.3.3. Relationship with Allen–Cahn Energy Functional As in the previous section, let us restrict to a single sublattice degree of freedom, $|\mathcal{A}_j| = 1$, and assume that $\tau_j^{(\alpha_j)} = 0$. Assume that v is an interlayer pair potential that is radially decaying in xy-direction, and set $\gamma_j = 0$. In addition, we restrict u_j to take values in the xy-plane.

We claim that, in the Cauchy–Born approximation, $e_{\mathrm{tot}}(u_1, 0)$, resp., $e_{\mathrm{tot}}(0, u_2)$, are modified Allen–Cahn functionals. For that, define a *stacking fault potential*

$$\Phi_j^{(\mathrm{misfit})}(x_{3-j}) := \frac{1}{|\Gamma_j|} \sum_{R_{3-j} \in \mathcal{R}_{3-j}} v\big(x_{3-j} - R_{3-j}\big) \tag{2.40}$$

for all $x_{3-j} \in \Gamma_{3-j}$, $j = 1, 2$. We note that the generalized stacking fault energy (GSFE) more commonly used in numerical computations of relaxation [24,27,28] approximates the misfit energy by a DFT computation on a periodic cell at zero twist angle. By construction, $\Phi_j^{(\text{misfit})}$ is periodic with respect to $\mathcal{R}_{3-j}$, $j = 1, 2$. $\Phi_j^{(\text{misfit})}(x_{3-j})$ is maximal on the lattice points $R_{3-j} \in \mathcal{R}_{3-j}$, which we will refer to as *AA stacking*, and minimal at

$$R_{3-j} + \frac{1}{3} A_{3-j} \begin{pmatrix} 1 \\ 1 \end{pmatrix},$$

which we will refer to as *AB stacking*, and at

$$R_{3-j} + \frac{2}{3} A_{3-j} \begin{pmatrix} 1 \\ 1 \end{pmatrix},$$

which we will refer to as *BA stacking*, see Figs. 1 and 5. In the AA stacking, nuclei from different layers are stacked on top of each other, while in the AB/BA stacking, they sit in between three nuclei.

Recalling (2.28) and (1.1), observe that we have the identities

$$\begin{aligned} \Psi_1^{(\text{inter})}[u_1, 0](x, D_{1\to 2}x) &= \Phi_1^{(\text{misfit})}(D_{1\to 2}x + u_1(x)), \\ \Psi_2^{(\text{inter})}[0, u_2](x, D_{2\to 1}x) &= \Phi_2^{(\text{misfit})}(D_{2\to 1}x + u_2(x)). \end{aligned} \tag{2.41}$$

Moreover, Lemma 4.6 implies that

$$\fint_{\Gamma_{\mathcal{M}}} \mathrm{d}x \; \Phi_{1,0}^{(\text{inter})}[\mathbf{u}](x) = \fint_{\Gamma_{\mathcal{M}}} \mathrm{d}x \; \Phi_{2,0}^{(\text{inter})}[\mathbf{u}](x).$$

In the Cauchy–Born approximation $a_0 \ll 1$, see (2.39), the total energy functional becomes

$$e_{\text{tot}}(\mathbf{u}) \approx \frac{1}{2} \sum_{j=1}^{2} \fint_{\Gamma_{\mathcal{M}}} \mathrm{d}x \left(Du_j(x) : \mathcal{E}_j : Du_j(x) + \Phi_{j,0}^{(\text{inter})}[\mathbf{u}](x) \right).$$

In particular, employing (2.41), we have for $a_0 \ll 1$ that

$$e_{\text{tot}}(u_1, 0) \approx \fint_{\Gamma_{\mathcal{M}}} \mathrm{d}x \left(\frac{1}{2} Du_1(x) : \mathcal{E}_1 : Du_1(x) + \Phi_1^{(\text{misfit})}\big(D_{1\to 2}x + u_1(x)\big) \right).$$

In order to recognize the scaling-behavior with $\theta \to 0$, let us rescale $y := D_{1\to 2}x$, and define $U_1(y) := u_1(D_{1\to 2}^{-1}y)$. For simplicity, we assume that the layers are purely twisted, i.e., $q = 1$. Then (A.1) and (A.3) below imply that

$$A_{\mathcal{M}} = 2\sin(\theta/2)\mathcal{J}A, \quad \mathcal{J} := \begin{pmatrix} 0 & -1 \\ 1 & 0 \end{pmatrix}.$$

Due to $D_{1\to 2} = -A_2 A_{\mathcal{M}}^{-1} = 2\sin(\theta/2)A_2 A^{-1}\mathcal{J}$, see Lemma 4.1, we obtain, defining $\varepsilon := 2\sin(\theta/2)$, for some $\tilde{\mathcal{E}}_1$

$$\fint_{\Gamma_2} \mathrm{d}y \left(\frac{\varepsilon^2}{2} DU_1(y) : \tilde{\mathcal{E}}_1 : DU_1(y) + \Phi_1^{(\text{misfit})}\big(y + U_1(y)\big) \right).$$

Rescaling this energy by $\frac{1}{\varepsilon}$, we thus obtain

$$\fint_{\Gamma_2} \mathrm{d}y \left(\frac{\varepsilon}{2} DU_1(y) : \tilde{\mathcal{E}}_1 : DU_1(y) + \frac{1}{\varepsilon} \Phi_1^{(\mathrm{misfit})}\big(y + U_1(y)\big) \right),$$

the algebraic form of the expression obtained in [28]. The obtained energy resembles the Allen–Cahn energy functional, except for the additional explicit dependence on x. Without setting $u_2 = 0$, one can show that for $U_2(y) := u_2(-D_{2\to 1}^{-1} y)$ the resulting rescaled energy takes the form

$$\begin{aligned} &\frac{\varepsilon}{2} \sum_{j=1}^{2} \fint_{\Gamma_{3-j}} \mathrm{d}y \; DU_j(y) : \tilde{\mathcal{E}}_j : DU_j(y) \\ &\quad + \frac{1}{\varepsilon} \int_{\mathbb{R}^2} \mathrm{d}y \; V\big(y + U_1(y) - U_2(y)\big), \end{aligned} \tag{2.42}$$

where $\tilde{\mathcal{E}}_2$ and $V = \frac{v}{|\Gamma_1||\Gamma_2|}$ are chosen appropriately.

2.3.4. Comparison with Previous Result We now give a more detailed comparison of the previous model (1.2) and our new model (1.4) in the simplest possible setting. Again, we restrict to a single sublattice degree of freedom in each layer, assume that the layers are centered at the origin, $\gamma_j = 0$, and not mismatched, $q = 1$. We will argue that the stacking fault energy $\Phi_j^{(\mathrm{misfit})}$, see (2.40), obtained in this work provides a microscopic model for the GSFE $\Phi_j^{(\mathrm{GSFE})}$ studied in [24,25,27,28], see Fig. 5. However, the resulting model even under this modelling assumption is different from ours obtained in this work.

Setting $\Phi_j^{(\mathrm{GSFE})} = \Phi_j^{(\mathrm{misfit})}$, we obtain, starting from the interlayer energy in (1.2),

$$\begin{aligned} &\frac{1}{|\Gamma_{\mathcal{M}}|} \int_{\Gamma_{\mathcal{M}}} \mathrm{d}x \; \Phi_j^{(\mathrm{GSFE})}\big(D_{j\to 3-j}x + u_j(x) - u_{3-j}(x)\big) \\ &\quad = \frac{1}{|\Gamma_{\mathcal{M}}||\Gamma_j|} \int_{\Gamma_{\mathcal{M}}} \mathrm{d}x \sum_{R_{3-j}\in\mathcal{R}_{3-j}} v\big(D_{j\to 3-j}x - R_{3-j} + u_j(x) - u_{3-j}(x)\big). \end{aligned}$$

As above, we rescale $y := D_{j\to 3-j}x$, and define $U_j(y) := u_j((-1)^{j+1} D_{j\to 3-j}^{-1} y)$. Then a straight-forward calculation using Lemma 4.1 yields

$$\frac{1}{|\Gamma_1||\Gamma_2|} \int_{\Gamma_{3-j}} \mathrm{d}y \sum_{R_{3-j}\in\mathcal{R}_{3-j}} v\big(y - R_{3-j} + U_j(y) - U_{3-j}(A_j A_{3-j}^{-1} y)\big).$$

Putting technicalities aside, we interchange orders of integration and summation and substitute $x - R_{3-j} \to x$ and use $\mathcal{R}_{3-j}$-periodicity of U_j to obtain

$$\frac{1}{|\Gamma_1||\Gamma_2|} \int_{\mathbb{R}^2} \mathrm{d}y \; v\big(y + U_j(y) - U_{3-j}(A_j A_{3-j}^{-1} y)\big).$$

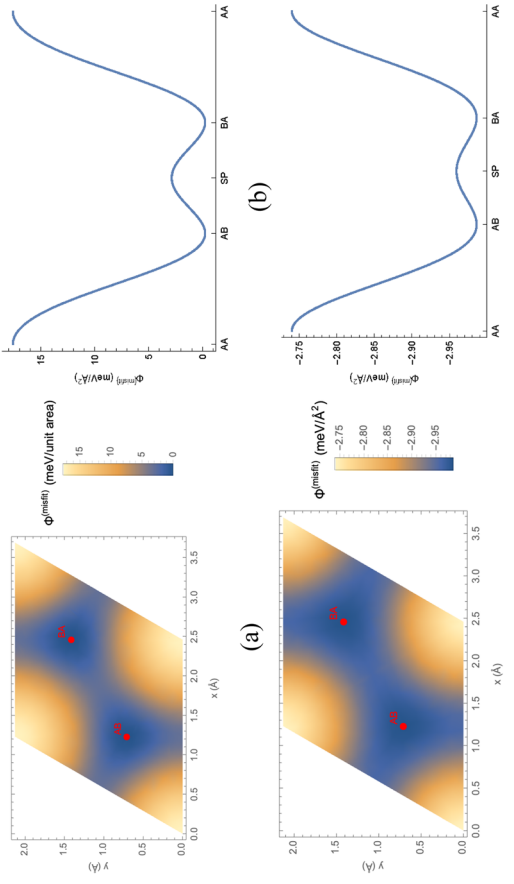

Fig. 5. Stacking fault energies for graphene-graphene interlayer potential. Red dots in left diagrams indicate AB and BA stacking, respectively. The corners correspond to AA stacking. On the right, the profile along the diagonal through the red dots is displayed. Figure 5a and b refer to the GSFE computed in [25]. Figure 5c and d refer to misfit energy computed from Morse potential with parametrization (E_0, κ_0, r_0)=(2.8437 meV, 1.8168 Å^{-1}, 3.6891 Å) taken from [75]

Including the monolayer contribution and rescaling the total energy by $\frac{1}{\varepsilon}$, we thus obtain

$$\frac{\varepsilon}{2}\sum_{j=1}^{2}\fint_{\Gamma_{3-j}} \mathrm{d}y\; DU_j(y) : \tilde{\mathcal{E}}_j : DU_j(y) + \frac{1}{\varepsilon}\int_{\mathbb{R}^2} \mathrm{d}y\; V\big(y + U_1(y) - U_2(R_{-\theta}y)\big)\,. \tag{2.43}$$

Comparing (2.43) and (2.42), we notice that U_2 in the argument of V is evaluated at different positions. The difference of arguments is of size $|x - R_{-\theta}x| \approx \varepsilon|x|$ as $\varepsilon \to 0$. It was shown in [27] that for a minimizer (U_1^{eq}, U_2^{eq}), $\|DU_j^{eq}\|_2 \lesssim \frac{1}{\varepsilon}$. In particular, numerical computations show that domain walls of thickness ε form, where U_j^{eq} has a transition of order $O(1)$ from AB to BA stacking. This phenomenon has been explained more rigorously in the context of the Allen–Cahn energy, see, e.g., [34] for a nice introduction. Consequently, we expect our derived energy to vary significantly, of order $O(1)$ at the domain walls, from that obtained in [28]. We plan to address this issue in future works.

2.3.5. Outlook In the Cauchy–Born and linear elasticity approximation, we can employ ideas from elliptic theory to establish existence, uniqueness, and regularity of energy minimizers. This remains true as long as the interlayer potential is a compact perturbation to the intralayer Cauchy–Born energy. In particular, one can use a contraction map argument as in [28]. We do not elaborate on further details here, and defer to future works instead.

Furthermore, one can extend the intralayer model that we use beyond linear elasticity, as was studied, e.g., in [44,45]. In order to include out-of-plane relaxation, we need to include an out-of-plane penalization for the monolayer contribution, see, e.g., [76] and example 2.13 above.

While we develop a model for bilayer systems only, we can extend the model to systems with an arbitrary finite number of layers, by summing over the pair-wise coupling of layers. For the case of many-body site potentials, we believe that the ideas presented in [28] lend themselves to extending our results to the multi-layer case.

2.4. Results for Rough Displacements

As stated above, it can be useful to access an energy functional when the displacement functions are not necessarily smooth. Due to the use of ergodicity, these results will only hold almost surely, up to some relative lattice shifts. We will see that to even formulate the problem for rougher conditions on the displacement functions, we need to introduce a weak notion of lattice dependence for the displacement functions. In contrast, above the existence of (moiré-)periodic continuous functions attaining assigned values on the lattices yields a strong constraint on the attainable values. We now introduce a weak lattice dependence, that we refer to as *reconstructability*, which will allow us to relax this constraint. Reconstructability in layer j means that there exists a single function u_j such that, for almost all lattice

origins γ_j, the values of u_j assigned to the corresponding shifted lattice $\gamma_j + \mathcal{R}_j$, allow us to recover all Fourier coefficients of u_j. Consequently, our statements will only hold up to a nullset of lattice shifts γ_1, γ_2.

We start by stating an almost sure and mean ergodic theorem that will allow us to rigorously analyze thermodynamic limits of elastic energies that are functions of non-smooth displacements $u_j \in L^1\big(\Gamma_{\mathcal{M}}; (\mathbb{R}^3)^{\mathcal{A}_j}\big)$.

Proposition 2.14. (Ergodic Theorem) *For all* $f \in L^1(\Gamma_{\mathcal{M}})$

$$\lim_{N\to\infty} \frac{1}{(2N+1)^2} \sum_{R_j \in \mathcal{R}_j(N)} f\left(\left\{R_j + \gamma_j\right\}_{\mathcal{M}}\right) = \fint_{\Gamma_{\mathcal{M}}} \mathrm{d}x \; f(x)\,.$$

converges almost everywhere in Γ_j *and also in the* $L^1(\Gamma_j)$*-sense.*

Proposition 2.14 follows from a more general ergodic theorem stated here as Proposition 3.1. Our first use of Proposition 2.14 will be to prove in Proposition 2.16 that the Fourier transform of $u_j \in L^1\big(\Gamma_{\mathcal{M}}; (\mathbb{R}^3)^{\mathcal{A}_j}\big)$ can be reconstructed as a thermodynamic limit from $u_j(\left\{\gamma_j + \mathcal{R}_j\right\}_{\mathcal{M}}, \mathcal{A}_j)$ for almost every $\gamma_j \in \Gamma_j$.

We now define lattice deformations based on $u_j \in L^1\big(\Gamma_{\mathcal{M}}; (\mathbb{R}^3)^{\mathcal{A}_j}\big)$.

Assumption 3. There exist displacements $u_j \in L^1\big(\Gamma_{\mathcal{M}}; (\mathbb{R}^3)^{\mathcal{A}_j}\big)$ such that the total positions on the reference collection of lattices

$$\big((\gamma_j + \mathcal{R}_j) \times \mathcal{A}_j\big)_{\gamma_j \in \Gamma_j}\,, \quad j \in \{1,2\}\,,$$

are given by the deformation (2.20).

Assumption 3 implies that whenever $\left\{\gamma_j + R_j\right\}_{\mathcal{M}} = \left\{\gamma_j' + R_j'\right\}_{\mathcal{M}}$, we have that the associated displacements

$$u_j\left(\left\{\gamma_j + R_j\right\}_{\mathcal{M}}, \alpha_j\right) = u_j\left(\left\{\gamma_j' + R_j'\right\}_{\mathcal{M}}, \alpha_j\right)$$

coincide. Since $(\mathcal{R}_1^*, \mathcal{R}_2^*)$ is incommensurate, this can only happen for $\gamma_j \neq \gamma_j'$, ensuring that we do not impose a moiré-periodicity constraint.

Observe that the total lattice positions are well-defined only up to a nullset of lattice shifts $\gamma_j \in \Gamma_j$. Next we will discuss in which sense the data of u_j on a single lattice suffices to reconstruct u_j.

Definition 2.15. We say that $u_j \in L^1\big(\Gamma_{\mathcal{M}}; (\mathbb{R}^3)^{\mathcal{A}_j}\big)$ is *reconstructable* along $\gamma_j + \mathcal{R}_j$ iff for all $G_{\mathcal{M}} \in \mathcal{R}_{\mathcal{M}}^*$, $\alpha_j \in \mathcal{A}_j$, we have that

$$\lim_{N\to\infty} \frac{1}{(2N+1)^2} \sum_{R_j \in \mathcal{R}_j(N)} e^{-iG_{\mathcal{M}}\cdot(\gamma_j + R_j)} u_j(\left\{\gamma_j + R_j\right\}_{\mathcal{M}}, \alpha_j) = \hat{u}_j(G_{\mathcal{M}}, \alpha_j)\,.$$

In particular, if $u_j \in L^p\big(\Gamma_{\mathcal{M}}; (\mathbb{R}^3)^{\mathcal{A}_j}\big)$, $p > 1$, is reconstructable along $\gamma_j + \mathcal{R}_j$, the Carleson-Hunt Theorem, see, e.g., [40, Chapter 1], implies that for almost all $x \in \Gamma_{\mathcal{M}}$ and all $\alpha_j \in \mathcal{A}_j$

$$u_j(x, \alpha_j) = \sum_{G_{\mathcal{M}} \in \mathcal{R}^*_{\mathcal{M}}} e^{iG_{\mathcal{M}} \cdot x} \lim_{N\to\infty} \frac{1}{(2N+1)^2} \sum_{R_j \in \mathcal{R}_j(N)} e^{-iG_{\mathcal{M}} \cdot (\gamma_j + R_j)} u_j(\{\gamma_j + R_j\}_{\mathcal{M}}, \alpha_j) .$$

If $u_j, v_j \in L^1\big(\Gamma_{\mathcal{M}}; (\mathbb{R}^3)^{\mathcal{A}_j}\big)$, we have the uniqueness property that

$$\hat{u}_j(G_{\mathcal{M}}, \alpha_j) = \hat{v}_j(G_{\mathcal{M}}, \alpha_j)$$

for all $(G_{\mathcal{M}}, \alpha_j) \in \mathcal{R}^*_{\mathcal{M}} \times \mathcal{A}_j$ implies that $u_j = v_j$, see [40, Corollary 1.11].

As a consequence of Proposition 2.14, we find the following result.

Proposition 2.16. (Almost sure reconstructability) *Every $u_j \in L^1\big(\Gamma_{\mathcal{M}}; (\mathbb{R}^3)^{\mathcal{A}_j}\big)$ is reconstructable along $\gamma_j + \mathcal{R}_j$ for almost every $\gamma_j \in \Gamma_j$.*

For a proof, we refer to Appendix A.

We are now ready to formulate the main result for rough displacements.

Theorem 2.17. *Assume that $\Phi_j^{(\mathrm{mono})}[u_j] \in L^1(\Gamma_{\mathcal{M}})$, and that $\Psi_j^{(\mathrm{inter})}[\mathbf{u}] \in L^1(\Gamma_{\mathcal{M}} \times \Gamma_{3-j})$ and for any $\boldsymbol{\gamma} = (\gamma_1, \gamma_2) \in \Gamma_1 \times \Gamma_2$ that $\Phi_{j,\boldsymbol{\gamma}}^{(\mathrm{inter})}[\mathbf{u}] \in L^1(\Gamma_{\mathcal{M}})$, respectively.*

In the case of interlayer pair potentials, let $r > 1$ and assume that, for $k = 1, 2$, $\alpha_k \in \mathcal{A}_k$, $u_k(\cdot, \alpha_k) \in L^\infty(\mathbb{R}^2)$, and that

$$v_{\boldsymbol{\alpha}} \in L^\infty_{2r}(\mathbb{R}^2 \times [-L^z_{\mathbf{u}}, L^z_{\mathbf{u}}]) .$$

We then have for almost all $\boldsymbol{\gamma} \in \Gamma_1 \times \Gamma_2$ that

$$\lim_{N\to\infty} e^{(\mathrm{mono})}_{j,N,\gamma_j}(u_j) = e^{(\mathrm{mono})}_j(u_j) , \quad \lim_{N\to\infty} e^{(\mathrm{inter})}_{j,N,\boldsymbol{\gamma}}(\mathbf{u}) = e^{(\mathrm{inter})}_{j,\boldsymbol{\gamma}}(\mathbf{u}) .$$

.

In the case of many-body potentials, this result is a direct consequence of the ergodic theorem Proposition 2.14. The proof that the conditions in the case of interlayer pair potentials are sufficient, are contained in Sect. 4.3.

2.5. Sketch of the Proof

The technical tools used for the thermodynamic limit stem from ergodic theory. We prove an almost sure and mean ergodic theorem, see Proposition 3.3, and a quantitative ergodic theorem, see Proposition 3.5. The latter is inspired by [30] which shows uniform convergence with respect to shifts of the lattice origin, for the one-dimensional case. In contrast to [30], our approach is two-dimensional and based on studying the convergence properties of the approximate Dirichlet kernel

associated with the ergodic average over the truncated lattice. We directly compute an L^1-limit for smooth functions, which, by density, yields a general L^1-limit. In order to obtain convergence almost everywhere, we invoke a general ergodic theorem 3.5 as stated, e.g., in [56]. For a more detailed description of our approach, see Sect. 3.

3. Ergodic Theorems

We start by stating ergodic theorems in a sufficiently general setting, as developed, e.g., in [54,56], see also [37]. Then we explain how these general ideas can be applied in the present setting.

3.1. Review of General Ergodic Theorems

Given a probability space $(\Omega, \Sigma, \mathbb{P})$ and a group G, recall that a group action $G \curvearrowright \Omega$ is *measure-preserving* iff

$$g.\mathbb{P}(B) := \mathbb{P}(g^{-1}.B) = \mathbb{P}(B)$$

for all $B \in \Sigma$ and $g \in G$. Moreover, we call a measurable map $f : \Omega \to \mathbb{R}$ *G-invariant* iff $g.f := f \circ g^{-1} = f$ for any $g \in G$ $\mathbb{P}-$almost surely. Similarly, we call measurable set B G-invariant iff $\mathbb{1}_B$ is G-invariant. Let Σ_G denote the sub σ-algebra of Σ of all G-invariant sets in Σ.

Given a measurable function $f : \Omega \to \mathbb{R}$ and a finite subset $H \subseteq G$, we define the *ergodic average*

$$\mathcal{A}_H(f) := \frac{1}{|H|} \sum_{g \in H} g^{-1}.f \,.$$

A sequence $(H_N)_{N\in\mathbb{N}}$ of non-empty finite subsets of G is called a *Følner sequence* iff

$$\lim_{N\to\infty} \frac{|gH_N \triangle H_N|}{|H_N|} = 0$$

for all $g \in G$, where $A \triangle B$ denotes the symmetric difference of sets A, B. $(H_N)_{N\in\mathbb{N}}$ is *tempered* iff there is $C > 0$ s.t.

$$\left| \bigcup_{k=1}^{N-1} H_k^{-1} H_N \right| \leq C|H_N|$$

for all $N \in \mathbb{N}$, $N \geq 2$.

We finish this general introduction with the following pointwise ergodic theorem as stated, e.g., in [56, Theorem 4.28]:

Proposition 3.1. (Pointwise Ergodic Theorem) *Let* $(\Omega, \Sigma, \mathbb{P})$ *be a probability space and* $G \curvearrowright \Omega$ *be a measure-preserving group action. Let* $(H_N)_{N\in\mathbb{N}}$ *be a tempered Følner sequence. Then we have that for all* $f \in L^1(\Omega)$ *and*

$$\lim_{N\to\infty} \mathcal{A}_{H_N}(f) = \mathbb{E}[f|\Sigma_G]$$

$\mathbb{P}-$*almost surely and in the* L^1*-sense, where* $\mathbb{E}[\cdot|\Sigma_G]$ *denotes the conditional expectation given the* σ*-algebra* Σ_G *of* G*-invariant events.*

Remark 3.2. Recall that the conditional expectation $\mathbb{E}[f|\Sigma_G]$ is the unique (Ω, Σ_G)-measurable function such that

$$\int_C \mathrm{d}\mathbb{P}(\omega)\, \mathbb{E}[f|\Sigma_G](\omega) = \int_C \mathrm{d}\mathbb{P}(\omega)\, f(\omega)$$

for all (G-invariant) sets $C \in \Sigma_G$.

3.2. Ergodicity in Incommensurate Bilayer Systems

We now turn to the system at hand and explore how ergodicity arises as a consequence of the underlying incommensurate geometry. To apply the general ergodic setting above, we set $G = \mathcal{R}_j$ and $H_N := \mathcal{R}_j(N)$, see (2.4). It is straightforward to verify that $(\mathcal{R}_j(N))_{N\in\mathbb{N}}$ is both Følner and tempered. We leave the details to the interested reader.

Let $\mathbb{T}^2 = \mathbb{R}^2/\mathbb{Z}^2$ denote the standard 2-torus, and

$$\Gamma_{\mathcal{M}}^{(\mathrm{per})} := A_{\mathcal{M}}\mathbb{T}^2, \quad \Gamma_{3-j}^{(\mathrm{per})} := A_{3-j}\mathbb{T}^2$$

denote the tori associated with the moiré unit cell $\Gamma_{\mathcal{M}}$ and with the unit cell Γ_{3-j} of layer $3-j$, respectively. Let $\mathcal{B}$ denote the respective Borel σ-algebra over Ω.

Then we choose $\Omega = \Gamma_{\mathcal{M}}^{(\mathrm{per})} \times \Gamma_{3-j}^{(\mathrm{per})}$ and study the Lebesgue-measure preserving group action of $\mathcal{R}_j$ on Ω given by translations, i.e., $R_j.\omega := \omega + (R_j, R_j)$. As a consequence of Proposition 3.1, we prove the following statement:

Proposition 3.3. (Pointwise and Mean Ergodic Theorem) *Let* $h \in L^1_{\mathrm{loc}}(\mathbb{R}^4)$ *be* $\mathcal{R}_{\mathcal{M}} \times \mathcal{R}_{3-j}$*-periodic. Then*

$$\begin{aligned}\lim_{N\to\infty} \mathcal{A}_{\mathcal{R}_j(N)}(h)(\omega_{\mathcal{M}}, \omega_{3-j}) &= \fint_{A_j^{-1}\Gamma_{\mathcal{M}}} \mathrm{d}\xi\; h\big(A_j\xi + \omega_{\mathcal{M}}, (A_j - A_{3-j})\xi + \omega_{3-j}\big)\\ &= \fint_{\Gamma_{\mathcal{M}}} \mathrm{d}x\; h\big(x, D_{j\to 3-j}(x - \omega_{\mathcal{M}}) + \omega_{3-j}\big)\\ &= \fint_{\Gamma_{3-j}} \mathrm{d}y\; h\big(D^{-1}_{j\to 3-j}(y - \omega_{3-j}) + \omega_{\mathcal{M}}, y\big)\end{aligned}$$

converges for almost all $(\omega_{\mathcal{M}}, \omega_{3-j}) \in \Gamma_{\mathcal{M}} \times \Gamma_{3-j}$ *and also in* $L^1(\Gamma_{\mathcal{M}} \times \Gamma_{3-j})$.

Remark 3.4. Let $h \in L^1_{loc}(\Gamma^{(\mathrm{per})}_{\mathcal{M}} \times \Gamma^{(\mathrm{per})}_{3-j})$.

In addition, let $\mathcal{B}_{\mathcal{R}_j}$ denote the σ-algebra of $\mathcal{R}_j$-invariant Borel subsets of $\Gamma^{(\mathrm{per})}_{\mathcal{M}} \times \Gamma^{(\mathrm{per})}_{3-j}$, where the $\mathcal{R}_j$-action is given as above by $R_j.\omega = \omega + (R_j, R_j)$. Then one can prove directly that

$$\mathbb{E}[h|\Sigma_{\mathcal{R}_j}](\omega_{\mathcal{M}}, \omega_{3-j}) = \fint_{A_j^{-1}\Gamma_{\mathcal{M}}} \mathrm{d}\xi \; h\big(A_j\xi + \omega_{\mathcal{M}}, (A_j - A_{3-j})\xi + \omega_{3-j}\big) .$$

Lebesgue-almost everywhere, where the conditional expectation on the l.h.s. is taken with respect to the uniform distribution on $\Gamma^{(\mathrm{per})}_{\mathcal{M}} \times \Gamma^{(\mathrm{per})}_{3-j}$.

We find the argument presented in the proof of Proposition 3.3 appealing because it provides a means to calculate the conditional expectation.

Using the notion of Diophantine 2D rotations, see Definition 2.4, we obtain the following quantitative ergodic theorem:

Proposition 3.5. (Quantitative Ergodic Theorem) *Let $q > 0$, $\sigma > \frac{1433}{1248}$, $s > 1$, and let θ be a (q, K, σ)-Diophantine 2D rotation for some $K > 0$. Let $f \in L^1(\Gamma_{\mathcal{M}})$ be such that $\mathcal{F}_{\Gamma_{\mathcal{M}}}\big(|\nabla|^{2(\sigma+s)} f\big) \in \ell^\infty(\mathcal{R}^*_{\mathcal{M}})$. Then we have for all $N \in \mathbb{N}$ large enough that*

$$\begin{aligned}
&\left| \frac{1}{(2N+1)^2} \sum_{R_j \in \mathcal{A}_{\mathcal{R}_j(N)}} f(\{R_j\}_{\mathcal{M}}) - \fint_{\Gamma_{\mathcal{M}}} \mathrm{d}x \; f(x) \right| \\
&\quad \leq \frac{2\sqrt{2}}{K} \Big(\frac{\rho_{\mathcal{M}} \|A\|_2}{2\pi} \Big)^{2(\sigma+s)} \big(\zeta(2s) + 2^{-s} \zeta(s)^2 \big) \\
&\quad \sup_{G_{\mathcal{M}} \in \mathcal{R}^*_{\mathcal{M}}} |G_{\mathcal{M}}|^{2(\sigma+s)} |\hat{f}(G_{\mathcal{M}})| \frac{1}{2N+1} .
\end{aligned}$$

For proofs of these ergodic theorems, we refer to Appendix C.

Remark 3.6. Our methods would allow us to adapt Proposition 3.5 to the more general setting in Proposition 3.3. However, for presentational purposes, we chose to omit such a result and leave the details to the interested reader.

We now want to motivate how to prove Propositions 3.3 and 3.5.

3.3. Dirichlet Kernel as a Discrepancy Function

Our idea is based on using periodicity of the functions which we are averaging over the individual lattices by representing them via their Fourier expansion. Averaging the corresponding Fourier basis $(\exp(iG \cdot (\cdot)))_G$ over a discrete set leads to the emergence of the Dirichlet kernel, normalized by the number of lattice points. This is a common idea in Fourier analysis, see, e.g., [40], and has been applied, e.g., in [33,84] to derive a discretization error in Riemann sums.

Let $h \in L^p(\Gamma_{\mathcal{M}} \times \Gamma_{3-j})$, $p > 1$. In addition to the Fourier transform defined in (2.35), for $h \in L^1(\Gamma_{\mathcal{M}} \times \Gamma_j)$ and $(G_{\mathcal{M}}, G_j) \in (\mathcal{R}^*_{\mathcal{M}}, \mathcal{R}^*_j)$, define

$$\begin{aligned} \hat{h}(G_{\mathcal{M}}, G_j) &:= \mathcal{F}_{\Gamma_{\mathcal{M}} \times \Gamma_j}(h)(G_{\mathcal{M}}) \\ &:= \fint_{\Gamma_j} \mathrm{d}y \fint_{\Gamma_{\mathcal{M}}} \mathrm{d}x \, e^{-i(G_{\mathcal{M}} \cdot x + G_j \cdot y)} h(x, y) \,. \end{aligned} \tag{3.1}$$

Here, we abuse notation and interpret $\hat{h}$ in the local context.

Using this Fourier transform, we obtain that for almost all $(\omega_{\mathcal{M}}, \omega_{3-j}) \in \Gamma^{(\mathrm{per})}_{\mathcal{M}} \times \Gamma^{(\mathrm{per})}_{3-j}$

$$\begin{aligned} &\frac{1}{(2N+1)^2} \sum_{R_j \in \mathcal{R}_j(N)} h\big(\{R_j + \omega_{\mathcal{M}}\}_{\mathcal{M}}, \{R_j + \omega_{3-j}\}_{3-j}\big) \\ &= \sum_{R_j \in \mathcal{R}_j(N)} \sum_{\substack{G_{3-j} \in \mathcal{R}^*_{3-j}, \\ G_{\mathcal{M}} \in \mathcal{R}^*_{\mathcal{M}}}} e^{i(G_{\mathcal{M}} \cdot \{R_j + \omega_{\mathcal{M}}\}_{\mathcal{M}} + G_{3-j} \cdot \{R_j + \omega_{3-j}\}_{3-j})} \hat{h}(G_{\mathcal{M}}, G_{3-j}) \,. \end{aligned}$$

Realizing that $\mathcal{R}^*_{\mathcal{M}} \cdot \lfloor x \rfloor_{\mathcal{M}} \subseteq 2\pi\mathbb{Z}$ for any $x \in \mathbb{R}^2$, we have that

$$e^{iG_{\mathcal{M}} \cdot \{x\}_{\mathcal{M}}} = e^{iG_{\mathcal{M}} \cdot x}$$

for any $x \in \mathbb{R}^2$. A straight-forward calculation analogous to the computation of the Dirichlet kernel yields

$$\begin{aligned} \mathbb{1}^{(N)}_{\mathcal{R}^*_j}(G) &:= \frac{1}{(2N+1)^2} \sum_{R_j \in \mathcal{R}_j(N)} e^{iG \cdot R_j} \\ &= \prod_{\ell=1}^{2} \frac{\sin\big((2N+1)(A_j^T G)_\ell / 2\big)}{(2N+1)\sin\big((A_j^T G)_\ell / 2\big)} \,, \end{aligned} \tag{3.2}$$

where y_ℓ denotes the ℓ^{th} Euclidean coordinate of y. Using this notation, we obtain that

$$\begin{aligned} &\frac{1}{(2N+1)^2} \sum_{R_j \in \mathcal{R}_j(N)} h\big(\{R_j + \omega_{\mathcal{M}}\}_{\mathcal{M}}, \{R_j + \omega_{3-j}\}_{3-j}\big) \\ &= \sum_{\substack{G_{3-j} \in \mathcal{R}^*_{3-j}, \\ G_{\mathcal{M}} \in \mathcal{R}^*_{\mathcal{M}}}} \mathbb{1}^{(N)}_{\mathcal{R}^*_j}(G_{3-j} + G_{\mathcal{M}}) \, \hat{h}(G_{\mathcal{M}}, G_{3-j}) e^{i(G_{\mathcal{M}} \cdot \omega_{\mathcal{M}} + G_{3-j} \cdot \omega_{3-j})} \,. \end{aligned} \tag{3.3}$$

If $f \in L^p(\Gamma_{\mathcal{M}})$, analogous steps yield

$$\frac{1}{(2N+1)^2} \sum_{R_j \in \mathcal{R}_j(N)} f(\{R_j\}_{\mathcal{M}}) = \sum_{G_{\mathcal{M}} \in \mathcal{R}^*_{\mathcal{M}}} \mathbb{1}^{(N)}_{\mathcal{R}^*_j}(G_{\mathcal{M}}) \, \hat{f}(G_{\mathcal{M}}) \,. \tag{3.4}$$

Next, we will study the convergence properties of $\mathbb{1}^{(N)}_{\mathcal{R}^*_j}$.

Properties of the Dirichlet kernel For all $G_j \in \mathcal{R}^*_j$, we have that

$$\mathbb{1}^{(N)}_{\mathcal{R}^*_j}(G_j) \,=\, 1\,.$$

Moreover, for all $G \in \mathbb{R}^2 \setminus \mathcal{R}^*_j$, it holds that

$$|\mathbb{1}^{(N)}_{\mathcal{R}^*_j}(G)| \,\leq\, \frac{1}{2N+1} \min_{\ell=1,2} \frac{1}{\left|\sin\left((A_j^T G)_\ell/2\right)\right|}\,.$$

In particular, we obtain that for all $G \in \mathbb{R}^2$

$$\lim_{N\to\infty} \mathbb{1}^{(N)}_{\mathcal{R}^*_j}(G) \,=\, \mathbb{1}_{\mathcal{R}^*_j}(G)\,.$$

In particular, if we can interchange the order of taking the limit $N \to \infty$ and summing over G_{3-j} and $G_{\mathcal{M}}$, (3.3) implies that

$$\begin{aligned}
&\frac{1}{(2N+1)^2} \sum_{R_j \in \mathcal{R}_j(N)} h\big(\{R_j+\omega_{\mathcal{M}}\}_{\mathcal{M}}\,, \{R_j+\omega_{3-j}\}_{3-j}\big) \\
&\xrightarrow{N\to\infty} \sum_{\substack{G_{3-j}\,\in\,\mathcal{R}^*_{3-j},\\ G_{\mathcal{M}}\,\in\,\mathcal{R}^*_{\mathcal{M}}}} \mathbb{1}_{\mathcal{R}^*_j}(G_{3-j}+G_{\mathcal{M}})\,\hat{h}(G_{\mathcal{M}}, G_{3-j}) e^{i(G_{\mathcal{M}}\cdot\omega_{\mathcal{M}}+G_{3-j}\cdot\omega_{3-j})}\,.
\end{aligned}$$

Again, assuming interchangeability of involved sums and integrals, we arrive, after a straight-forward calculation, at

$$\fint_{A_j^{-1}\Gamma_{\mathcal{M}}} \mathrm{d}x\; h\big(A_j x+\omega_{\mathcal{M}}, (A_j-A_{3-j})x+\omega_{3-j}\big)\,,$$

as stated in Proposition 3.3. In order to interchange limits, sums, and integrals, we use the fact that we study the convergence in $L^1(\Gamma^{(\mathrm{per})}_{\mathcal{M}} \times \Gamma^{(\mathrm{per})}_{3-j})$, in order to restrict to C^∞-smooth functions.

In order to extract a rate of convergence in (3.3), we need to analyze the tail-behavior of $\mathbb{1}^{(N)}_{\mathcal{R}^*_j}$. For general irrational angles, the rate of convergence can be arbitrarily slow. However, we show in the proof of Proposition 3.5, in Appendix C, that for Diophantine 2D rotations θ, see Definition 2.4, and all $G_{\mathcal{M}} \in \mathcal{R}^*_{\mathcal{M}} \setminus \{0\}$, we have that

$$|\mathbb{1}^{(N)}_{\mathcal{R}^*_j}(G_{\mathcal{M}})| \,\leq\, \frac{C_{\sigma,q,A,\theta}|G_{\mathcal{M}}|^{2\sigma}}{2N+1} \tag{3.5}$$

for any $\sigma > \frac{1433}{1248}$, where $C_{\sigma,q,A,\theta}$ depends only on σ, q, A, and θ. In particular, employing (3.5), (3.4) implies that

$$\begin{aligned}
&\left|\frac{1}{(2N+1)^2} \sum_{R_j \in \mathcal{R}_{j(N)}} f\big(\{R_j\}_{\mathcal{M}}\big) \,-\, \fint_{\Gamma_{\mathcal{M}}} \mathrm{d}x\; f(x)\right| \\
&\quad\leq\, C_{\sigma,q,A,\theta} \sum_{G_{\mathcal{M}}\in\mathcal{R}^*_{\mathcal{M}}\setminus\{0\}} |G_{\mathcal{M}}|^{2\sigma}|\hat{f}(G_{\mathcal{M}})| \frac{1}{2N+1}\,.
\end{aligned}$$

Lemma A.1 then implies for any $s > 1$ that

$$\begin{aligned}&\left|\frac{1}{(2N+1)^2}\sum_{R_j\in\mathcal{R}_j(N)} f\big(\{R_j\}_{\mathcal{M}}\big) - \fint_{\Gamma_{\mathcal{M}}} \mathrm{d}x\ f(x)\right| \\ &\leq C_{\sigma,q,A,\theta}\, 4\Big(\frac{\rho_{\mathcal{M}}\|A\|_2}{2\pi}\Big)^{2s}\big(\zeta(2s)+2^{-s}\zeta(s)^2\big) \\ &\sup_{G_{\mathcal{M}}\in\mathcal{R}^*_{\mathcal{M}}} |G_{\mathcal{M}}|^{2(\sigma+s)}|\hat{f}(G_{\mathcal{M}})|\frac{1}{2N+1}\,,\end{aligned} \tag{3.6}$$

where the constant $C_{\sigma,q,A,\theta}$ is the same as in (3.5).

4. Proofs of Results

We now want to show how the ergodic theorems obtained in the previous section can be used to show the existence of the thermodynamic limits of the mechanical energy densities presented above. To that end, we show that the energy densities for lattice truncations can be represented as averages over appropriate periodic functions. In the case of interlayer pair potentials, we show how to represent the resulting limit energy density in a more convenient way.

4.1. Equivalence of Disregistries

Recall the disregistry matrices

$$D_{j\to 3-j} = I - A_{3-j}A_j^{-1}\,;$$

see (2.13) and (2.1) above.

Lemma 4.1. *The disregistry matrices have the following properties:*

(1) $D_{j\to 3-j} = (-1)^j A_{3-j}A_{\mathcal{M}}^{-1}$,
(2) $-D_{3-j\to j}D_{j\to 3-j}^{-1} = -D_{j\to 3-j}^{-1}D_{3-j\to j} = A_jA_{3-j}^{-1} = I - D_{3-j\to j}$,
(3) $|D_{j\to 3-j}^{-1}x| = q^{(-1)^{j+1}1/2}\rho_{\mathcal{M}}^{-1}|x|$,
(4) $|(D_{j\to 3-j}^{-1} - I)x| = q^{(-1)^j 1/2}\rho_{\mathcal{M}}^{-1}|x|$.

Proof. We show the computations for $j = 1$; $j = 2$ can be computed analogously. We have proved (1) already above in (2.13). For (2), we employ (1) and obtain

$$-D_{2\to 1}D_{1\to 2}^{-1} = A_1A_{\mathcal{M}}^{-1}A_{\mathcal{M}}A_2^{-1} = A_1A_2^{-1} = I - D_{2\to 1}\,,$$

where, in the last step, we employ (2.13). Similarly, using (1) again, we have that

$$\begin{aligned}-D_{1\to 2}^{-1}D_{2\to 1} &= A_{\mathcal{M}}A_2^{-1}A_1A_{\mathcal{M}}^{-1} = A_{\mathcal{M}}(A_2^{-1}A_1 - I)A_{\mathcal{M}}^{-1} + I \\ &= -A_{\mathcal{M}}A_{\mathcal{M}}^{-1}A_1A_{\mathcal{M}}^{-1} + I = A_1A_2^{-1}\,.\end{aligned}$$

Observe that, due to (2.1), $|A_2 x| = q^{\frac{1}{2}}|Ax|$. By (1), we thus have that

$$|D_{1\to 2}^{-1}x| \;=\; |A_2 A_{\mathcal{M}}^{-1}x| \;=\; q^{1/2}|A A_{\mathcal{M}}^{-1}x| \;=\; q^{\frac{1}{2}}\rho_{\mathcal{M}}^{-1}|x|\,,$$

where, in the last step, we employed Lemma 2.1. By (2), we have that

$$D_{1\to 2}^{-1} - I \;=\; D_{1\to 2}^{-1}(I - D_{1\to 2}) \;=\; -D_{2\to 1}^{-1}\,,$$

which is why (4) follows from (3). This concludes the proof. □

Lemma 4.1 establishes a relation between the different disregistry notions. Next, we will specify this relation. Define

$$v_{\Gamma_j} \;:=\; A_j \begin{pmatrix} 1 \\ 1 \end{pmatrix}.$$

Lemma 4.2. *Let $R_j \in \mathcal{R}_j$, $j \in \{1,2\}$. Then we have that*

$$\begin{aligned} \{R_1\}_2 \;&=\; D_{1\to 2}\{R_1\}_{\mathcal{M}} \;+\; v_{\Gamma_2}\,, \\ \{R_2\}_1 \;&=\; D_{2\to 1}\{R_2\}_{\mathcal{M}}\,. \end{aligned}$$

Proof. Observe that $A_2 A_k^{-1} R_k \in \mathcal{R}_2$ for $R_k \in \mathcal{R}_k$, $k \in \{1, \mathcal{M}\}$. Hence we find that

$$\begin{aligned} \{R_1\}_2 \;&=\; \{D_{1\to 2}R_1\}_2 \;=\; \left\{-A_2 A_{\mathcal{M}}^{-1} R_1\right\}_2 \\ &=\; \left\{-A_2 A_{\mathcal{M}}^{-1}\{R_1\}_{\mathcal{M}}\right\}_2 \;=\; D_{1\to 2}\{R_1\}_{\mathcal{M}} + v_{\Gamma_2} \in \Gamma_2\,, \end{aligned}$$

where, in the last step, we used the fact that $v_{\Gamma_2} \in \mathcal{R}_2$. The second identity follows analogously. This concludes the proof. □

Remark 4.3. Lemma 4.2 is sensitive to the lattice origin. More precisely, there is no affine map between $\{x\}_{3-j}$ and $\{x\}_{\mathcal{M}}$ for general $x \in \mathbb{R}^2$. In fact, assume that there is a matrix M such that for all $x \in \mathbb{R}^2$,

$$x \;=\; M(x + \mathcal{R}_{\mathcal{M}}) \;+\; \mathcal{R}_{3-j}\,.$$

In particular, this requires $M\mathcal{R}_{\mathcal{M}} \subseteq \mathcal{R}_{3-j}$, which implies

$$M \in A_{\mathcal{M}}^{-1} A_{3-j}\mathbb{Z}^{2\times 2}\,.$$

However, e.g., $(I - M)\sqrt{2}v_{\Gamma_{3-j}} \notin \mathcal{R}_{3-j}$. Thus, no such M exists.

4.2. Lattice Reduction Formulae

Recall definitions (2.28) of $\Psi_j^{(\mathrm{inter})}[\mathbf{u}]$ and (2.30) of $\Phi_{j,\boldsymbol{\gamma}}^{(\mathrm{inter})}[\mathbf{u}]$.

Lemma 4.4. *For all $x \in \mathbb{R}^2$ and all $\gamma_{3-j} \in \Gamma_{3-j}$, we have that*

$$\frac{1}{|\Gamma_j|} \sum_{\alpha_j \in \mathcal{A}_j} V_{j,\alpha_j}^{(\mathrm{inter})} \left(\Big(Y_j(x, \alpha_j) \, - \, Y_{3-j}(R_{3-j} + \gamma_{3-j}, \alpha_{3-j}) \Big)_{\substack{R_{3-j} \in \mathcal{R}_{3-j}, \\ \alpha_{3-j} \in \mathcal{A}_{3-j}}} \right)$$
$$= \Psi_j^{(\mathrm{inter})}[\mathbf{u}](\{x\}_{\mathcal{M}}, \{x - \gamma_{3-j}\}_{3-j}) .$$

In the case $x = R_j \in \mathcal{R}_j$ and $\gamma_{3-j} = 0$, we even have

$$\frac{1}{|\Gamma_j|} \sum_{\alpha_j \in \mathcal{A}_j} V_{j,\alpha_j}^{(\mathrm{inter})} \left(\Big(Y_j(R_j, \alpha_j) \, - \, Y_{3-j}(R_{3-j}, \alpha_{3-j}) \Big)_{\substack{R_{3-j} \in \mathcal{R}_{3-j}, \\ \alpha_{3-j} \in \mathcal{A}_{3-j}}} \right)$$
$$= \Phi_{j,0}^{(\mathrm{inter})}[\mathbf{u}](\{R_j\}_{\mathcal{M}}) .$$

Proof. By translation-invariance of $V_{j,\alpha_j}^{(\mathrm{inter})}$, we may shift the index

$$R_{3-j} \to R_{3-j} + \lfloor x - \gamma_{3-j} \rfloor_{3-j} .$$

Employing $\mathcal{R}_{\mathcal{M}}$-periodicity of u_j and definition (2.17) of $\lfloor x \rfloor_{3-j}$, the first claim then follows from definition (2.28).

In the case $x = R_j \in \mathcal{R}_j$ and $\gamma_{3-j} = 0$, recall from Lemma 4.2 that

$$\{R_j\}_{3-j} \, = \, D_{j \to 3-j} \{R_j\}_{\mathcal{M}} \, + \, v_{\Gamma_2} \delta_{j,1} .$$

Then the statement follows from (2.30) after shifting $R_{3-j} \to R_{3-j} + v_{\Gamma_2} \delta_{j,1}$ and using translation-invariance. This concludes the proof. □

Define for all $y \in \mathbb{R}^2$

$$\begin{aligned} g_{j,\boldsymbol{\alpha},\gamma_{3-j}}(y) \, := \tau_j^{(\alpha_j)} - \tau_{3-j}^{(\alpha_{3-j})} \, + \, u_j(D_{j \to 3-j}^{-1}(y + \gamma_{3-j}), \alpha_j) \\ - \, u_{3-j}(D_{j \to 3-j}^{-1}(y + \gamma_{3-j}) - y, \alpha_{3-j}) . \end{aligned} \tag{4.1}$$

We now establish sufficient conditions on the pair potentials $v_{\boldsymbol{\alpha}}$ for the ergodic theorems above to be applicable.

Lemma 4.5. *Let $r > 1$. Assume that, for $\alpha_j \in \mathcal{A}_j$, $j = 1, 2$, $u_j(\cdot, \alpha_j) \in L^\infty(\Gamma_{\mathcal{M}})$, and that $f \in L^\infty_{2r}(\mathbb{R}^2 \times [-L^z_{\mathbf{u}}, L^z_{\mathbf{u}}])$. Then we have that*

$$\int_{\mathbb{R}^2} \mathrm{d}x \, |f(x + g_{j,\boldsymbol{\alpha},\gamma_{3-j}}(x))| \, \leq \frac{5^{r-1}\pi}{r-1} \left(1 + d_{\mathcal{A}_1,\mathcal{A}_2} \, + \, \|u_1\|_\infty + \|u_2\|_\infty\right)^{2r}$$
$$\|\langle \cdot \rangle^{2r} f\|_{L^\infty(\mathbb{R}^2 \times [-L^z_{\mathbf{u}}, L^z_{\mathbf{u}}])} .$$

Proof. Recalling definition 2.2 of $\langle\cdot\rangle$, we have that

$$\begin{aligned}&\int_{\mathbb{R}^2} \mathrm{d}x\ |f(x+g_{j,\boldsymbol{\alpha},\gamma_{3-j}}(x))|\\ &\quad\leq \|\langle\cdot\rangle^{2r} f(\cdot+g_{j,\boldsymbol{\alpha},\gamma_{3-j}})\|_{L^\infty(\mathbb{R}^2)} \int_{\mathbb{R}^2} \mathrm{d}x\ \langle x\rangle^{-2r}\,.\end{aligned} \tag{4.2}$$

Observe that

$$\begin{aligned}\langle x+y\rangle^{2r} &= (1+|x+y|^2)^r\\ &\leq \big(1+2(|x|^2+|y|^2)\big)^r\,,\end{aligned}$$

by Cauchy-Schwarz and monotonicity of $t\mapsto t^r$. Using convexity of $t\mapsto t^r$, we thus find that

$$\begin{aligned}\langle x+y\rangle^{2r} &\leq 5^r\Big(\frac{1}{5}+\frac{2}{5}\big(|x|^2+|y|^2\big)\Big)^r\\ &\leq 2\cdot 5^{r-1}\big(1+|x|^{2r}+|y|^{2r}\big)\,.\end{aligned} \tag{4.3}$$

Recall from (2.31) that

$$d_{\mathcal{A}_1,\mathcal{A}_2} = \max_{\substack{\alpha_j\in\mathcal{A}_j\\ j=1,2}} |\tau_1^{(\alpha_1)}-\tau_2^{(\alpha_2)}|\,.$$

The definition (4.1) of $g_{j,\boldsymbol{\alpha},\gamma_{3-j}}$ thus implies

$$\|g_{j,\boldsymbol{\alpha},\gamma_{3-j}}\|_\infty \leq d_{\mathcal{A}_1,\mathcal{A}_2} + \|u_1\|_\infty + \|u_2\|_\infty\,, \tag{4.4}$$

and that

$$\|(g_{j,\boldsymbol{\alpha},\gamma_{3-j}})_z\|_\infty \leq d_{\mathcal{A}_1,\mathcal{A}_2} + \|u_{1,z}\|_\infty + \|u_{2,z}\|_\infty = L^z_{\mathbf{u}}\,, \tag{4.5}$$

see definition (2.32) of $L^z_{\mathbf{u}}$. A straight-forward computation yields

$$\int_{\mathbb{R}^2} \mathrm{d}x\ \langle x\rangle^{-2r} = \frac{\pi}{2(r-1)}\,. \tag{4.6}$$

In addition, observe that for any $x\in\ell^1(\mathbb{Z})$ we have that

$$\|x\|_{\ell^r} \leq \|x\|_{\ell^\infty}^{\frac{r-1}{r}} \|x\|_{\ell^1}^{\frac{1}{r}} \leq \|x\|_{\ell^1}\,. \tag{4.7}$$

Collecting (4.3), (4.4), (4.5), and (4.6), (4.2) implies

$$\begin{aligned}&\int_{\mathbb{R}^2} \mathrm{d}x\ |f(x+g_{j,\boldsymbol{\alpha},\gamma_{3-j}}(x))|\\ &\quad\leq \frac{5^{r-1}\pi}{r-1}\Big(\|\big(1+|\cdot+g_{j,\boldsymbol{\alpha},\gamma_{3-j}}|^{2r}\big) f(\cdot+g_{j,\boldsymbol{\alpha},\gamma_{3-j}})\|_{L^\infty(\mathbb{R}^2)}\\ &\qquad + \||g_{j,\boldsymbol{\alpha},\gamma_{3-j}}|^{2r} f(\cdot+g_{j,\boldsymbol{\alpha},\gamma_{3-j}})\|_{L^\infty(\mathbb{R}^2)}\Big)\\ &\quad\leq \frac{5^{r-1}\pi}{r-1}\big(1+d_{\mathcal{A}_1,\mathcal{A}_2} + \|u_1\|_\infty+\|u_2\|_\infty\big)^{2r}\\ &\quad\|\langle\cdot\rangle^{2r} f\|_{L^\infty(\mathbb{R}^2\times[-L^z_{\mathbf{u}},L^z_{\mathbf{u}}])}\,,\end{aligned}$$

where, in the last step, we applied (4.7). This concludes the proof. □

Lemma 4.6. *Let $r > 1$ and $\gamma_{3-j} \in \Gamma_{3-j}$. Assume that, for $\alpha_j \in \mathcal{A}_j$, $j = 1, 2$, $u_j(\cdot, \alpha_j) \in L^\infty(\Gamma_\mathcal{M})$, and that*

$$v_{\boldsymbol{\alpha}} \in L^\infty_{2r}(\mathbb{R}^2 \times [-L^z_{\mathbf{u}}, L^z_{\mathbf{u}}])\,.$$

Then we have that $\Phi^{(\mathrm{inter})}_{j,\boldsymbol{\gamma}}[\mathbf{u}] \in L^1(\Gamma_\mathcal{M})$ and that

$$\begin{aligned}
&\mathcal{F}_{\Gamma_\mathcal{M}}(\Phi^{(\mathrm{inter})}_{j,\boldsymbol{\gamma}}[\mathbf{u}])(G_\mathcal{M}) \\
&\quad = \frac{1}{2|\Gamma_\mathcal{M}|} \sum_{\substack{\alpha_k \in \mathcal{A}_k \\ k=1,2}} \int_{\mathbb{R}^2} \mathrm{d}x\; e^{-iG_\mathcal{M}\cdot(A_j x + \gamma_j)} v_{\boldsymbol{\alpha}}\big(A_1 x + \gamma_1 + \tau_1^{(\alpha_1)} \\
&\qquad + u_1(A_1 x + \gamma_1, \alpha_1) - A_2 x - \gamma_2 - \tau_2^{(\alpha_2)} - u_2(A_2 x + \gamma_2, \alpha_2)\big)\,.
\end{aligned}$$

In particular, we have that

$$\fint_{\Gamma_\mathcal{M}} \mathrm{d}x\; \Phi^{(\mathrm{inter})}_{j,\boldsymbol{\gamma}}[\mathbf{u}](x) \;=\; \fint_{\Gamma_\mathcal{M}} \mathrm{d}x\; \Phi^{(\mathrm{inter})}_{3-j,\boldsymbol{\gamma}}[\mathbf{u}](x)\,.$$

Proof. Assume that $v_{\boldsymbol{\alpha}}$ and u_j are simple functions. Interchanging integration and summation, we then have that

$$\begin{aligned}
&\mathcal{F}_{\Gamma_\mathcal{M}}(\Phi^{(\mathrm{inter})}_{j,\boldsymbol{\gamma}}[\mathbf{u}])(G_\mathcal{M}) \\
&\quad = \frac{1}{2|\Gamma_j|} \sum_{\substack{\alpha_k \in \mathcal{A}_k \\ k=1,2}} \sum_{R_{3-j} \in \mathcal{R}_{3-j}} \fint_{\Gamma_\mathcal{M}} \mathrm{d}x\; e^{-iG_\mathcal{M}\cdot x} v_{\boldsymbol{\alpha}}\big(D_{j\to 3-j} x - R_{3-j} \\
&\qquad + A_{3-j}A_j^{-1}\gamma_j - \gamma_{3-j} + \tau_j^{(\alpha_j)} - \tau_{3-j}^{(\alpha_{3-j})} + u_j(x, \alpha_j) \\
&\qquad - u_{3-j}(R_{3-j} + A_{3-j}A_j^{-1}\gamma_j + \gamma_{3-j} + (I - D_{j\to 3-j})x, \alpha_{3-j})\big)\,.
\end{aligned}$$

Substituting $y := D_{j\to 3-j}x + A_{3-j}A_j^{-1}\gamma_j - R_{3-j} - \gamma_{3-j}$ and interchanging integration and summation again, we obtain

$$\begin{aligned}
\mathcal{F}_{\Gamma_\mathcal{M}}(\Phi^{(\mathrm{inter})}_{j,\boldsymbol{\gamma}}[\mathbf{u}])(G_\mathcal{M}) = \frac{|\det(D^{-1}_{j\to 3-j})|}{2|\Gamma_\mathcal{M}||\Gamma_j|} &\sum_{\substack{\alpha_k \in \mathcal{A}_k \\ k=1,2}} \int_{\mathbb{R}^2} \mathrm{d}y \\
&\sum_{R_{3-j} \in \mathcal{R}_{3-j}} e^{-iG_\mathcal{M}\cdot D^{-1}_{j\to 3-j}(y - A_{3-j}A_j^{-1}\gamma_j + R_{3-j} + \gamma_{3-j})} \\
&\mathbb{1}_{D_{j\to 3-j}\Gamma_\mathcal{M} + A_{3-j}A_j^{-1}\gamma_j - R_{3-j} - \gamma_{3-j}}(y)\, v_{\boldsymbol{\alpha}}\Big(y + \tau_j^{(\alpha_j)} - \tau_{3-j}^{(\alpha_{3-j})} \\
&+ u_j(D^{-1}_{j\to 3-j}(y - A_{3-j}A_j^{-1}\gamma_j + R_{3-j} + \gamma_{3-j}), \alpha_j) \\
&- u_{3-j}(D^{-1}_{j\to 3-j}(y - A_{3-j}A_j^{-1}\gamma_j + R_{3-j} + \gamma_{3-j}) - y, \alpha_{3-j})\Big)\,.
\end{aligned} \tag{4.8}$$

Observe that, by (2.13), (2.13), (2.3), and (2.12),

$$|\det(D_{j\to 3-j})| \;=\; \frac{|\det(A_{3-j})|}{|\det(A_\mathcal{M})|} \;=\; \frac{|\Gamma_{3-j}|}{|\Gamma_\mathcal{M}|}\,. \tag{4.9}$$

In addition, by (2.13), (2.13), and (2.6), we have that

$$D_{j\to 3-j}^{-T}\mathcal{R}_{\mathcal{M}}^{*} \;=\; \mathcal{R}_{3-j}^{*}\,. \tag{4.10}$$

Furthermore, Lemma 4.2 implies that

$$D_{j\to 3-j}\Gamma_{\mathcal{M}} \;=\; (-1)^{j}\Gamma_{3-j}\,, \tag{4.11}$$

and that

$$D_{j\to 3-j}^{-1}\mathcal{R}_{3-j} \;=\; \mathcal{R}_{\mathcal{M}}\,. \tag{4.12}$$

Collecting (4.9), (4.10), (4.11), (4.12), and using the facts that

$$\bigcup_{R_{3-j}\in\mathcal{R}_{3-j}} \big((-1)^{j}\Gamma_{3-j} - R_{3-j} - \gamma_{3-j}\big) \;=\; \mathbb{R}^2\,,$$

and that $u_k(\cdot,\alpha_k)$ is $\mathcal{R}_{\mathcal{M}}$-periodic, (4.8) yields

$$\begin{aligned}
&\mathcal{F}_{\Gamma_{\mathcal{M}}}(\Phi_{j,\boldsymbol{\gamma}}^{(\mathrm{inter})}[\mathbf{u}])(G_{\mathcal{M}})\\
&\quad= \frac{1}{2|\Gamma_1||\Gamma_2|}\sum_{\substack{\alpha_k\in\mathcal{A}_k\\ k=1,2}}\int_{\mathbb{R}^2}\mathrm{d}y\; e^{-iG_{\mathcal{M}}\cdot D_{j\to 3-j}^{-1}(y-A_{3-j}A_j^{-1}\gamma_j+\gamma_{3-j})}\\
&\quad v_{\boldsymbol{\alpha}}\Big(y+\tau_j^{(\alpha_j)}-\tau_{3-j}^{(\alpha_{3-j})}\\
&\quad+u_j(D_{j\to 3-j}^{-1}(y-A_{3-j}A_j^{-1}\gamma_j+\gamma_{3-j}),\alpha_j)\\
&\quad-u_{3-j}(D_{j\to 3-j}^{-1}(y-A_{3-j}A_j^{-1}\gamma_j+\gamma_{3-j})-y,\alpha_{3-j})\Big)\,.
\end{aligned} \tag{4.13}$$

Using the fact that

$$A_j - A_{3-j} \;=\; D_{j\to 3-j}A_j \;=\; (-1)^{j}A_{3-j}A_{\mathcal{M}}^{-1}A_j\,,$$

see Lemma 4.1, and substituting $y=(A_j-A_{3-j})\xi+\gamma_j-\gamma_{3-j}$, we obtain

$$\begin{aligned}
&\mathcal{F}_{\Gamma_{\mathcal{M}}}(\Phi_{j,\boldsymbol{\gamma}}^{(\mathrm{inter})}[\mathbf{u}])(G_{\mathcal{M}})\\
&\quad= \frac{1}{2|\Gamma_{\mathcal{M}}|}\sum_{\substack{\alpha_k\in\mathcal{A}_k\\ k=1,2}}\int_{\mathbb{R}^2}\mathrm{d}\xi\; e^{-iG_{\mathcal{M}}\cdot(A_j\xi+\gamma_j)}v_{\boldsymbol{\alpha}}\big(A_1\xi+\gamma_1+\tau_1^{(\alpha_1)}\\
&\qquad+u_1(A_1\xi+\gamma_1,\alpha_1)-A_2\xi-\gamma_2-\tau_2^{(\alpha_2)}-u_2(A_2\xi+\gamma_2,\alpha_2)\big)\,,
\end{aligned} \tag{4.14}$$

where we also employed that $v_{\boldsymbol{\alpha}}$ is even. Due to Lemma 4.5, we can extend (4.13), and thus (4.14), to all

$$v_{\boldsymbol{\alpha}} \in L^{\infty}_{2r}(\mathbb{R}^2\times[-L_{\mathbf{u}}^{z},L_{\mathbf{u}}^{z}])\,.$$

This finishes the proof. □

Define for almost all $x, y \in \mathbb{R}^2$

$$h_{j,\boldsymbol{\alpha}}(x, y) := \tau_j^{(\alpha_j)} - \tau_{3-j}^{(\alpha_{3-j})} + u_j(x, \alpha_j) - u_{3-j}(x - y, \alpha_{3-j}) .$$

For a pair-potential (2.26), (2.28) becomes

$$\Psi_j^{(\text{inter})}[\mathbf{u}](x, y) = \frac{1}{2|\Gamma_j|} \sum_{\substack{\alpha_k \in \mathcal{A}_k \\ k=1,2}} \sum_{\substack{R_{3-j} \\ \in \mathcal{R}_{3-j}}} v_{\boldsymbol{\alpha}}\big(y - R_{3-j} + h_{j,\boldsymbol{\alpha}}(x, y - R_{3-j})\big) .$$

Lemma 4.7. *Let $r > 1$. Assume that, for $\alpha_j \in \mathcal{A}_j$, $j = 1, 2$, $u_j(\cdot, \alpha_j) \in L^\infty(\Gamma_\mathcal{M})$, and that*

$$v_{\boldsymbol{\alpha}} \in L^\infty_{2r}(\mathbb{R}^2 \times [-L^z_{\mathbf{u}}, L^z_{\mathbf{u}}]) .$$

Then we have that $\Psi_j^{(\text{inter})}[\mathbf{u}] \in L^1(\Gamma_\mathcal{M} \times \Gamma_{3-j})$.

Proof. The idea of this proof follows the steps in the proofs of the two previous Lemmata. As above, assume that $v_{\boldsymbol{\alpha}}$ and u_j are simple functions.

Let

$$\psi(x, y) := \frac{1}{2|\Gamma_j|} \sum_{\substack{\alpha_k \in \mathcal{A}_k \\ k=1,2}} v_{\boldsymbol{\alpha}}\big(y + h_{j,\boldsymbol{\alpha}}(x, y)\big) .$$

Then we have that

$$\begin{aligned} &\int_{\Gamma_\mathcal{M}} \mathrm{d}x \int_{\Gamma_{3-j}} \mathrm{d}y \, |\Psi_j^{(\text{inter})}[\mathbf{u}](x, y)| \\ &\quad \le \sum_{R_{3-j} \in \mathcal{R}_{3-j}} \int_{\Gamma_\mathcal{M}} \mathrm{d}x \int_{\Gamma_{3-j}} \mathrm{d}y \, |\psi(x - R_{3-j}, y)| . \end{aligned}$$

Shifting $x - R_{3-j} \to x$, we obtain

$$\begin{aligned} &\int_{\Gamma_\mathcal{M}} \mathrm{d}x \int_{\Gamma_{3-j}} \mathrm{d}y \, |\Psi_j^{(\text{inter})}[\mathbf{u}](x, y)| \\ &\quad \le \sum_{R_{3-j} \in \mathcal{R}_{3-j}} \int_{\Gamma_{3-j} - R_{3-j}} \mathrm{d}x \int_{\Gamma_\mathcal{M}} \mathrm{d}y \, |\psi(x, y)| \\ &\quad = \int_{\mathbb{R}^2} \mathrm{d}x \int_{\Gamma_\mathcal{M}} \mathrm{d}y \, |\psi(x, y)| , \end{aligned} \tag{4.15}$$

where, again, we used the fact that

$$\bigcup_{R_{3-j} \in \mathcal{R}_{3-j}} \big(\Gamma_{3-j} - R_{3-j}\big) = \mathbb{R}^2 .$$

Due to

$$\int_{\mathbb{R}^2} \mathrm{d}x \, \langle x \rangle^{-2r} \, < \, \infty$$

for $r > 1$, (4.15) implies

$$\begin{aligned} &\int_{\Gamma_{\mathcal{M}}} \mathrm{d}x \int_{\Gamma_{3-j}} \mathrm{d}y \, |\Psi_j^{(\mathrm{inter})}[\mathbf{u}](x,y)| \\ &\lesssim \|\langle x \rangle^{2r} \psi(x,y)\|_{L^\infty_{x,y}} \, . \end{aligned}$$

With analogous steps as in the proof of Lemma 4.5, we have that

$$\begin{aligned} \|\langle x \rangle^{2r} \psi(x,y)\|_{L^\infty_{x,y}} \lesssim (1 + d_{\mathcal{A}_1,\mathcal{A}_2} + \|u_1\|_\infty + \|u_2\|_\infty)^{2r} \\ \sum_{\substack{\alpha_k \in \mathcal{A}_k \\ k=1,2}} \|\langle \cdot \rangle^{2r} v_{\boldsymbol{\alpha}}\|_{L^\infty(\mathbb{R}^2 \times [-L^z_{\mathbf{u}}, L^z_{\mathbf{u}}])} \, < \, \infty \end{aligned}$$

by assumption on $v_{\boldsymbol{\alpha}}$. This concludes the proof. □

4.3. Proofs of Main Theorems

Proof of Theorem 2.10. We are left with proving the upper bound in the case of interlayer pair potentials. Observe that, due to $\sigma > \frac{1433}{1248}$ and $s > 1$, we have that $\lceil \sigma + s \rceil \geq 3$. We choose $s = 3 - \sigma$ for some $\sigma \in \left(\frac{1433}{1248}, 2\right)$.

Employing the first part of the theorem, we have that

$$|e^{(\mathrm{inter})}_{j,N,0}(\mathbf{u}) - e^{(\mathrm{inter})}_{j,0}(\mathbf{u})| \, \leq \, \frac{\mathrm{err}^{(\mathrm{MB})}}{2N+1} \tag{4.16}$$

with $\mathrm{err}^{(\mathrm{MB})}$ given in (2.36), with the choice $s = 3 - \sigma$, $\ell = \mathrm{inter}$, by

$$\begin{aligned} \mathrm{err}^{(\mathrm{MB})}_j \, = \, &\frac{2\sqrt{2}}{K} \Big(\frac{\rho_{\mathcal{M}} \|A\|_2}{2\pi} \Big)^6 \big(\zeta(6 - 2\sigma) + 2^{\sigma-3} \zeta(3-\sigma)^2 \big) \\ &\sup_{G_{\mathcal{M}} \in \mathcal{R}^*_{\mathcal{M}}} |G_{\mathcal{M}}|^6 |\mathcal{F}_{\Gamma_{\mathcal{M}}}(\Phi^{(\mathrm{inter})}_{j,0}[\mathbf{u}])(G_{\mathcal{M}})| \, . \end{aligned} \tag{4.17}$$

Since $\sigma \in \left(\frac{1433}{1248}, 2\right)$ was arbitrary, (4.16) and (4.17) imply

$$\begin{aligned} |e^{(\mathrm{inter})}_{j,N,0}(\mathbf{u}) - e^{(\mathrm{inter})}_{j,0}(\mathbf{u})| \, \leq &2\sqrt{2} \Big(\frac{\sqrt{3}|\Gamma_{\mathcal{M}}|}{2^3 \pi^2} \Big)^3 M^{(\mathrm{pair})}(\theta) \\ &\sup_{G_{\mathcal{M}} \in \mathcal{R}^*_{\mathcal{M}}} |G_{\mathcal{M}}|^6 |\mathcal{F}_{\Gamma_{\mathcal{M}}}(\Phi^{(\mathrm{inter})}_{j,0}[\mathbf{u}])(G_{\mathcal{M}})| \, , \end{aligned} \tag{4.18}$$

where we recall definition (2.37) of $M^{(\mathrm{pair})}(\theta)$. (4.13) in the proof of Lemma 4.6 implies

$$\begin{aligned}
&\mathcal{F}_{\Gamma_{\mathcal{M}}}(\Phi^{(\mathrm{inter})}_{j,\boldsymbol{\gamma}}[\mathbf{u}])(G_{\mathcal{M}}) \\
&\quad = \frac{1}{2|\Gamma_1||\Gamma_2|} \sum_{\substack{\alpha_k \in \mathcal{A}_k \\ k=1,2}} \int_{\mathbb{R}^2} \mathrm{d}y \, e^{-iD^{-T}_{j\to 3-j} G_{\mathcal{M}}\cdot(y+\gamma_{3-j})} v_{\boldsymbol{\alpha}}\big(y + \tau_j^{(\alpha_j)} \\
&\qquad - \tau_{3-j}^{(\alpha_{3-j})} + u_j(D^{-1}_{j\to 3-j} y, \alpha_j) - u_{3-j}(D^{-1}_{j\to 3-j} y - y, \alpha_{3-j})\big) .
\end{aligned}$$

In particular, we have that $\mathcal{F}_{\Gamma_{\mathcal{M}}}(\Phi^{(\mathrm{inter})}_{j,0}[\mathbf{u}])(0) = e^{(\mathrm{inter})}_{j,0}(\mathbf{u})$. As in (4.1), we define

$$g_{j,\boldsymbol{\alpha}}(y) := \tau_j^{(\alpha_j)} - \tau_{3-j}^{(\alpha_{3-j})} + u_j(D^{-1}_{j\to 3-j} y, \alpha_j) - u_{3-j}(D^{-1}_{j\to 3-j} y - y, \alpha_{3-j}) . \tag{4.19}$$

Now let $\sigma \in \left(\frac{1433}{1248}, 2\right)$ be arbitrary. Using Lemma 4.1 and the definition of the fractional derivative $|\nabla|$ via Fourier multiplication, we find that

$$\begin{aligned}
&|G_{\mathcal{M}}|^6 \mathcal{F}_{\Gamma_{\mathcal{M}}}(\Phi^{(\mathrm{inter})}_{j,0}[\mathbf{u}])(G_{\mathcal{M}}) \\
&\quad = \frac{1}{2|\Gamma_1||\Gamma_2|} \Big(\frac{\rho_{\mathcal{M}}}{q^{(-1)^{j+1}1/2}}\Big)^6 \sum_{\substack{\alpha_k \in \mathcal{A}_k \\ k=1,2}} \int_{\mathbb{R}^2} \mathrm{d}y \, e^{-iD^{-T}_{j\to 3-j} G_{\mathcal{M}}\cdot y} \\
&|\nabla_y|^6 \Big(v_{\boldsymbol{\alpha}}\big(y + g_{j,\boldsymbol{\alpha}}(y)\big)\Big) \\
&\quad \leq \frac{1}{2|\Gamma_1||\Gamma_2|} \Big(\frac{\rho_{\mathcal{M}}}{q^{(-1)^{j+1}1/2}}\Big)^6 \sum_{\substack{\alpha_k \in \mathcal{A}_k \\ k=1,2}} \|(-\Delta)^3 v_{\boldsymbol{\alpha}}(\cdot + g_{j,\boldsymbol{\alpha}})\|_1 .
\end{aligned} \tag{4.20}$$

For any $n \in \mathbb{N}$, define

$$R(n) := \{\mathbf{r}_n \in \mathbb{N}_0^n \mid \sum_{j=1}^n j r_j = n\} . \tag{4.21}$$

Using the Faá di Bruno formula and recalling (4.21), we have that

$$\begin{aligned}
&\|(-\Delta)^3 v_{\boldsymbol{\alpha}}(\cdot + g_{j,\boldsymbol{\alpha}})\|_1 \\
&\quad \leq 6! \sum_{\mathbf{r}_6 \in R(6)} \big\| \big(D^{|\mathbf{r}_6|_1} v_{\boldsymbol{\alpha}}\big)(\cdot + g_{j,\boldsymbol{\alpha}})\big\|_1 \\
&\quad \prod_{k=1}^6 \frac{1}{r_k!} \Big(\frac{\delta_{k,1} + \|D^k g_{j,\boldsymbol{\alpha}}\|_\infty}{k!} \Big)^{r_k} \\
&\quad \leq 6! \sum_{\mathbf{r}_6 \in R(6)} \big\| \big(D^{|\mathbf{r}_6|_1} v_{\boldsymbol{\alpha}}\big)(\cdot + g_{j,\boldsymbol{\alpha}})\big\|_1 \\
&\quad \Big(1 + \sum_{k=1}^6 \|D^k g_{j,\boldsymbol{\alpha}}\|_\infty\Big)^{|\mathbf{r}_6|_1} \prod_{k=1}^6 \frac{1}{r_k!(k!)^{r_k}} .
\end{aligned} \tag{4.22}$$

Employing definition (4.21), we obtain that

$$1 \le |\mathbf{r}_6|_1 = \sum_{k=1}^{6} r_k \le \sum_{k=1}^{6} k r_k = 6$$

for all $\mathbf{r}_6 \in R(6)$. Hence, (4.22) yields

$$\|(-\Delta)^3 v_{\boldsymbol{\alpha}}(\cdot + g_{\boldsymbol{\alpha}})\|_1 \le B_6 \sum_{k=1}^{6} \left\| \left(D^k v_{\boldsymbol{\alpha}}\right)(\cdot + g_{j,\boldsymbol{\alpha}}) \right\|_1 \left(1 + \sum_{\ell=1}^{6} \|D^\ell g_{\boldsymbol{\alpha}}\|_\infty\right)^6, \tag{4.23}$$

where

$$B_6 := 6! \sum_{\mathbf{r}_6 \in R(6)} \prod_{k=1}^{6} \frac{1}{r_k!(k!)^{r_k}} = \partial_\lambda^6 \Big|_{\lambda=0} e^{e^\lambda - 1} = 203 \tag{4.24}$$

denotes the 6^{th} Bell number.

Recalling definition (4.19) of $g_{j,\boldsymbol{\alpha}}$ and employing Lemma 4.1, we find that

$$\begin{aligned}
\|D^\ell g_{j,\boldsymbol{\alpha}}\|_\infty \le & \|D^\ell u_j(D_{j\to 3-j}^{-1}(\cdot), \alpha_j)\|_\infty \\
& + \|D^\ell u_{3-j}((D_{j\to 3-j}^{-1} - I)(\cdot), \alpha_{3-j})\|_\infty \\
\le & \left(\frac{q^{(-1)^{j+1}1/2}}{\rho_{\mathcal{M}}}\right)^\ell \|D^\ell u_1(\cdot, \alpha_1)\|_\infty \\
& + \left(\frac{q^{(-1)^{j}1/2}}{\rho_{\mathcal{M}}}\right)^\ell \|D^\ell u_2(\cdot, \alpha_2)\|_\infty \\
\le & \frac{q^{(-1)^{j+1}\ell/2} + q^{(-1)^{j}\ell/2}}{\rho_{\mathcal{M}}^\ell} \left(\|D^\ell u_1\|_\infty + \|D^\ell u_2\|_\infty\right).
\end{aligned} \tag{4.25}$$

Lemma 4.5 implies

$$\begin{aligned}
& \left\| \left(D^k v_{\boldsymbol{\alpha}}\right)(\cdot + g_{j,\boldsymbol{\alpha}}) \right\|_1 \\
& \quad \le \frac{5^{r-1}\pi}{r-1} \left(1 + d_{\mathcal{A}_1,\mathcal{A}_2} + \|u_1\|_\infty + \|u_2\|_\infty\right)^{2r} \\
& \quad \|\langle\cdot\rangle^{2r} \left(D^k v_{\boldsymbol{\alpha}}\right)\|_{L^\infty(\mathbb{R}^2 \times [-L_{\mathbf{u}}^z, L_{\mathbf{u}}^z])}.
\end{aligned} \tag{4.26}$$

Collecting (4.20), (4.22), (4.23), (4.24), (4.25), and (4.26), and recalling the weighted Sobolev norm (2.33), we obtain

$$\begin{aligned}
& \sup_{G_{\mathcal{M}}} \left| |G_{\mathcal{M}}|^6 \mathcal{F}_{\Gamma_{\mathcal{M}}}(\Phi_{j,0}^{(\text{inter})}[\mathbf{u}])(G_{\mathcal{M}}) \right| \\
& \quad \le 203 \frac{1 + q^{(-1)^j 6}}{2|\Gamma_1||\Gamma_2|} \frac{5^{r-1}\pi}{r-1} \\
& \quad \left(1 + d_{\mathcal{A}_1,\mathcal{A}_2} + \|u_1\|_{W^{6,\infty}} + \|u_2\|_{W^{6,\infty}}\right)^{6+2r} \\
& \quad \sum_{\substack{\alpha_k \in \mathcal{A}_k \\ k=1,2}} \|v_{\boldsymbol{\alpha}}\|_{W_{2r}^{6,\infty}(\mathbb{R}^2 \times [-L_{\mathbf{u}}^z, L_{\mathbf{u}}^z])}.
\end{aligned}$$

Together with (4.18), this concludes the proof. □

Proof of Theorem 2.17. We are left with proving that the conditions in the case of interlayer pair potentials are sufficient.

Lemma 4.7 implies that $\Psi_j^{(\mathrm{inter})}[\mathbf{u}] \in L^1(\Gamma_{\mathcal{M}} \times \Gamma_{3-j})$. Moreover, Lemma 4.6 implies that $\Phi_1^{(\mathrm{inter})}[u] \in L^1(\Gamma_{\mathcal{M}})$. Thus, the conditions of Proposition 3.3 are satisfied. □

Acknowledgements. MH's and ML's research was partially supported by Targeted Grant Award No. 896630 through the Simons Foundation. AW's and ML's research was supported in part by DMREF Award No. 1922165 through the National Science Foundation. AW's research was supported in part by DMS Award No. 2406981 through the National Science Foundation. The authors are grateful to Eric Cancès and Xiaowen Zhu for helpful comments on the first version of the manuscript. The authors are grateful to Tianyu Kong for providing Figs. 1 and 3. The authors would like to thank Dmitriy Bilyk, Max Chaudkhari, Max Engelstein, Fabian Faustlich, and Ziyan (Zoe) Zhu for helpful comments, stimulating discussions, and for pointing out helpful references.

Data availablity The manuscript has no associated data.

Declarations

financial or non-financial interests The authors do not declare financial or non-financial interests that are directly or indirectly related to the work submitted for publication.

Publisher's Note Springer Nature remains neutral with regard to jurisdictional claims in published maps and institutional affiliations.

Springer Nature or its licensor (e.g. a society or other partner) holds exclusive rights to this article under a publishing agreement with the author(s) or other rightsholder(s); author self-archiving of the accepted manuscript version of this article is solely governed by the terms of such publishing agreement and applicable law.

A. Lattice Calculus

Proof of Lemma 2.1. By definitions (2.8) and (2.1), we have that

$$A_{\mathcal{M}} = (A_1^{-1} - A_2^{-1})^{-1} = (q^{1/2}R_{\theta/2} - q^{-1/2}R_{-\theta/2})^{-1}A\,. \tag{A.1}$$

Consequently, we obtain that

$$B_{\mathcal{M}} = (q^{1/2}R_{-\theta/2} - q^{-1/2}R_{\theta/2})2\pi\, A^{-T}\,. \tag{A.2}$$

Observe that

$$q^{1/2}R_{\theta/2} - q^{-1/2}R_{-\theta/2} = \begin{pmatrix} (q^{1/2} - q^{-1/2})\cos(\theta/2) & -(q^{1/2} + q^{-1/2})\sin(\theta/2) \\ (q^{1/2} + q^{-1/2})\sin(\theta/2) & (q^{1/2} - q^{-1/2})\cos(\theta/2) \end{pmatrix}. \tag{A.3}$$

A straight-forward calculation yields

$$|(q^{1/2}R_{\theta/2} - q^{-1/2}R_{-\theta/2})x|^2 \;=\; [(q^{1/2} - q^{-1/2})^2 \;+\; 4\sin^2(\theta/2)]|x|^2\,.$$

Consequently, we have that

$$|(q^{1/2}R_{\theta/2} - q^{-1/2}R_{-\theta/2})^{-1}x| \;=\; [(q^{1/2} - q^{-1/2})^2 \;+\; 4\sin^2(\theta/2)]^{-\frac{1}{2}}|x|\,.$$

Together with (A.1) resp. (A.2), this concludes the proof. □

Proof of Proposition 2.16. By Proposition 3.1, let $(\mathcal{N}_{G_\mathcal{M}}))_{G_\mathcal{M}\in\mathcal{R}^*_\mathcal{M}}$ be a sequence of nullsets such that for all $G_\mathcal{M} \in \mathcal{R}^*_\mathcal{M}$ and all $\gamma_j \in \Gamma_j \setminus \mathcal{N}_{G_\mathcal{M}}$

$$\begin{aligned}\lim_{N\to\infty} \frac{1}{(2N+1)^2} \sum_{R_j\in\mathcal{R}_j(N)} e^{-iG_\mathcal{M}\cdot(\gamma_j+R_j)}u_j(\gamma_j+R_j,\alpha_j)\\ =\; \fint_{\Gamma_\mathcal{M}} \mathrm{d}x\; e^{-iG_\mathcal{M}\cdot x}u_j(x,\alpha_j) \;=\; \hat{u}_j(G_\mathcal{M},\alpha_j)\,,\end{aligned}$$

where we used the fact that

$$e^{-iG_\mathcal{M}\cdot x} \;=\; e^{-iG_\mathcal{M}\cdot\{x\}_\mathcal{M}}\,.$$

Then

$$\mathcal{N} := \bigcup_{G_\mathcal{M}\in\mathcal{R}^*_\mathcal{M}} \mathcal{N}_{G_\mathcal{M}}$$

is a nullset, and for all $\gamma_j \in \Gamma_j \setminus \mathcal{N}$, we have that

$$\lim_{N\to\infty} \frac{1}{(2N+1)^2} \sum_{R_j\in\mathcal{R}_j(N)} e^{-iG_\mathcal{M}\cdot(\gamma_j+R_j)}u_j(\gamma_j+R_j,\alpha_j) \;=\; \hat{u}_j(G_\mathcal{M},\alpha_j)\,.$$

This concludes the proof. □

Lemma A.1. *Let $s > 1$. Then we have that*

$$\sum_{G_\mathcal{M}\in\mathcal{R}^*_\mathcal{M}\setminus\{0\}} \frac{1}{|G_\mathcal{M}|^{2s}} \;\le\; 4\Big(\frac{\rho_\mathcal{M}\|A\|_2}{2\pi}\Big)^{2s}\big(\zeta(2s) + 2^{-s}\zeta(s)^2\big)\,.$$

Proof. Lemma 2.1 yields

$$\begin{aligned}|B_\mathcal{M}n|^2 \;&=\; (2\pi)^2\rho_\mathcal{M}^{-2}|A^{-T}n|^2\\ &\ge\; (2\pi)^2\rho_\mathcal{M}^{-2}\|A\|_2^{-2}|n|^2 &\text{(A.4a)}\\ &\ge\; 2\cdot(2\pi)^2\rho_\mathcal{M}^{-2}\|A\|_2^{-2}|n_1|\cdot|n_2|\,, &\text{(A.4b)}\end{aligned}$$

where, in the last step, we applied the geometric-quadratic-mean inequality. We split the sum over $\mathcal{R}^*_\mathcal{M} \setminus \{0\}$ into

$$\{B_\mathcal{M}n \mid n_1n_2 = 0, (n_1,n_2) \neq (0,0)\}\dot\cup\{B_\mathcal{M}n \mid n_1,n_2 \neq 0\}\,.$$

Applying (A.4a) on $G_{\mathcal{M}}$ in the first set and (A.4b) on the latter, we obtain

$$\sum_{G_{\mathcal{M}} \in \mathcal{R}^*_{\mathcal{M}} \setminus \{0\}} \frac{1}{|G_{\mathcal{M}}|^{2s}} \leq \left(\frac{\rho_{\mathcal{M}} \|A\|_2}{2\pi}\right)^{2s} \left[4 \sum_{n \in \mathbb{N}} \frac{1}{n^{2s}} + 2^{-s} \left(2 \sum_{n \in \mathbb{N}} \frac{1}{n^s}\right)^2\right]$$
$$= 4 \left(\frac{\rho_{\mathcal{M}} \|A\|_2}{2\pi}\right)^{2s} \left(\zeta(2s) + 2^{-s} \zeta(s)^2\right),$$

where we recognize the Riemann zeta function $\zeta(\sigma) = \sum_{m \in \mathbb{N}} \frac{1}{m^\sigma}$, $\sigma > 1$. This concludes the proof. □

B. Existence of Diophantine 2D Rotations

We now prove Proposition 2.5. It suffices to show that for almost every $\theta \in \mathbb{R}$ and all $\sigma > \frac{1433}{1248}$, there exists $K > 0$ such that for all $n \in \mathbb{Z}^2 \setminus \{0\}$

$$\operatorname{dist}\left(q A^T R_\theta A^{-T} n, \mathbb{Z}^2\right) \geq \frac{K}{|n|^{2\sigma}}$$

holds.

Due to 2π-periodicity of R_θ, it suffices to show that Lebesgue-almost every $\theta \in [0, 2\pi)$ is a Diophantine 2D rotation. We follow the classical strategy to apply the Borel-Cantelli Lemma to the complement. In particular, let

$$\Omega := \bigcap_{\sigma > \frac{1433}{1248}} \bigcup_{\substack{K>0, \\ N \in \mathbb{N}}} \bigcap_{\substack{n \in \mathbb{Z}^2: \\ |n|^2 \geq N}} \bigcap_{m \in \mathbb{Z}^2} \left\{\theta \in [0, 2\pi) \mid |q A^T R_\theta A^{-T} n - m| \geq \frac{K}{|n|^{2\sigma}}\right\}.$$

Ω consists of all $\theta \in [0, 2\pi)$ such that for all $\sigma > \frac{1433}{1248}$ there exists $K > 0$ and $N \in \mathbb{N}$ s.t. for all $n \in \mathbb{Z}^2$ with $|n|^2 \geq N$ we have that

$$\operatorname{dist}\left(q A^T R_\theta A^{-T} n, \mathbb{Z}^2\right) \geq \frac{K}{|n|^{2\sigma}}. \tag{B.1}$$

Taking $\tilde{K} := \min\left\{K, \min_{|n|^2 < N} \operatorname{dist}\left(q A^T R_\theta A^{-T} n, \mathbb{Z}^2\right)\right\}$, we can extend (B.1) to hold for all $n \in \mathbb{Z}^2 \setminus \{0\}$ by lowering K to $\tilde{K}$. Our goal is to show that $|\Omega| = 2\pi$. Let

$$E_N(\sigma) := \bigcap_{K>0} \bigcup_{\substack{n \in \mathbb{Z}^2 \\ |n|^2 = N}} \bigcup_{m \in \mathbb{Z}^2} \left\{\theta \in [0, 2\pi) \mid |q A^T R_\theta A^{-T} n - m| < \frac{K}{|n|^{2\sigma}}\right\}.$$

Since A is invertible, we have that $|A^T \cdot|$ and $|\cdot|$ are equivalent norms. More precisely, we have that

$$\|A^T\|_2^{-1} |A^T v| \leq |v| \leq \|A^{-T}\|_2 |A^T v|, \tag{B.2}$$

where $\|\cdot\|_2$ denotes the spectral/Hilbert-Schmidt norm. In particular, we have that

$$E_N(\sigma) \subseteq \bigcup_{\substack{n\in\mathbb{Z}^2\\ |n|^2=N}} \bigcup_{m\in\mathbb{Z}^2} \left\{\theta\in[0,2\pi) \mid |qR_\theta A^{-T}n - A^{-T}m| < \frac{1}{|n|^{2\sigma}}\right\},$$

In order to apply Borel-Cantelli, we need to control the asymptotic behavior of the Lebesgue measures of the sets E_N in order to study their summability. We have that

$$\begin{aligned}&|E_N(\sigma)|\\ &\leq \sum_{\substack{n\in\mathbb{Z}^2\\ |n|^2=N}} \sum_{\substack{m\in\mathbb{Z}^2\\ \left||A^{-T}m|-|qA^{-T}n|\right|<\frac{1}{|n|^{2\sigma}}}} \int_0^{2\pi} d\theta\, \mathbb{1}_{B_{\frac{1}{|n|^{2\sigma}}}(A^{-T}m)}\big(qR_\theta A^{-T}n\big). \end{aligned} \tag{B.3}$$

Observe that for large $|n|$, we have that $|A^{-T}m| \approx_\sigma |qA^{-T}n|$. In particular, the integrand vanishes unless θ is on an arc of length $\sim |n|^{-2\sigma}$ for a circle of radius $|qA^{-T}n| \sim |n|$, see (B.2), about the angle defined by $A^{-T}n$. In particular, we obtain that

$$\int_0^{2\pi} \mathrm{d}\theta\, \mathbb{1}_{B_{\frac{1}{|n|^{2\sigma}}}(A^{-T}m)}\big(R_\theta A^{-T}n\big) \lesssim_{q,\sigma,A} \frac{1}{|n|^{1+2\sigma}} \tag{B.4}$$

for sufficiently large n. In addition, for $r>0$, Levitan [63] obtained the bound

$$|B_r \cap qA^{-T}\mathbb{Z}^2| = \frac{\pi r^2}{|\det(qA^{-T})|} + O_{r\to\infty}(r^{\frac{2}{3}}),$$

see also [61] for a related works, and also [47]. As a consequence, we find that

$$\begin{aligned}&\sum_{m\in\mathbb{Z}^2} \mathbb{1}_{B_{|n|-2\sigma}(qA^{-T}n)}(A^{-T}m)\\ &\leq \left|\left(B_{|qA^{-T}n|+\frac{1}{|n|^{2\sigma}}} \setminus B_{|qA^{-T}n|-\frac{1}{|n|^{2\sigma}}}\right)\cap A^{-T}\mathbb{Z}^2\right|\\ &= \big(|qA^{-T}n| + \frac{1}{|n|^{2\sigma}}\big)^2 - \big(|qA^{-T}n| - \frac{1}{|n|^{2\sigma}}\big)^2 + O_{|n|\to\infty}(|n|^{\frac{2}{3}})\\ &\lesssim_{q,\sigma,A} |n|^{\frac{2}{3}}, \end{aligned} \tag{B.5}$$

for $2\sigma>1$. In addition, Huxley [51] showed that

$$|B_r\cap\mathbb{Z}^2| = \pi r^2 + O_{r\to\infty}(r^{\frac{131}{208}}\log(r)^{\frac{18627}{8320}}),$$

see also [11,18,60] for recent progress. Consequently, we obtain that

$$\begin{aligned}|\{n\in\mathbb{Z}^2 \mid |n|^2=N\}| &\leq \left|\left((B_{\sqrt{N}+\delta}\setminus B_{\sqrt{N}-\delta})\cap\mathbb{Z}^2\right)\right|\\ &\lesssim N^{\frac{131}{416}+\varepsilon}\end{aligned} \tag{B.6}$$

for any $\delta,\varepsilon>0$.

Collecting (B.4), (B.5), and (B.6), (B.3) yields

$$|E_N(\sigma)| \lesssim_{\sigma,A} N^{\frac{131}{416}+\frac{1}{3}-\frac{1}{2}-\sigma+\varepsilon} = N^{\frac{185}{1248}-\sigma+\varepsilon}$$

for any $N \in \mathbb{N}$ large enough. In particular, choosing any

$$\sigma > \frac{185}{1248} + 1 = \frac{1433}{1248}$$

and any $0 < \varepsilon < \sigma - \frac{1433}{1248}$, we obtain that

$$\sum_{N\in\mathbb{N}} |E_N(\sigma)| < \infty .$$

Then the Borel-Cantelli Lemma yields that

$$\Big| \bigcap_{N_0=1}^{\infty} \bigcup_{N=N_0}^{\infty} E_N(\sigma) \Big| = 0 . \tag{B.7}$$

Observe that $E_N(\sigma)$ is decreasing in σ, i.e.,

$$E_N(\sigma') \subseteq E_N(\sigma)$$

for $\sigma \leq \sigma'$. Thus, and using (B.7), we obtain that

$$\begin{aligned} \Big| \bigcup_{\sigma > \frac{1433}{624}} \bigcap_{N_0=1}^{\infty} \bigcup_{N=N_0}^{\infty} E_N(\sigma) \Big| &\leq \sum_{\ell=1}^{\infty} \Big| \bigcap_{N_0=1}^{\infty} \bigcup_{N=N_0}^{\infty} E_N\big(\frac{1433}{1248} + \frac{1}{\ell}\big) \Big| \\ &= 0 . \end{aligned}$$

Using the fact that

$$\Omega \supseteq \Big(\bigcup_{\sigma > \frac{1433}{1248}} \bigcap_{N_0=1}^{\infty} \bigcup_{N=N_0}^{\infty} E_N(\sigma) \Big)^c ,$$

we finish the proof.

C. Proofs of Ergodic Theorems

Proof of Proposition 3.3. Proposition 3.1 implies almost sure pointwise convergence. For both, almost sure and L^1-convergence, imply convergence in probability, it suffices to compute the L^1-limit. Using standard approximation arguments, we may assume that h is a C^∞-smooth function. By dominated convergence, it suffices the almost sure pointwise limit.
W.l.o.g. we set $j = 1$.

(3.3) implies that

$$\begin{aligned}&\mathcal{A}_{\mathcal{R}_1(N)}(h)(\omega_{\mathcal{M}},\omega_2)\\&\quad=\sum_{\substack{G_2\in\mathcal{R}_2^*,\\ G_{\mathcal{M}}\in\mathcal{R}_{\mathcal{M}}^*}}\mathbb{1}^{(N)}_{\mathcal{R}_1^*}(G_2+G_{\mathcal{M}})\,\hat{h}(G_{\mathcal{M}},G_2)e^{i[G_{\mathcal{M}}\cdot\omega_{\mathcal{M}}+G_2\cdot\omega_2]}\end{aligned}$$

Using dominated convergence, we obtain that

$$\begin{aligned}&\lim_{N\to\infty}\mathcal{A}_{\mathcal{R}_1(N)}(h)(\omega_{\mathcal{M}},\omega_2)\\&\quad=\sum_{\substack{G_2\in\mathcal{R}_2^*,\\ G_{\mathcal{M}}\in\mathcal{R}_{\mathcal{M}}^*}}\mathbb{1}_{\mathcal{R}_1^*}(G_2+G_{\mathcal{M}})\,\hat{h}(G_{\mathcal{M}},G_2)e^{i[G_{\mathcal{M}}\cdot\omega_{\mathcal{M}}+G_2\cdot\omega_2]}\,.\end{aligned}\tag{C.1}$$

Now observe that, due to (2.13), (2.13),

$$\begin{aligned}D_{1\to2}^TG_2&=-{A_{\mathcal{M}}}^{-T}A_2^TG_2\in\mathcal{R}_{\mathcal{M}}^*\,,\\(I-D_{1\to2}^T)G_2&=A_1^{-T}A_2^TG_2\in\mathcal{R}_1^*\,.\end{aligned}$$

Thus, and using the fact that $(\mathcal{R}_1,\mathcal{R}_{\mathcal{M}})$ is incommensurate, we have that

$$\mathbb{1}_{\mathcal{R}_1^*}(G_2+G_{\mathcal{M}})=\mathbb{1}_{\mathcal{R}_1^*}(D_{1\to2}^TG_2+G_{\mathcal{M}})=\delta_{G_{\mathcal{M}},-D_{1\to2}^TG_2}\,.\tag{C.2}$$

Employing (C.2), (C.1) implies

$$\begin{aligned}&\lim_{N\to\infty}\mathcal{A}_{\mathcal{R}_1(N)}(h)(\omega_{\mathcal{M}},\omega_2)\\&\quad=\sum_{G_2\in\mathcal{R}_2^*}\hat{h}(-D_{1\to2}^TG_2,G_2)e^{i[-D_{1\to2}^TG_2\cdot\omega_{\mathcal{M}}+G_2\cdot\omega_2]}\,.\end{aligned}\tag{C.3}$$

Recalling (2.35) and (3.1), and using Fubini, we have that

$$\begin{aligned}&\sum_{G_2\in\mathcal{R}_2^*}\hat{h}(-D_{1\to2}^TG_2,G_2)e^{i[-D_{1\to2}^TG_2\cdot\omega_{\mathcal{M}}+G_2\cdot\omega_2]}\\&\quad=\sum_{G_2\in\mathcal{R}_2^*}\fint_{\Gamma_{\mathcal{M}}}\mathrm{d}x\;\mathcal{F}_{\Gamma_2}[h(x,\cdot)](G_2)e^{iG_2\cdot[D_{1\to2}(x-\omega_{\mathcal{M}})+\omega_2]}\,.\end{aligned}$$

Using Fubini again, we thus find that

$$\begin{aligned}&\sum_{G_2\in\mathcal{R}_2^*}\hat{h}(-D_{1\to2}^TG_2,G_2)e^{i[-D_{1\to2}^TG_2\cdot\omega_{\mathcal{M}}+G_2\cdot\omega_2]}\\&\quad=\fint_{\Gamma_{\mathcal{M}}}\mathrm{d}x\sum_{G_2\in\mathcal{R}_2^*}e^{iG_2\cdot[D_{1\to2}(x-\omega_{\mathcal{M}})+\omega_2]}\mathcal{F}_{\Gamma_2}[h(x,\cdot)](G_2)\\&\quad=\fint_{\Gamma_{\mathcal{M}}}\mathrm{d}x\;h\big(x,D_{1\to2}(x-\omega_{\mathcal{M}})+\omega_2\big)\,,\end{aligned}\tag{C.4}$$

where, in the second-to-last step, we used the Fourier inversion formula. Substituting $x = A_1\xi + \omega_{\mathcal{M}}$, and recalling (2.13), yields

$$\begin{aligned} &\fint_{\Gamma_{\mathcal{M}}} \mathrm{d}x\; h\big(x, D_{1\to 2}(x-\omega_{\mathcal{M}})+\omega_2\big) \\ &\quad = \fint_{A_1^{-1}\Gamma_{\mathcal{M}}} \mathrm{d}\xi\; h\big(A_1\xi+\omega_{\mathcal{M}}, (A_1-A_2)\xi+\omega_2\big) \end{aligned} \tag{C.5}$$

Collecting (C.3), (C.4), and (C.5), we conclude the proof. □

Proof of Proposition 3.5. We start by calculating for $G_{\mathcal{M}} = B_{\mathcal{M}} n \in \mathcal{R}^*_{\mathcal{M}}$

$$\begin{aligned} A_1^T G_{\mathcal{M}} &= A_1^T B_{\mathcal{M}} n \\ &= 2\pi (I - A_1^T A_2^{-T}) n \\ &= 2\pi (I - A^T R_\theta A^{-T}) n\,, \end{aligned} \tag{C.6}$$

where we recall (2.1), (2.5), and (2.8). Similarly, we find that

$$A_2^T G_{\mathcal{M}} = 2\pi (q^{-1} A^T R_{-\theta} A^{-T} - I) n\,. \tag{C.7}$$

In particular, using (C.6), (C.7), and (3.2), a straight-forward calculation yields

$$\begin{aligned} &\mathbb{1}^{(N)}_{\mathcal{R}^*_j}(B_{\mathcal{M}} n) \\ &\quad = \prod_{\ell=1}^{2} \frac{\sin\Big(\pi \operatorname{dist}\big((q^{(-1)^{j+1}} A^T R_{(-1)^{j+1}\theta} A^{-T} n)_\ell, \mathbb{Z}\big)(2N+1)\Big)}{(2N+1)\sin\Big(\pi \operatorname{dist}\big((q^{(-1)^{j+1}} A^T R_{(-1)^{j+1}\theta} A^{-T} n)_\ell, \mathbb{Z}\big)\Big)}\,. \end{aligned} \tag{C.8}$$

Observe that

$$\frac{\operatorname{dist}(x,\mathbb{Z})}{|\sin(\pi x)|} = \frac{\operatorname{dist}(x,\mathbb{Z})}{|\sin\big(\pi \operatorname{dist}(x,\mathbb{Z})\big)|} \le \frac{1}{\pi} \sup_{0<y<\pi/2} \frac{y}{\sin(y)} \le \frac{1}{2}\,.$$

Let $n \in \mathbb{Z}^2 \setminus \{0\}$. Recalling (C.8), we thus obtain that

$$\begin{aligned} &\max_{\ell=1,2} \operatorname{dist}\big((q^{(-1)^{j+1}} A^T R_{(-1)^{j+1}\theta} A^{-T} n)_\ell, \mathbb{Z}\big) \mathbb{1}^{(N)}_{\mathcal{R}^*_j}(B_{\mathcal{M}} n) \\ &\quad \le \frac{1}{\pi(2N+1)} \sup_{0<y<\pi/2} \frac{y}{\sin(y)} \\ &\quad = \frac{1}{2(2N+1)}\,. \end{aligned} \tag{C.9}$$

Using (C.9) and employing the fact that $\sqrt{a^2+b^2} \le \sqrt{2}\max\{|a|,|b|\}$, we find that

$$\begin{aligned} &|\mathbb{1}^{(N)}_{\mathcal{R}^*_j}(B_{\mathcal{M}}n)| \\ &\quad = \frac{\max_{\ell=1,2}\operatorname{dist}\left((q^{(-1)^{j+1}}A^T R_{(-1)^{j+1}\theta}A^{-T}n)_\ell, \mathbb{Z}\right)|\mathbb{1}^{(N)}_{\mathcal{R}^*_j}(B_{\mathcal{M}}n)|}{\operatorname{dist}\left(q^{(-1)^{j+1}}A^T R_{(-1)^{j+1}\theta}A^{-T}n, \mathbb{Z}^2\right)} \\ &\qquad \times \frac{\operatorname{dist}\left(q^{(-1)^{j+1}}A^T R_{(-1)^{j+1}\theta}A^{-T}n, \mathbb{Z}^2\right)}{\max_{\ell=1,2}\operatorname{dist}\left((q^{(-1)^{j+1}}A^T R_{(-1)^{j+1}\theta}A^{-T}n)_\ell, \mathbb{Z}\right)} \\ &\quad \le \frac{|n|^{2\sigma}}{\sqrt{2}K(2N+1)}\,. \end{aligned} \tag{C.10}$$

Here, we recognize the Diophantine condition (2.19) in the second line of (C.10). Recall from (A.4a) that

$$|n| \le \frac{\rho_{\mathcal{M}}\|A\|_2}{2\pi}|B_{\mathcal{M}}n|\,.$$

In particular, we arrive at

$$|\mathbb{1}^{(N)}_{\mathcal{R}^*_j}(G_{\mathcal{M}})| \le \frac{1}{\sqrt{2}K}\Big(\frac{\rho_{\mathcal{M}}\|A\|_2}{2\pi}\Big)^{2\sigma}|G_{\mathcal{M}}|^{2\sigma}\frac{1}{2N+1} \tag{C.11}$$

for any $G_{\mathcal{M}} \in \mathcal{R}^*_{\mathcal{M}} \setminus \{0\}$. Using (C.11) and the steps leading to (3.6), we thus conclude the proof. □

References

1. Arendt, W., Daners, D.: Semilinear elliptic equations on rough domains. *J. Differ. Equ.* **346**, 376–415, 2023
2. Aubry, S.: The new concept of transitions by breaking of analyticity in a crystallographic model. In: Bishop, A.R., Schneider, T. (eds.) Solitons Condens. Matter Phys., pp. 264–277. Springer, Berlin Heidelberg (1978)
3. Aubry, S., André, G.: Analyticity breaking and Anderson localization in incommensurate lattices. *Ann. Israel Phys. Soc.* **3**(133), 18, 1980
4. Aubry, S., Le Daeron, P.-Y.: The discrete Frenkel-Kontorova model and its extensions: I. Exact results for the ground-states. *Phys. D* **8**(3), 381–422, 1983
5. Becker, S., Embree, M., Wittsten, J., Zworski, M.: Mathematics of magic angles in a model of twisted bilayer graphene. *Probab. Math. Phys.* **3**(1), 69–103, 2022
6. Becker, S., Humbert, T., Zworski, M. (2022). Fine structure of flat bands in a chiral model of magic angles. arXiv:2208.01628, 2022
7. Bellissard, J., Testard, D.: Quasi periodic Hamiltonians: a mathematical approach. *Oper. Algebras Appl.* **2**, 579, 1982
8. Bellissard, J.: Coherent and dissipative transport in aperiodic solids: An overview. In: Garbaczewski, P., Olkiewicz, R. (eds.) Dynamics of dissipation, pp. 413–485. Springer, Berlin (2002)
9. Bellissard, J., van Elst, A., Schulz-Baldes, H.: The noncommutative geometry of the quantum Hall effect. *J. Math. Phys.* **35**(10), 5373–5451, 1994
10. Beresnevich, V., Ramírez, F., Velani, S.: Metric Diophantine approximation: aspects of recent work. *Dyn. Anal. Number Theory* **437**, 1–95, 2016

11. Berndt, B.C., Kim, S., Zaharescu, A.: The Circle problem of Gauss and the divisor problem of Dirichlet—still unsolved. *Am. Math. Mon.* **125**(2), 99–114, 2018
12. Bilyk, D.: Discrepancy theory and harmonic analysis. Uniform distribution and quasi-Monte Carlo methods, pp 45–62 (2014)
13. Bilyk, D., Ma, X., Pipher, J., Spencer, C.: Directional discrepancy in two dimensions. *Bull. Lond. Math. Soc.* **43**(6), 1151–1166, 2011
14. Bilyk, D., Ma, X., Pipher, J., Spencer, C.: Diophantine approximations and directional discrepancy of rotated lattices. *Trans. Am. Math. Soc.* **368**(6), 3871–3897, 2016
15. Bistritzer, R., MacDonald, A.H.: Moiré bands in twisted double-layer graphene. *Proc. Natl. Acad. Sci.* **108**(30), 12233–12237, 2011
16. Blanc, X., Le Bris, C., Lions, P.-L.: From molecular models to continuum mechanics. *Arch. Ration. Mech. Anal.* **164**, 341–381, 2002
17. Bourgain, J.: A quantitative Oppenheim theorem for generic diagonal quadratic forms. *Israel J. Math.* **215**(1), 503–512, 2016
18. Bourgain, J., Watt, N.: Mean square of zeta function, circle problem and divisor problem revisited. arXiv:1709.04340 (2017)
19. Buterus, P., Götze, F., Hille, T., Margulis, G.: Distribution of values of quadratic forms at integral points. *Invent. Math.* **227**(3), 857–961, 2022
20. Cabre, X., Cinti, E., Serra, J.: Stable solutions to the fractional Allen-Cahn equation in the nonlocal perimeter regime. arXiv:2111.06285 (2021)
21. Cancès, E., Cazeaux, P., Luskin, M.: Generalized Kubo formulas for the transport properties of incommensurate 2d atomic heterostructures. *J. Math. Phys.* **58**(6), 063502, 2017
22. Cao, Y., Fatemi, V., Demir, A., Fang, S., Tomarken, S.L., Luo, J.Y., Sanchez-Yamagishi, J.D., Watanabe, K., Taniguchi, T., Kaxiras, E., Ashoori, R.C., Jarillo-Herrero, P.: Correlated insulator behaviour at half-filling in magic-angle graphene superlattices. *Nature* **556**(7699), 80–84, 2018
23. Cao, Y., Fatemi, V., Fang, S., Watanabe, K., Taniguchi, T., Kaxiras, E., Jarillo-Herrero, P.: Unconventional superconductivity in magic-angle graphene superlattices. *Nature* **556**(7699), 43–50, 2018
24. Carr, S., Massatt, D., Torrisi, S.B., Cazeaux, P., Luskin, M., Kaxiras, E.: Relaxation and domain formation in incommensurate two-dimensional heterostructures. *Phys. Rev. B* **98**, 12, 2018
25. Carr, S., Massatt, D., Torrisi, S.B., Cazeaux, P., Luskin, M., Kaxiras, E.: Relaxation and domain formation in incommensurate two-dimensional heterostructures. *Phys. Rev. B* **98**(22), 224102, 2018
26. Catarina, G., Amorim, B., Castro, E.V., Lopes, J.M.V.P., Peres, N.M.R.: Twisted bilayer graphene: low-energy physics, electronic and optical properties. *Handbook of Graphene* **3**, 177–232, 2019
27. Cazeaux, P., Clark, D., Engelke, R., Kim, P., Luskin, M.: Relaxation and domain wall structure of bilayer moiré systems. *J. Elasticit.* **154**(1), 443–466, 2023
28. Cazeaux, P., Luskin, M., Massatt, D.: Energy minimization of two dimensional incommensurate heterostructures. *Arch. Ration. Mech. Anal.* **235**, 1289–1325, 2020
29. Cazeaux, P., Luskin, M., Tadmor, E.B.: Analysis of rippling in incommensurate one-dimensional coupled chains. *Multis. Model. Simul.* **15**(1), 56–73, 2017
30. Cazeaux, P.: Cauchy-Born strain energy density for coupled incommensurate elastic chains. *ESAIM: M2AN* **52**(2), 729–749, 2018
31. Cazenave, T.: An introduction to semilinear elliptic equations. Editora do IM-UFRJ, Rio de Janeiro (2006)
32. Champagne, J., Roy, D.: Diophantine approximation with constraints. *Acta Arith* **207**(1), 57–99, 2023
33. Chen, T., Hott, M.: On the emergence of quantum Boltzmann fluctuation dynamics near a Bose-Einstein condensate. *J. Stat. Phys.* **190**(4), 85, 2023

34. Chodosh, O.: Lecture notes on geometric features of the Allen–Cahn equation (Princeton, 2019). https://web.stanford.edu/~ochodosh/AllenCahnSummerSchool2019.pdf (2023). Accessed 15 June 2024
35. Cinti, E., Davila, J., Del Pino, M.: Solutions of the fractional Allen-Cahn equation which are invariant under screw motion. *J. Lond. Math. Soc.* **94**(1), 295–313, 2016
36. Dai, S., Xiang, Y., Srolovitz, D.J.: Twisted bilayer graphene: Moiré with a twist. *Nano Lett.* **16**(9), 5923–5927, 2016
37. Damanik, D.: One-dimensional ergodic Schrödinger operators. In: Graduate studies in mathematics, vol. 221. American Mathematical Society, Providence, Rhode Island (2022)
38. Dean, C., Lei Wang, P., Maher, C.F., Fereshte Ghahari, Y., Gao, J.K., Ishigami, M., Moon, P., Koshino, M., Takashi Taniguchi, K., Watanabe, K.S., Hone, J., Kim, P.: Hofstadter's butterfly and the fractal quantum Hall effect in moiré superlattices. *Nature* **497**, 598, 2013
39. Díaz, G.: Large solutions of elliptic semilinear equations non-degenerate near the boundary. *Commun. Pure Appl. Anal.* **22**(3), 686–735, 2023
40. Duoandikoetxea, J.: Fourier analysis. In: Graduate studies in mathematics, vol. 29. American Mathematical Society, Providence, Rhode Island (2001)
41. Dupaigne, L.: Stable solutions of elliptic partial differential equations, vol. 143. Chapman & Hall/CRC Monographs and Surveys in Pure and Applied Mathematics. Chapman & Hall/CRC, Boca Raton, FL (2011)
42. Dupaigne, L., Farina, A.: Regularity and symmetry for semilinear elliptic equations in bounded domains. *Commun. Contemp. Math.* **25**(5), 2250018, 2023
43. Eskin, A., Margulis, G., Mozes, S.: Quadratic forms of signature (2, 2) and eigenvalue spacings on rectangular 2-tori. *Ann. Math.* **161**(2), 679–725, 2005
44. Español, M.I., Golovaty, D., Patrick Wilber, J.: Discrete-to-continuum modelling of weakly interacting incommensurate two-dimensional lattices. *Proc. R. Soc. A.* **474**(2209), 20170612, 2018
45. Español, M.I., Golovaty, D., Patrick Wilber, J.: A discrete-to-continuum model of weakly interacting incommensurate two-dimensional lattices: The hexagonal case. *J. Mech. Phys. Solids* **173**, 105229, 2023
46. Figalli, A., Serra, J.: On stable solutions for boundary reactions: a De Giorgi-type result in dimension 4+ 1. *Invent. Math.* **219**(1), 153–177, 2020
47. Fricker, F.: Einführung in die Gitterpunktlehre, volume 73 of Lehrbücher und Monographien aus dem Gebiete der Exakten Wissenschaften (LMW). Mathematische Reihe [Textbooks and Monographs in the Exact Sciences. Mathematical Series]. Birkhäuser Verlag, Basel-Boston, Mass. (1982)
48. Ghosh, A., Kelmer, D.: A quantitative Oppenheim theorem for generic ternary quadratic forms. *J. Mod. Dyn.* **12**, 1–8, 2018
49. Guo, B., Pei, Y.: Periodic solutions of Ginzburg-Landau theory for atomic Fermi gases near the BCS-BEC crossover. *Appl. Anal.* **101**(4), 1199–1210, 2022
50. Hammonds, T., Kim, S., Miller, S.J., Nigam, A., Onghai, K., Saikia, D., Sharma, L.M.: k-Diophantine m-tuples in finite fields. *Int. J. Number Theory* **19**(4), 891–912, 2023
51. Huxley, M.N.: Exponential sums and lattice points iii. *Proc. Lond. Math. Soc.* **87**(3), 591–609, 2003
52. Ignat, R., Jerrard, R.L.: Renormalized energy between vortices in some Ginzburg-Landau models on 2-dimensional Riemannian manifolds. *Arch. Ration. Mech. Anal.* **239**(3), 1577–1666, 2021
53. Joseph, A., Sankar, L.: Singular semilinear elliptic problems on unbounded domains in $\mathbb{R}^n$. *J. Math. Anal. Appl.* **520**(2), 126903, 2023
54. Kechris, A. S.: Global aspects of ergodic group actions, vol. 160. Mathematical Surveys and Monographs. American Mathematical Society, Providence, RI (2010)

55. Kennes, D.M., Claassen, M., Xian, L., Georges, A., Millis, A.J., Hone, J., Dean, C.R., Basov, D.N., Pasupathy, A.N., Rubio, A.: Moiré heterostructures as a condensed-matter quantum simulator. *Nat. Phys.* **17**(2), 155–163, 2021
56. Kerr, D., Li, H.: Ergodic theory: independence and dichotomies. Springer monographs in mathematics. Springer, Cham (2016)
57. Kolmogorov, A.N., Crespi, V.H.: Registry-dependent interlayer potential for graphitic systems. *Phys. Rev. B* **71**, 235415, 2005
58. Koshino, M., Son, Y.W.: Moiré phonons in twisted bilayer graphene. *Phys. Rev. B* **100**, 8, 2019
59. Kuipers, L., Niederreiter, H.: Uniform distribution of sequences. Pure and applied mathematics. Wiley-Interscience, New York (1974)
60. Kuratsubo, S., Nakai, E.: Multiple Fourier series and lattice point problems. *J. Funct. Anal.* **282**(1), 109272, 2022
61. Lax, P.D., Phillips, R.S.: The asymptotic distribution of lattice points in Euclidean and non-Euclidean spaces. *J. Funct. Anal.* **46**(3), 280–350, 1982
62. Leven, I., Maaravi, T., Azuri, I., Kronik, L., Hod, O.: Interlayer potential for graphene/h-BN heterostructures. *J. Chem. Theory Comput.* **12**(6), 2896–2905, 2016
63. Levitan, B.M.: Asymptotic formulae for the number of lattice points in Euclidean and Lobachevskii spaces. *Russ. Math. Surv.* **42**(3), 13, 1987
64. Lu, J.Z., Zhu, Z., Angeli, M., Larson, D.T., Kaxiras, E.: Low-energy moiré phonons in twisted bilayer van der waals heterostructures. *Phys. Rev. B* **106**, 144305, 2022
65. Maggi, F., Restrepo, D.: Uniform stability in the Euclidean isoperimetric problem for the Allen-Cahn energy. *Anal. PDE* **17**(5), 1761–1830, 2024
66. Marom, N., Bernstein, J., Garel, J., Tkatchenko, A., Joselevich, E., Kronik, L., Hod, O.: Stacking and registry effects in layered materials: The case of hexagonal boron nitride. *Phys. Rev. Lett.* **105**, 046801, 2010
67. Massatt, D., Carr, S., Luskin, M.: Electronic observables for relaxed bilayer 2D heterostructures in momentum space. *Multiscale Model. Simul.* **21**(4), 1344–1378, 2023
68. Massatt, D., Luskin, M., Ortner, C.: Electronic density of states for incommensurate layers. *SIAM J. Multiscale Model. Simul.* **15**, 476–499, 2017
69. Massatt, D., Luskin, M., Ortner, C.: Electronic density of states for incommensurate layers. *Multiscale Model. Simul.* **15**(1), 476–499, 2017
70. Musil, F., Grisafi, A., Bartók, A.P., Ortner, C., Csányi, G., Ceriotti, M.: Physics-inspired structural representations for molecules and materials. *Chem. Rev.* **121**(16), 9759–9815, 2021
71. Mutalik, P.: Solution: Magic Moiré in Twisted Graphene. Quanta Magazine, July 2019. https://www.quantamagazine.org/puzzle-solution-magic-moire-in-graphene-20190726/, Accessed 22 Mar 2023
72. Nam, N.N., Koshino, M.: Lattice relaxation and energy band modulation in twisted bilayer graphene. *Phys. Rev. B* **96**(7), 075311, 2017
73. O'Dorney, E.: Diophantine approximation on conics. *Proc. Amer. Math. Soc.* **151**(5), 1889–1905, 2023
74. Ortner, C., Theil, F.: Justification of the Cauchy-born approximation of elastodynamics. *Arch. Ration. Mech. Anal.* **207**(3), 1025–1073, 2013
75. O'connor, Thomas C., Andzelm, Jan, Robbins, Mark O.: AIREBO-M: a reactive model for hydrocarbons at extreme pressures. *J. Chem. Phys.* **142**, 024903, 2015
76. Peng, Z., Chen, X., Fan, Y., Srolovitz, D.J., Lei, D.: Strain engineering of 2d semiconductors and graphene: from strain fields to band-structure tuning and photonic applications. *Light Sci. Appl.* **9**(1), 190, 2020
77. Pablo San-Jose, A., Gutiérrez-Rubio, M.S., Guinea, F.: Spontaneous strains and gap in graphene on boron nitride. *Phys. Rev. B* **90**, 075428, 2014
78. Savin, O.: Minimal surfaces and minimizers of the Ginzburg–Landau energy. *Cont. Math. Mech. Anal. AMS* **526**, 43–58, 2010

79. Schmidt, K.M., Buettner, A.B., Graeve, O.A., Vasquez, V.R.: Interatomic pair potentials from DFT and molecular dynamics for Ca, Ba, and Sr hexaborides. *J. Mater. Chem. C* **3**(33), 8649–8658, 2015
80. Serfaty, S.: Mean field limits of the Gross-Pitaevskii and parabolic Ginzburg-Landau equations. *J. Am. Math. Soc.* **30**(3), 713–768, 2017
81. Shapeev, A.V.: Moment tensor potentials: a class of systematically improvable interatomic potentials. *Multiscale Model. Simul.* **14**(3), 1153–1173, 2016
82. Tachim Medjo, T.: Large deviation principles for a 2D stochastic Allen–Cahn–Navier–Stokes driven by jump noise.". *Stoch. Dyn.* **22**(04), 2250005, 2022
83. Tarnopolsky, G., Kruchkov, A.J., Vishwanath, A.: Origin of magic angles in twisted bilayer graphene. *Phys. Rev. Lett.* **122**(10), 106405, 2019
84. Trefethen, L.N., Weideman, J.A.C.: The exponentially convergent trapezoidal rule. *SIAM Rev.* **56**, 385–458, 2014
85. Tritsaris, G.A., Shirodkar, S.N., Kaxiras, E., Cazeaux, P., Luskin, M., Plechác, P., Cancès, E.: Perturbation theory for weakly coupled two-dimensional layers. *J. Mater. Res.* **31**, 959–966, 2016
86. Watson, A.B., Luskin, M.: Existence of the first magic angle for the chiral model of bilayer graphene. *J. Math. Phys.* **62**(9), 091502, 2021
87. Yoo, H., Engelke, R., Carr, S., Fang, S., Zhang, K., Cazeaux, P., Sung, S.H., Hovden, R., Tsen, A.W., Taniguchi, T., Watanabe, K.: Atomic and electronic reconstruction at the van der Waals interface in twisted bilayer graphene. *Nat. Mater.* **18**(5), 448–453, 2019
88. Zhang, K., Tadmor, E.B.: Structural and electron diffraction scaling of twisted graphene bilayers. *J. Mech. Phys. Solids* **112**, 12, 2017
89. Zhang, X., Tsai, K.-T., Zhu, Z., Ren, W., Luo, Y., Carr, S., Luskin, M., Kaxiras, E., Wang, K.: Correlated insulating states and transport signature of superconductivity in twisted trilayer graphene superlattices. *Phys. Rev. Lett.* **127**(16), 166802, 2021
90. Zhou, S., Han, J., Dai, S., Sun, J., Srolovitz, D.J.: van der Waals bilayer energetics: generalized stacking-fault energy of graphene, boron nitride, and graphene/boron nitride bilayers. *Phys. Rev. B* **92**, 155438, 2015
91. Zhu, Z., Carr, S., Massatt, D., Luskin, M., Kaxiras, E.: Twisted trilayer graphene: a precisely tunable platform for correlated electrons. *Phys. Rev. Lett.* **125**(11), 116404, 2020
92. Zhu, Z., Cazeaux, P., Luskin, M., Kaxiras, E.: Modeling mechanical relaxation in incommensurate Trilayer van der Waals heterostructures. *Phys. Rev. B* **101**(22), 224107, 2020

Michael Hott · Alexander B. Watson · Mitchell Luskin
School of Mathematics,
University of Minneapolis, Twin Cities,
Minneapolis
MN
55455 USA.
e-mail: mhott@umn.edu; abwatson@umn.edu; luskin@umn.edu

(*Received November 11, 2023 / Accepted September 16, 2024*)
Published online October 24, 2024
© *The Author(s), under exclusive licence to Springer-Verlag GmbH Germany, part of Springer Nature* (*2024*)